Optimal Underdamped Langevin MCMC Method

Zhengmian Hu, Feihu Huang, Heng Huang
Department of Electrical and Computer Engineering
University of Pittsburgh, Pittsburgh, PA 15213, USA
{huzhengmian,huangfeihu2018}@gmail.com, heng.huang@pitt.edu

Abstract

In the paper, we study the underdamped Langevin diffusion (ULD) with strongly-convex potential consisting of finite summation of N smooth components, and propose an efficient discretization method, which requires $O(N + d^{\frac{1}{3}}N^{\frac{2}{3}}/\varepsilon^{\frac{2}{3}})$ gradient evaluations to achieve ε-error (in $\sqrt{\mathbb{E}\|\cdot\|_2^2}$ distance) for approximating d-dimensional ULD. Moreover, we prove a lower bound of gradient complexity as $\Omega(N + d^{\frac{1}{3}}N^{\frac{2}{3}}/\varepsilon^{\frac{2}{3}})$, which indicates that our method is optimal in dependence of N, ε, and d. In particular, we apply our method to sample the strongly-log-concave distribution and obtain gradient complexity better than all existing gradient based sampling algorithms. Experimental results on both synthetic and real-world data show that our new method consistently outperforms the existing ULD approaches.

1 Introduction

Sampling is an important research problem in statistics learning with many applications such as Bayesian inference [1], multi-arm bandit optimization [2], and reinforcement learning [3]. One of the fundamental problems in these applications is to sample from a high-dimensional strongly-log-concave distribution. Recently, several Markov chain Monte Carlo (MCMC) based methods were proposed to solve this problem based on underdamped Langevin diffusion (ULD). This continuous diffusion process converges to the target distribution exponentially fast. Thus, the methods approximating a ULD process could be used to sample from the target distribution within certain accuracy.

Multiple discretization methods have been proposed for approximating ULD. Among them, the Euler-Maruyama discretization [4] is the simplest one but generates the largest error. Recently the left point method (LPM) [1] [5] was introduced to fix the gradient term in ULD to be the gradient at k-th iteration, and then integrate the new linear stochastic differential equation (SDE) with a small time-interval. Subsequently, Shen and Lee [6] proposed randomized midpoint method (RMM) with smaller error. There are also discretization schemes based on splitting [7] or Runge-Kutta method [8, 9]. More recently, Cao et al. [10] derived an information-based complexity lower bound for simulating a d-dimensional ULD. Under the assumption that the full gradient oracle $\nabla f(\boldsymbol{x})$ is evaluated at most n times, they show a lower bound for worst-case error by perturbation analysis, which matches the discretization error upper bound of RMM in the dependence of d and n.

Although the ULD-MCMC methods with full gradient oracle are largely understood, many real-world applications involve summation form of potential function and large-scale data, which leads to the need of stochastic gradient methods. The vanilla stochastic gradient methods have been used to replace full gradient [5]. Albeit the computational cost for each iteration is reduced, the variance of

[1] Although this method is mostly just denoted as ULD-MCMC, we adopt the name LPM to distinguish it from other discretization methods. The name comes from the fact that gradient is evaluated at the left point of the time interval.

35th Conference on Neural Information Processing Systems (NeurIPS 2021).

Table 1: Summary of gradient complexity of sampling methods, which is defined as number of gradient evaluation of $\nabla f_i(\boldsymbol{x})$ needed to sample from m-strongly-log-concave distributions up to $\varepsilon\sqrt{d/m}$ accuracy in 2-Wasserstein distance where $\varepsilon \leq 1$ is the target accuracy, d is the dimension. ULA, LPM, RMM, and ALUM are full gradient methods, therefore, gradient complexities for them are sample size N times the iteration complexities. Only dependence on d, ε, and N are shown below. The dependence of batch size b is made clear in Table 3. The dependence of condition number κ is discussed in Section 7.

Algorithms	Gradient complexities
Unadjusted Langevin Algorithm (ULA) [15, 16]	$\widetilde{O}(N\varepsilon^{-2})$
LPM [17]	$\widetilde{O}(N\varepsilon^{-1})$
RMM [6]	$\widetilde{O}(N\varepsilon^{-\frac{2}{3}})$
ALUM (Ours)	$\widetilde{O}(N\varepsilon^{-\frac{2}{3}})$
Stochastic Gradient LPM (SG-LPM) [5]	$\widetilde{O}(\varepsilon^{-2})$
SVRG-LPM [11][2]	$\widetilde{O}(N+\varepsilon^{-1}+N^{\frac{2}{3}}\varepsilon^{-\frac{2}{3}})$
CV-ULD [18][3]	$\widetilde{O}(N+\varepsilon^{-3})$
SVRG-ALUM (Ours)	$\widetilde{O}(N+N^{\frac{2}{3}}\varepsilon^{-\frac{2}{3}})$
SAGA-ALUM (Ours)	$\widetilde{O}(N+N^{\frac{2}{3}}\varepsilon^{-\frac{2}{3}})$

stochastic gradient is much larger than the discretization error and therefore degenerates the overall performance. Previous works [11, 12] used stochastic variance reduced gradient (SVRG) [13] and SAGA [14] instead, but the gradient complexities of these methods are still worse than the full gradient RMM in terms of dependence on accuracy ε. Thus, there exists a natural question:

What is the optimal ULD-MCMC method with sum-decomposable potential?

In this paper, we focus on optimal dependence of dimension d, components number N and accuracy ε in gradient complexity for estimating a ULD process. We answer this question by two parts. We first provide a novel ULD-MCMC method and derive the corresponding complexity upper bound in Sections 4 and 5. After that, we analyze the worse case error and show that the lower bound matches the upper bound in Section 6. The major contributions of our paper can be summarized as follows.

1. We propose a new full gradient ULD-MCMC method, called as AcceLerated ULD method (ALUM), whose discretization error has the same order dependence on dimension d, step size h as RMM. Although RMM already has optimal asymptotic complexity in full gradient setting, ALUM is still of practical interest. Compared with RMM, which uses two gradient evaluations at each iteration, ALUM uses gradient less frequently and only requires one gradient at each iteration to achieve constant speedup.
2. We further propose VR-ALUM methods, including SVRG-ALUM and SAGA-ALUM, which utilize the unbiased variance reduction techniques in ALUM under sum-decomposable setting. We show that these methods achieve better gradient complexity than all existing gradient based MCMC approaches. These gradient complexities for sampling from a strongly-log-concave distribution are compared in Table 1.
3. We derive an information-based lower bound on worst-case error for estimating a ULD process with only gradient oracle and weighted Brownian motion oracle. We show that in order to achieve ε approximation accuracy, $\Omega(N + d^{\frac{1}{3}}N^{\frac{2}{3}}\varepsilon^{-\frac{2}{3}})$ single component gradient evaluations are needed. This lower bound matches the upper bound for VR-ALUM in terms of dependence of dimension d, sample size N, and accuracy ε. Therefore, our VR-ALUM methods are indeed optimal for estimating a ULD process under sum-decomposable setting.

[2] In Zou et al. [11], the authors call their method SVR-HMC. However, their method is not based on Hamiltonian Monte Carlo (HMC), but based on ULD. Their method is just applying SVRG to replace full gradient in LPM.

[3] Further explanation and comparison is shown in Appendix A.2.

2 Related work

Though we mainly use the gradient oracle in this paper, there is also a large body of sampling algorithms which leverage zeroth order potential value oracle. For example, Metropolis-Hastings accept-reject step could be used to ensure an MCMC converges to a stationary distribution equal to the target distribution [19, 20, 21, 22, 23] and the linear convergence can be obtained. For example, MALA [24, 21, 25], as Metropolis-adjusted ULA, can achieve ε error in total variation distance within $O(d^2 \log(1/\varepsilon))$ steps under certain initialization [26]. Note that purely gradient based sampling algorithms typically only converge sub-linearly because the stationary distribution is different from the target distribution.

Other diffusion processes could also be used for constructing MCMC. ULA, a discretization of Langevin diffusion (LD) [27, 24], is the first commonly used gradient-based MCMC. We will provide an overview for some LD-based and ULD-based methods in Appendix A.1. Later, higher order diffusion process is also discussed. Although the path is even smoother than ULD, currently it is not clear whether such higher order smoothness of path could be leveraged to accelerate the convergence without extra assumptions on potential function. Mou et al. [28] studied third-order diffusion, but their acceleration requires special structure or high order smoothness of potential. The more general diffusion process, which converges to the target distribution, was studied in Ma et al. [29].

3 Preliminary

The problem of sampling from a strongly-log-concave distribution involves a probability density function $p^*(\boldsymbol{x})$ defined on a real vector space $\mathbb{R}^d$. A corresponding potential function $f(\boldsymbol{x}) = -\log(p^*(\boldsymbol{x}))$ can be defined such that $f(\boldsymbol{x})$ is strongly convex. One way to solve this sampling problem is constructing a Markov chain that converges to a stationary distribution that is the same as or similar to the target distribution. In Appendix A.1, we introduce several such Markov chains as discretization of certain continuous stochastic processes, and we roughly analyze discretization error of these methods with pointing out the bottleneck.

We use $\widetilde{O}(f) = O(f)\log^{O(1)}(f)$ to omit logarithm factor. $\|\cdot\|_2$ means the Euclidean norm. We define a norm of random vector as $\|\cdot\|_{\mathbb{L}_2} = \sqrt{\mathbb{E}\|\cdot\|_2^2}$. Next, we list our assumptions on potential $f(\boldsymbol{x})$.

Assumption 1 (Sum-decomposable)**.** *$f(\boldsymbol{x}) = \sum_{i=1}^N f_i(\boldsymbol{x})$, where integer N is the sample size.*

Assumption 2 (Smoothness)**.** *Each function f_i is twice differentiable on $\mathbb{R}^d$ and there exists a constant $L > 0$, such that $\boldsymbol{\nabla}^2 f_i(\boldsymbol{x}) \preccurlyeq \frac{L}{N} I$ for any $\boldsymbol{x} \in \mathbb{R}^d$ where I is the identity matrix. It can be easily verified that $f(\boldsymbol{x})$ is L-smooth.*

Assumption 3 (Strong Convexity)**.** *There exists a constant $m > 0$ such that: $f(\boldsymbol{x}) - f(\boldsymbol{y}) \geq \langle \nabla f(\boldsymbol{y}), \boldsymbol{x} - \boldsymbol{y}\rangle + \frac{m}{2}\|\boldsymbol{x} - \boldsymbol{y}\|_2^2$. We define the condition number $\kappa \coloneqq L/m$.*

We finally define the 2-Wasserstein distance between distributions. For any pair of probability measures μ and ν on the same parameter space, a transference plan ζ between μ and ν is a joint distribution such that the marginal distributions on two sets of coordinates are μ and ν, respectively. We denote $\Gamma(\mu, \nu)$ as the set of all transference plans, and define the 2-Wasserstein distance between μ and ν as follows:

$$W_2^2(\mu, \nu) = \inf_{\zeta \in \Gamma(\mu,\nu)} \int \|\boldsymbol{x} - \boldsymbol{y}\|_2^2 d\zeta(x, y).$$

4 AcceLerated ULD-MCMC (ALUM) methods

In this section, we propose a class of AcceLerated ULD-MCMC (ALUM) methods based on approximation of the continuous ULD process:

$$d\boldsymbol{X}_t = \boldsymbol{V}_t dt,\ d\boldsymbol{V}_t = -\nabla f(\boldsymbol{X}_t)dt - \gamma \boldsymbol{V}_t dt + \sqrt{2\gamma} d\boldsymbol{B}_t. \tag{1}$$

The gradient term in the above SDE could be highly non-linear such that closed form solution is not available. Thus, we propose an estimation of SDE solution at time point h which only requires

gradient evaluation at one single point:

$$\begin{aligned}
\boldsymbol{X}_h^{(o)} &= \boldsymbol{X}_0 + \psi_1(h)\boldsymbol{V}_0 - h\psi_1(h-ah)\nabla f(\boldsymbol{X}_{ah}^{(e)}) + \boldsymbol{e}_{x,[0,h]}, \\
\boldsymbol{V}_h^{(o)} &= \psi_0(h)\boldsymbol{V}_0 - h\psi_0(h-ah)\nabla f(\boldsymbol{X}_{ah}^{(e)}) + \boldsymbol{e}_{v,[0,h]}, \\
\boldsymbol{X}_{ah}^{(e)} &= \boldsymbol{X}_0 + \psi_1(ah)\boldsymbol{V}_0 + \boldsymbol{e}_{x,[0,ah]},
\end{aligned} \tag{2}$$

where the random variable a is uniform random variable in $[0,1]$, $\psi_i(\cdot)$ and noise terms $\boldsymbol{e}_{x,[0,h]}$, $\boldsymbol{e}_{v,[0,h]}$, $\boldsymbol{e}_{x,[0,ah]}$ are defined as follows [4].

$$\begin{gathered}
\psi_0(h) = e^{-\gamma h}, \psi_1(h) = \frac{1}{\gamma}(1-e^{-\gamma h}), \\
\boldsymbol{e}_{x,[0,h]} = \sqrt{2\gamma}\int_0^h \psi_1(h-s)d\boldsymbol{B}_s, \;\; \boldsymbol{e}_{v,[0,h]} = \sqrt{2\gamma}\int_0^h \psi_0(h-s)d\boldsymbol{B}_s.
\end{gathered} \tag{3}$$

4.1 Full gradient ALUM

In this subsection, we propose a full gradient ALUM method, which is shown in Algorithm 1. Specifically, the update rule is obtained by setting $\boldsymbol{x}_{k+1}^{(o)}, \boldsymbol{v}_{k+1}^{(o)}$ to $\boldsymbol{X}_h^{(o)}, \boldsymbol{V}_h^{(o)}$ where the ULD starts from $\boldsymbol{X}_0 = \boldsymbol{x}_k^{(o)}, \boldsymbol{V}_0 = \boldsymbol{v}_k^{(o)}$ and h is a small step size.

Next, we compare our method with both RMM and Nesterov's accelerated gradient method (NAG) which has been shown optimal for gradient based optimization. **Compared to RMM:** By comparing the formula in (19) and (2), it is easy to see that ALUM and RMM differ in one single term $-\psi_2(ah)\nabla f(\boldsymbol{X}_0)$.

Our motivation of dropping this term is to reduce the computations. By deleting this term from the algorithm, only one gradient evaluation at a randomized midpoint is needed at each iteration. This compares favorably to the RMM, which requires two gradient evaluations at each iteration.

Algorithm 1: Full gradient ALUM Method

Input: Initial point $(\boldsymbol{x}_0^{(o)}, \boldsymbol{v}_0^{(o)})$, parameter γ, iteration number K, and step size $h > 0$.
for $k = 0$ **to** $K-1$ **do**
  Randomly sample a_k uniformly from $[0,1]$;
  Generate $\boldsymbol{e}_{x,[0,h],k}$, $\boldsymbol{e}_{v,[0,h],k}$, $\boldsymbol{e}_{x,[0,a_kh],k}$ according to Appendix A.5;
  $\boldsymbol{x}_k^{(e)} = \boldsymbol{x}_k^{(o)} + \psi_1(a_kh)\boldsymbol{v}_k^{(o)} + \boldsymbol{e}_{x,[0,a_kh],k}$;
  Calculate full gradient $\nabla f(\boldsymbol{x}_k^{(e)})$;
  $\boldsymbol{x}_{k+1}^{(o)} =$
  $\boldsymbol{x}_k^{(o)} + \psi_1(h)\boldsymbol{v}_k^{(o)} - h\psi_1(h-a_kh)\nabla f(\boldsymbol{x}_k^{(e)}) + \boldsymbol{e}_{x,[0,h],k}$;
  $\boldsymbol{v}_{k+1}^{(o)} = \psi_0(h)\boldsymbol{v}_k^{(o)} - h\psi_0(h-a_kh)\nabla f(\boldsymbol{x}_k^{(e)}) + \boldsymbol{e}_{v,[0,h],k}$;
end for
Output: $\boldsymbol{x}_K^{(o)}$.

However, could this method still estimate ULD accurately with only half gradient evaluations? We firmly answer this question with rigorous error analysis in Theorem 2. Roughly speaking, if we only consider the error's dependence on step size h, the answer is yes. In this section, we only give an intuition of how that is possible.

In Appendix A.1, we show that RMM has very low bias and high variance. Therefore, the bottleneck is the variance, and increasing the bias slightly would not degenerate the overall performance much if the bias is not larger than the error introduced by variance. The dropped term $-\psi_2(ah)\nabla f(\boldsymbol{X}_0)$ has norm $O(h^2)$, and the coefficient of gradient in $\boldsymbol{V}_h$ is $O(h)$. Thus, the bias introduced in single step is $O(h^3)$ when we use step size h. After accumulating for $T/h = O(h^{-1})$ iterations, the bias is $O(h^2)$, which still has better dependence on h than the square root of variance $O(h^{3/2})$.

With increased bias, the complexities of ALUM and some other variants[5] still have the same dependence on ε as RMM, the highest order dependence on κ could deteriorate as discussed in Section 7.

Compared to Nesterov's accelerated gradient (NAG) method: NAG is a gradient based optimization method [30]. Based on [31], NAG could be formulated as the following momentum method:

[4] $\boldsymbol{e}_{x,[0,ah]}$ is obtained by simply substituting h with ah in the definition of $\boldsymbol{e}_{x,[0,h]}$.

[5] We can drop $\boldsymbol{e}_{x,[0,h],k}$ and $\boldsymbol{e}_{x,[0,a_kh],k}$ in (2) to derive other variants of ALUM. The bias of these variants increases to $O(h^{3/2})$, which is still no larger than the square root of variance. The maximum order dependence on h is the same, thus the final iteration complexity has the same dependence on ε as RMM.

$$\boldsymbol{x}_{k+1} = \boldsymbol{x}_k + c_k\boldsymbol{x}_k + c_k'\nabla f(\boldsymbol{x}_k^{(e)}), \quad \boldsymbol{v}_{k+1} = c_k\boldsymbol{x}_k + c_k'\nabla f(\boldsymbol{x}_k^{(e)}), \quad \boldsymbol{x}_k^{(e)} = \boldsymbol{x}_k + c_k\boldsymbol{x}_k\,. \quad (4)$$

We can see that the main differences between Algorithm 1 and (4) are coefficients and additional Gaussian noise terms. The coefficients in NAG are set in a deterministic way. However, the coefficients in ALUM could be random values from fixed distributions. The additional noise terms in ALUM come from the Brownian motion term in ULD and are necessary for sampling methods.

Despite the differences, both NAG and ALUM use one gradient at each iteration, and both of them take a big jump along current momentum direction to calculate the gradient instead of directly computing the gradient at current iterate.

4.2 Variance-reduced ALUM (VR-ALUM)

In the subsection, we propose variance-reduced stochastic ALUM (VR-ALUM) methods based on two common unbiased [6] variance-reduced techniques: stochastic variance reduced gradient (SVRG) [13] and SAGA [14]. VR-ALUM comes from simply replacing all full gradient in Algorithm 1 with a gradient estimation $\widetilde{\nabla}_k$. We show Algorithm 2 in the Appendix A.6 due to the limit of space.

Next, we briefly introduce these two variance reduction techniques. SVRG utilizes the following gradient estimation (B_k is the batch of k-th iteration and b is the batch size): $\widetilde{\nabla}_k^{\text{SVRG}} = \frac{N}{b}\sum_{i\in B_k}\left(\nabla f_i(\boldsymbol{x}_k^{(e)\widetilde{\nabla}}) - \nabla f_i(\overline{\boldsymbol{x}})\right) + \sum_{i=1}^N \nabla f_i(\overline{\boldsymbol{x}})$. The full gradient $\sum_{i=1}^N \nabla f_i(\overline{\boldsymbol{x}})$ and point $\overline{\boldsymbol{x}}$ are updated after every τ evaluations of $\widetilde{\nabla}_k^{\text{SVRG}}$. We call the hyperparameter τ as epoch length.

SAGA estimates the gradient in the following way, where $\boldsymbol{\phi}_{k+1}^i$ is set as $\boldsymbol{x}_k^{(e)\widetilde{\nabla}}$ if and only if $i \in B_k$, otherwise $\boldsymbol{\phi}_{k+1}^i = \boldsymbol{\phi}_k^i$: $\widetilde{\nabla}_k^{\text{SAGA}} = \frac{N}{b}\sum_{i\in B_k}\left(\nabla f_i(\boldsymbol{x}_k^{(e)\widetilde{\nabla}}) - \nabla f_i(\boldsymbol{\phi}_k^i)\right) + \sum_{i=1}^N \nabla f_i(\boldsymbol{\phi}_k^i)$. SAGA does not re-compute but stores the latest gradient information $\nabla f_i(\boldsymbol{\phi}_k^i)$ for each f_i. Therefore, SAGA does not introduce extra gradient evaluation except for initialization, but has much larger storage requirements.

Both SVRG and SAGA are unbiased, which means $\mathbb{E}_{B_k}\widetilde{\nabla}_k = \nabla f(\boldsymbol{x}_k^{(e)\widetilde{\nabla}})$, where $\mathbb{E}_{B_k}$ means expectation over random batch at k-th iteration. Moreover, both SVRG and SAGA reduce the mean-squared error of gradient estimation and satisfy bounded MSE property proposed in Appendix B.3.

5 Theoretical analysis

We provide non-asymptotic upper bounds on sampling error and discretization error for our methods, including full gradient ALUM and VR-ALUMs. The proof is shown in Appendix B. Throughout this section, we assume $W_2(p_0, p^*) = O(1)\sqrt{d/m}$ when deriving asymptotic results. This means the initialization is not too far away from the target distribution, and can be achieved under multiple setting as discussed in Appendix A.7.

5.1 Convergence analysis of full gradient ALUM

Recall that ALUM can be used for solving two different but related problems: strongly-log-concave sampling and approximating the ULD. We show the upper bound for sampling error in Theorem 1 and the upper bound for approximation error in Theorem 2 separately.

Theorem 1. *Suppose Assumptions 1 to 3 hold. Given an initial distribution $p_0(\boldsymbol{x})$, we initialize ALUM with random $\boldsymbol{x}_0^{(o)}$ based on probability p_0 and random $\boldsymbol{v}_0^{(o)}$ from standard Gaussian distribution. Assume $L = 1$ and let $\gamma = 2$, p_k be the distribution of $\boldsymbol{x}_k^{(o)}$ and p^* be the target distribution. Assume we use step size $h \le \frac{m}{22}$. After running the ALUM for k iterations, we have the following upper bound of sampling error in 2-Wasserstein distance:*

$$W_2(p_k, p^*) \le 2(1 - \frac{mh}{4})^k W_2(p_0, p^*) + 12\sqrt{\frac{h^3 d}{m}}. \quad (5)$$

[6] The reason we choose unbiased variance reduction instead of biased one is that bias accumulates quicker than variance, therefore generates higher overall error.

Table 2: Iteration complexities for full gradient ALUM on both sampling and approximation problem.

Problem	Accuracy	Step size h	Iteration complexity
Sampling	$\varepsilon\sqrt{d/m}$ in W_2	$h = O(\min(\varepsilon^{\frac{2}{3}}, m))$	$\widetilde{O}(\max(\kappa/\varepsilon^{\frac{2}{3}}, \kappa^2))$
Approximating	ε in $\mathbb{L}_2$	$h = O(\min(m^{\frac{2}{3}}\varepsilon^{\frac{2}{3}}d^{-\frac{1}{3}}, m))$	$O(\max(T\kappa^{\frac{2}{3}}\varepsilon^{-\frac{2}{3}}d^{\frac{1}{3}}, T\kappa))$

Theorem 2. *With same assumptions and setup in Theorem 1, we consider $\boldsymbol{X}_{kh}$ which comes from a continuous ULD starting from the same position as $\boldsymbol{x}_0^{(o)}$ with probability 1. We have the following upper bound of discretization error:*

$$\|\boldsymbol{x}_k^{(o)} - \boldsymbol{X}_{kh}\|_{\mathbb{L}_2} \leq 38\sqrt{\frac{h^3}{m}}W_2(p_0, p^*) + 31\sqrt{\frac{h^3 d}{m}}. \tag{6}$$

Remark 1. *The assumption $L = 1$ actually does not limit the availability of the algorithm. For any function $f(\boldsymbol{x})$ with $L \neq 1$, we can define another function $f'(\boldsymbol{x}') = f(\frac{1}{\sqrt{L}}\boldsymbol{x}')$ which satisfies $L = 1$. ALUM with step size $h \leq \frac{m}{22L}$ and initial momentum from the standard Gaussian distribution can be used to sample $\boldsymbol{x}'$ from the distribution $p'(\boldsymbol{x}') \propto \exp(-f'(\boldsymbol{x}'))$. The sample $\boldsymbol{x}$ from distribution $p(\boldsymbol{x}) \propto \exp(-f(\boldsymbol{x}))$ could be obtained by a transform $\boldsymbol{x} = \frac{1}{\sqrt{L}}\boldsymbol{x}'$. This is essentially the same as directly incorporating L into ULD process as in Appendix A.3.*

Thus, we can derive the iteration complexity for both problems. For sampling problem, we define the iteration complexity as the number of iterations K needed to achieve $W_2(p_K, p^*) \leq \varepsilon\sqrt{d/m}$ with certain step size h. For approximating the ULD at a given time point T, we define the iteration complexity as the number of iterations K needed to achieve $\|\boldsymbol{x}_K^{(o)} - \boldsymbol{X}_T\|_{\mathbb{L}_2} \leq \varepsilon$ with step size $h = T/K$. The results are shown in Table 2. Detailed derivations can be found at Appendix A.8.

5.2 Convergence analysis of variance-reduced ALUM (VR-ALUM)

We show the upper bound for sampling error in Theorem 3 and the upper bound for discretization error in Theorem 4 separately.

Theorem 3. *With same assumptions in Theorem 1, we use SVRG-ALUM with epoch length $\tau = \lceil N/b \rceil$ or SAGA-ALUM. We introduce an extra assumption $h^3 \leq \frac{1}{2304c}b^3 m N^{-2}$. We have the following upper bound of sampling error in 2-Wasserstein distance.*

$$W_2(p_k, p^*) \leq 2(1 - \frac{mh}{4})^k W_2(p_0, p^*) + 92\sqrt{\frac{h^3}{m}}\sqrt{c}\frac{N}{b^{\frac{3}{2}}}W_2(p_0, p^*) + (12 + 57\sqrt{c}\frac{N}{b^{\frac{3}{2}}}))\sqrt{\frac{h^3 d}{m}}. \tag{7}$$

The constant c is defined as $c = 1$ for SVRG-ALUM and $c = 2$ for SAGA-ALUM.

Theorem 4. *With the same assumptions in Theorem 3, we consider $\boldsymbol{X}_{kh}$ which comes from a continuous ULD starting from the same position as $\boldsymbol{x}_0^{(o)\widetilde{\nabla}}$ with probability 1. We have the following upper bound of discretization error.*

$$\|\boldsymbol{x}_k^{(o)\widetilde{\nabla}} - \boldsymbol{X}_{kh}\|_{\mathbb{L}_2} \leq (38 + 92\sqrt{c}\frac{N}{b^{\frac{3}{2}}})\sqrt{\frac{h^3}{m}}W_2(p_0, p^*) + (31 + 57\sqrt{c}\frac{N}{b^{\frac{3}{2}}})\sqrt{\frac{h^3 d}{m}}. \tag{8}$$

Remark 2. *Theorems 1 to 4 are specializations of more general results in Appendix B.1, where full gradient, SVRG and SAGA are unified under the framework of bounded MSE property that is defined in Appendix B.3. A unified approach not only simplifies the proof, but also indicates that our analysis could easily generalize to other gradient estimations that satisfy bounded MSE property.*

Similar to the full gradient case, we derive the iteration complexity K in Appendix A.9. Moreover, we define gradient complexity as the number of single component gradient evaluation $\nabla f_i(\boldsymbol{x})$ needed to achieve certain accuracy. We show the results in Table 3 and add the derivations in Appendix A.9. We finally simplify the result by only considering the dependence of d, N, b, and ε.

Corollary 1. *When $b \leq O(N^{\frac{2}{3}})$, the gradient complexity of SAGA-ALUM and SVRG-ALUM for sampling problem is $\widetilde{O}(N + N^{\frac{2}{3}}\varepsilon^{-\frac{2}{3}})$ and their gradient complexity for ULD approximation problem is $O(N + d^{\frac{1}{3}}N^{\frac{2}{3}}\varepsilon^{-\frac{2}{3}})$.*

Table 3: Gradient complexity for SAGA-ALUM and SVRG-ALUM.

Problem	Accuracy	Gradient complexity
Sampling	$\varepsilon\sqrt{d/m}$ in W_2	$\widetilde{O}(N+(b\kappa+N^{\frac{2}{3}}\kappa^{\frac{4}{3}})(1+\varepsilon^{-\frac{2}{3}})+b\kappa^2$
Approximating	ε in $\mathbb{L}_2$	$O(N+T(\kappa b+\kappa^{\frac{1}{3}}N^{\frac{2}{3}})+T\kappa^{\frac{2}{3}}d^{\frac{1}{3}}\varepsilon^{-\frac{2}{3}}(b+N^{\frac{2}{3}}))$

6 Information-based complexity

We first declare our setup for the problem class and accessible information. Then we show information-based lower bound for approximation error and oracle complexity. The proof is shown in Appendix C.

6.1 Setup

Class of possible potential functions: We denote the class of possible potential functions as $\mathcal{U} = \mathcal{U}(d,N,m,L) = \{(f_1,\ldots,f_N)|\boldsymbol{\nabla}^2 f_i(\boldsymbol{x}) \preccurlyeq (L/N)I, mI \preccurlyeq \boldsymbol{\nabla}^2\sum_{i=1}^N f_i(\boldsymbol{x})$ and $\|\mathbb{E}_{p^*}[\boldsymbol{X}]\|_2 \leq \sqrt{d/m}\}$ where $0<m<L$ and $p^*(\boldsymbol{X}) \propto \exp(-\sum_{i=1}^N f_i(\boldsymbol{X}))$.

Besides Assumptions 1 to 3 used in the previous sections, we introduce a new assumption that the target distributions have mean in a ball of constant radius around the origin. This is necessary because the lower bound could be arbitrarily large if the mean is far away from the initialization point.

Solution mapping: We denote the probability space for Brownian motion in the ULD process as $(\mathbb{M},\Sigma,\mathbb{P})$. Then, the true solution of ULD process starting from the origin $\mathbf{0}$ at time T can be denoted as the solution mapping $\boldsymbol{X}_T : (\omega,U) \in (\mathbb{M}\times\mathcal{U}) \mapsto \boldsymbol{X}_T(\omega,U) \in \mathbb{R}^d$.

Gradient oracle: For a given set of potential functions $U=(f_1,\ldots,f_N)$, the single component gradient oracle is $\Upsilon_U : (i,\boldsymbol{x}) \in [N]\times\mathbb{R}^d \mapsto \nabla f_i(\boldsymbol{x}) \in \mathbb{R}^d$.

Brownian oracle: We assume the Brownian motion at a given time $t>0$ could be evaluated with oracle $\boldsymbol{B}_t(\omega)\in\mathbb{R}^d$ for any event $\omega\in\mathbb{M}$. We further assume that the weighted Brownian motion is also admissible. $\boldsymbol{B}_t^{(\theta)}(\omega) = \int_0^T e^{\theta s} d\boldsymbol{B}_s(\omega)$.

Deterministic algorithm: A deterministic algorithm starts from empty information $I_0=()$. At i-th step, one oracle and corresponding parameters are picked by certain procedure. If the gradient oracle is picked, the algorithm will generate an index i and a point $\boldsymbol{x}$. If the weighted gradient oracle is picked, the parameters are order θ for weighted Brownian motion and time t. The picked oracle and parameters are represented by $\phi_i(I_i)$. The evaluation result is represented by $\Upsilon(\phi(I_i),\omega,U)$ where $\omega\in\mathbb{M}$ and $U\in\mathcal{U}$. The picked oracle, parameters, and result will be stored as new information, hence $I_{i+1} = (I_i,\phi(I_i),\Upsilon(\phi(I_i),\omega,U))$.

We consider deterministic algorithms that stop at n-th step. The final estimation is generated with a mapping $Y(I_n)\in\mathbb{R}^d$. We expect $Y(I_n)$ to be as close as possible to true solution $\boldsymbol{X}_T(\omega,U)$.

We denote a deterministic algorithm as a mapping A from $\mathbb{M}\times\mathcal{U}$ to $\mathbb{R}^d$ and $A(\omega,U)=Y(I_n)$ for some ϕ and Y. The family of all such algorithms is denoted by $\mathcal{A}_n^{\text{Det}}$.

Randomized algorithm: We consider another probability space $(\widetilde{\mathbb{M}},\widetilde{\Sigma},\widetilde{\mathbb{P}})$ as the source of randomness. A randomized algorithm A with n steps is a mapping from $\mathbb{M}\times\widetilde{\mathbb{M}}\times\mathcal{U}$ to $\mathbb{R}^d$ such that $A(\cdot,\widetilde{\omega},\cdot)\in\mathcal{A}_n^{\text{Det}}$ for any $\widetilde{\omega}\in\widetilde{\mathbb{M}}$. The family of all such randomized algorithms is denoted by $\mathcal{A}_n$.

Worst error of algorithms: We care about the following worst-case error for any possible algorithms:

$$e^2_{\mathcal{A},\mathcal{U}} := \inf_{A\in\mathcal{A}}\sup_{U\in\mathcal{U}} \mathbb{E}_{\omega\in\mathbb{P}}\mathbb{E}_{\widetilde{\omega}\in\widetilde{\mathbb{P}}}\|\boldsymbol{X}_T(\omega,U) - A(\omega,\widetilde{\omega},U)\|_2^2 \tag{9}$$

We always assume $T>0$ to avoid trivial cases.

6.2 Lower bounds

We first provide lower bounds on worst-case estimation error.

Theorem 5. *When $n < N$ which means that gradient evaluation number is less than components number, we have $e^2_{\mathcal{A}_n,\mathcal{U}} \geq dC_1$, where C_1 is positive and independent of d, N, and n.*

The above theorem is based on the fact that no algorithm can accurately estimate the global minimum point of the sum of quadratic potentials $\sum_{i=1}^{N} f_i(\boldsymbol{x})$ with information from only $N-1$ components.

Theorem 6. *When the gradient evaluation number n is a multiple of N, we have $e^2_{\mathcal{A}_n,\mathcal{U}} \geq dC_2 \frac{N^2}{n^3}$, where C_2 is positive and independent of d, N, and n.*

The method we use to prove the above theorem is to show that an algorithm that uses a limited number of gradient evaluations cannot distinguish a class of perturbed quadratic functions.

Next, we use the above lower bounds on error to derive a lower bound on gradient complexity.

Corollary 2. *For small enough target accuracy ε such that $\varepsilon^2 < dC_1$, in order to achieve $e_{\mathcal{A}_n,\mathcal{U}} \leq \varepsilon$, the minimum number of single component gradient oracle evaluations is $\Omega(N + d^{\frac{1}{3}} N^{\frac{2}{3}} \varepsilon^{-\frac{2}{3}})$.*

This lower bound matches the upper bound in Corollary 1 which indicates that gradient complexity of variance-reduced ALUM for estimating a ULD is optimal in the dependence of d, components number N, and approximation accuracy ε.

7 Optimality

In this section, we discuss in what sense our ALUM is optimal (or not), and point out possible improvements for future work.

Optimal for approximating problem: ALUM can be used for two tasks: (1) estimating a ULD process, (2) sampling from a strongly-log-concave distribution. ALUM is only optimal for the first task, and is not necessarily optimal for the second one. For example, we see in Section 5 that there exists a logarithm factor in the gradient complexity for sampling problem. We believe some proper adaptive step size method could cancel that extra term.

Dependency on κ: ALUM is only optimal on the dependence of d, N, ε, but not optimal in κ dependence. Actually both our method and our analysis may not be optimized for the dependence of κ. Currently, there is no information-based lower bound with clear dependence on condition number κ, therefore no matter how good the dependence on κ is, it is not sufficient to say it is optimal. For sampling problem, it is believed that $O(\min(\kappa, d^2))$ is the "natural barrier" [6] for iterations needed for achieving $W_2 \leq \varepsilon\sqrt{d/m}$ with $\varepsilon = 1/2$. Currently, the best dependence on κ is achieved by RMM with $O(\kappa^{7/6})$. For ALUM, the maximum dependence is $O(\kappa^2)$. This dependence is worse for two reasons. First, the analysis is not optimized for κ. Based on the analysis of bias and variance in Appendix A.10, we conjecture that the dependence could be improved to $O(\kappa^{3/2})$. Second, the method is not optimized for κ. We save one extra gradient compared to RMM, at the price of a slightly increased bias. This degenerates the dependence of κ.

Despite the max dependence order being larger than 1, in the high-precision regime, when ε is small enough, the term $\kappa/\varepsilon^{\frac{2}{3}}$ is dominant, therefore, both full-gradient ALUM and full-gradient RMM achieve $O(\kappa)$ dependence.

We note the complexity for VR-ALUM increases the dependence of κ to $\kappa^{4/3}$ in high-precision regime. We conjecture that this is an artifact of error-based analysis compared to momentum-based analysis, and could be improved by some tighter analysis.

Assumptions: Finally, we point out that our method and analysis are based on Assumptions 1 to 3 and the gradient oracle. It is natural to obtain better algorithm by introducing new assumptions or new oracle.

Many higher order integrators [8, 9] leverage higher order smoothness assumption to reduce discretization error. Assumptions on structure of potential [28] have also been shown to make acceleration possible together with high order diffusion process. Apart from the gradient oracle, many Metropolis-adjusted algorithms [24, 26] leverage zeroth-order oracle to achieve linear convergence. Second order oracle [17] has also been incorporated into estimating ULD.

8 Experiments

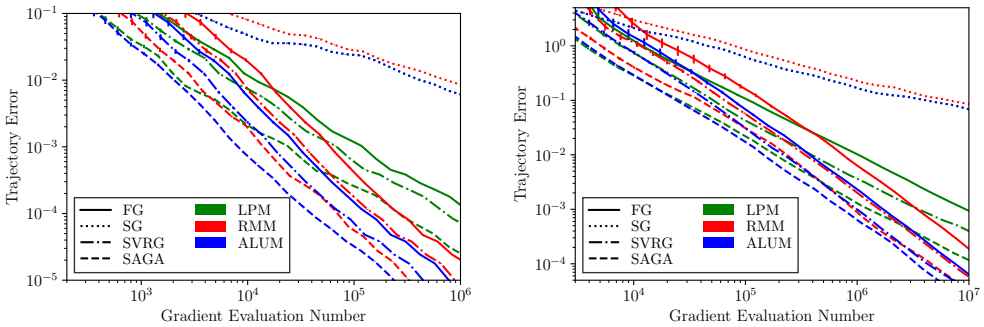

(a) Gaussian model

(b) Logistic regression on australian dataset

Figure 1: Trajectory error for different algorithms[7]. The vertical lines are the error bar. FG means full gradient, SG means stochastic gradient.

In this section, we compare different algorithms for estimating a ULD process on both Gaussian model and Bayesian logistic regression model. For the Gaussian model, the potential is defined as:

$$f_i(\boldsymbol{x}) = \frac{1}{2N}(\boldsymbol{d}_i - \boldsymbol{x})^\top \Sigma^{-1}(\boldsymbol{d}_i - \boldsymbol{x})\,, \tag{10}$$

where $\boldsymbol{d}_i$ and Σ is generated randomly to satisfy $d = 5$,$N = 100$,$m = 1$ and $L = 10$. For logistic regression model, the potential is:

$$f_i(\boldsymbol{x}) = \frac{m}{2N}\|\boldsymbol{x}\|_2^2 + \sum_{i=1}^{N} \log(1 + \exp(-y_i \boldsymbol{a}_i^\top \boldsymbol{x}))\,, \tag{11}$$

where m is set such that $\kappa = 10^4$ and y_i, $\boldsymbol{a}_i$ are data points in australian dataset from LIBSVM [32].

We calculate the trajectory error which is defined as $\frac{1}{K}\sum_{i=1}^{K}\sqrt{\|\boldsymbol{x}_k - \boldsymbol{x}_k'\|_2^2 + \|\boldsymbol{v}_k - \boldsymbol{v}_k'\|_2^2}$, where $\boldsymbol{x}_k$ and $\boldsymbol{v}_k$ are generated by ALUM, VR-ALUMs or other algorithms. $\boldsymbol{x}_k'$ and $\boldsymbol{v}_k'$ come from a reference path that is very close to true solution. We specify how we generate this reference path in Appendix D.1. The reason for us to average the error along the path instead of just reporting error at the final iterate is that we need more data points to reduce the variance.

Figure 1 shows the error for ALUM, LPM, and RMM with full gradient, stochastic gradient, SVRG and SAGA.[8] The detailed setup can be found in Appendix D.2. We summarize the messages in Figure 1 as follows:

- SAGA-ALUM achieves the best efficiency in the sense that with same number evaluations of single component gradient $\nabla f_i(\boldsymbol{x})$, SAGA-ALUM has smaller discretization error than any other algorithms. Results on more dataset are shown in Appendix D.3.
- Variance reduced algorithms constantly outperform full gradient algorithm of the same type by a large margin.
- For full gradient method, the discretization error of ALUM and RMM has similar asymptotic dependence on gradient evaluation number, and they are better than LPM. This phenomenon will be shown clearer in Figure 2.
- ALUM achieves constant acceleration compared to RMM by saving one gradient evaluation per iteration.

[7]Most of the error bars are too small to be visible. The SG-ALUM and SG-LPM highly overlap.

[8]Currently there is no theoretical result for RMM with stochastic gradient, SVRG or SAGA. We also didn't provide a theoretical result for ALUM with stochastic gradient. However, this doesn't prevent us from evaluating them experimentally.

We also show the relationship between discretization error and step size in Figure 2. Only full gradient method are shown here due to the limit of space, and more results for VR-ALUMs are shown in Appendix D.4.

Our analysis in Theorem 2 gives upper bound of discretization error of ALUM as $O(h^{3/2})$. Figure 2 shows that our analysis is tight. Moreover, the discretization error of ALUM is almost the same as RMM. Due to the fact that ALUM requires only half gradient evaluations per step than RMM, ALUM achieves better efficiency.

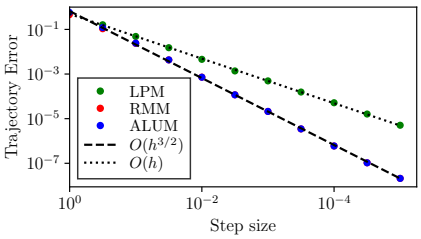

Figure 2: Discretization error of full gradient methods on australian dataset.[9]

Next, we discuss the effect of batch size. According to our theory in Corollary 1, our method is not sensitive to this hyperparameter introduced by SAGA or SVRG when batch size is relatively small, as the gradient complexity remains the same for $b = O(N^{2/3})$. We verify that in Figure 3, where the sampling efficiency is almost same for small batch sizes, and only deteriorate for very large batch size. We give further discussion on why our method is not sensitive to step size in Appendix D.5.

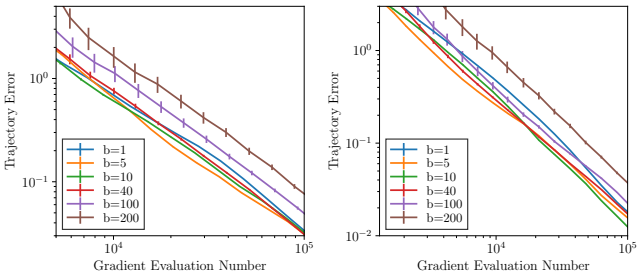

(a) SVRG-ALUM (b) SAGA-ALUM

Figure 3: Discretization error for SVRG-ALUM and SAGA-ALUM with different batch sizes on australian dataset.

Finally, we apply ALUM and VR-ALUMs to sample from a target distribution in Appendix D.6.

9 Conclusion

In this paper, we propose a class of MCMC methods for finite sum form of strongly-convex potential. Our methods are proven to be optimal in the sense that the discretization error has the best possible asymptotic dependence on dimension, number of potential summands, and number of gradient evaluations. Experiments on both synthetic and real data verify the superior performance of our algorithm. We also discuss possible improvements for future work.

Acknowledgments and Disclosure of Funding

This work was partially supported by NSF IIS 1845666, 1852606, 1838627, 1837956, 1956002, OIA 2040588.

References

[1] Andrew Gelman, John B Carlin, Hal S Stern, David B Dunson, Aki Vehtari, and Donald B Rubin. *Bayesian data analysis*. CRC press, 2013.

[2] Daniel Russo, Benjamin Van Roy, Abbas Kazerouni, Ian Osband, and Zheng Wen. A tutorial on thompson sampling. *arXiv preprint arXiv:1707.02038*, 2017.

[3] Deepak Ramachandran and Eyal Amir. Bayesian inverse reinforcement learning. In *IJCAI*, volume 7, pages 2586–2591, 2007.

[4] Peter E Kloeden and Eckhard Platen. *Numerical solution of stochastic differential equations*, volume 23. Springer Science & Business Media, 2013.

[5] Xiang Cheng, Niladri S. Chatterji, Peter L. Bartlett, and Michael I. Jordan. Underdamped langevin mcmc: A non-asymptotic analysis. In *Proceedings of the 31st Conference On Learning Theory*, volume 75, pages 300–323, 2018.

[9] The ALUM and RMM highly overlap.

[6] Ruoqi Shen and Yin Tat Lee. The randomized midpoint method for log-concave sampling. In *Advances in Neural Information Processing Systems*, volume 32, 2019.

[7] Benedict Leimkuhler, Charles Matthews, and Gabriel Stoltz. The computation of averages from equilibrium and nonequilibrium langevin molecular dynamics. *IMA Journal of Numerical Analysis*, 36(1):13–79, 2016.

[8] GN Milstein and Michael V Tretyakov. Quasi-symplectic methods for langevin-type equations. *IMA journal of numerical analysis*, 23(4):593–626, 2003.

[9] James Foster, Terry Lyons, and Harald Oberhauser. The shifted ode method for underdamped langevin mcmc. *arXiv preprint arXiv:2101.03446*, 2021.

[10] Yu Cao, Jianfeng Lu, and Lihan Wang. Complexity of randomized algorithms for underdamped langevin dynamics. *arXiv preprint arXiv:2003.09906*, 2020.

[11] Difan Zou, Pan Xu, and Quanquan Gu. Stochastic variance-reduced hamilton monte carlo methods. In *Proceedings of the 35th International Conference on Machine Learning*, volume 80, pages 6023–6032, 2018.

[12] Zhize Li, Tianyi Zhang, Shuyu Cheng, Jun Zhu, and Jian Li. Stochastic gradient hamiltonian monte carlo with variance reduction for bayesian inference. *Machine Learning*, 108(8):1701–1727, 2019.

[13] Rie Johnson and Tong Zhang. Accelerating stochastic gradient descent using predictive variance reduction. In *Advances in neural information processing systems*, pages 315–323, 2013.

[14] Aaron Defazio, Francis Bach, and Simon Lacoste-Julien. Saga: A fast incremental gradient method with support for non-strongly convex composite objectives. In *Advances in neural information processing systems*, pages 1646–1654, 2014.

[15] Alain Durmus and Eric Moulines. High-dimensional bayesian inference via the unadjusted langevin algorithm. *Bernoulli*, 25(4A):2854–2882, 2019.

[16] Arnak Dalalyan. Further and stronger analogy between sampling and optimization: Langevin monte carlo and gradient descent. In *Conference on Learning Theory*, pages 678–689, 2017.

[17] Arnak S Dalalyan and Lionel Riou-Durand. On sampling from a log-concave density using kinetic langevin diffusions. *Bernoulli*, 26(3):1956–1988, 2020.

[18] Niladri Chatterji, Nicolas Flammarion, Yian Ma, Peter Bartlett, and Michael Jordan. On the theory of variance reduction for stochastic gradient monte carlo. In *Proceedings of the 35th International Conference on Machine Learning*, pages 764–773, 2018.

[19] Claude JP Bélisle, H Edwin Romeijn, and Robert L Smith. Hit-and-run algorithms for generating multivariate distributions. *Mathematics of Operations Research*, 18(2):255–266, 1993.

[20] László Lovász and Miklós Simonovits. Random walks in a convex body and an improved volume algorithm. *Random structures & algorithms*, 4(4):359–412, 1993.

[21] Gareth O Roberts and Richard L Tweedie. Geometric convergence and central limit theorems for multidimensional hastings and metropolis algorithms. *Biometrika*, 83(1):95–110, 1996.

[22] Kerrie L Mengersen and Richard L Tweedie. Rates of convergence of the hastings and metropolis algorithms. *Annals of Statistics*, 24(1):101–121, 1996.

[23] László Lovász and Santosh Vempala. The geometry of logconcave functions and sampling algorithms. *Random Structures & Algorithms*, 30(3):307–358, 2007.

[24] Gareth O Roberts and Richard L Tweedie. Exponential convergence of langevin distributions and their discrete approximations. *Bernoulli*, 2(4):341–363, 1996.

[25] Gareth O Roberts and Jeffrey S Rosenthal. Optimal scaling of discrete approximations to langevin diffusions. *Journal of the Royal Statistical Society: Series B (Statistical Methodology)*, 60(1):255–268, 1998.

[26] Raaz Dwivedi, Yuansi Chen, Martin J Wainwright, and Bin Yu. Log-concave sampling: Metropolis-hastings algorithms are fast! In *Conference on Learning Theory*, pages 793–797, 2018.

[27] G Parisi. Correlation functions and computer simulations. *Nuclear Physics B*, 180(3):378–384, 1981.

[28] Wenlong Mou, Yi-An Ma, Martin J Wainwright, Peter L Bartlett, and Michael I Jordan. High-order langevin diffusion yields an accelerated mcmc algorithm. *Journal of Machine Learning Research*, 22(42):1–41, 2021.

[29] Yi-An Ma, Tianqi Chen, and Emily B. Fox. A complete recipe for stochastic gradient mcmc. In *Proceedings of the 28th International Conference on Neural Information Processing Systems - Volume 2*, page 2917–2925, 2015.

[30] Yurii Nesterov. *Lectures on convex optimization*, volume 137. Springer, 2018.

[31] Ilya Sutskever, James Martens, George Dahl, and Geoffrey Hinton. On the importance of initialization and momentum in deep learning. In *International conference on machine learning*, pages 1139–1147, 2013.

[32] Chih-Chung Chang and Chih-Jen Lin. Libsvm: a library for support vector machines. *ACM transactions on intelligent systems and technology (TIST)*, 2(3):1–27, 2011.

[33] Simon Duane, Anthony D Kennedy, Brian J Pendleton, and Duncan Roweth. Hybrid monte carlo. *Physics letters B*, 195(2):216–222, 1987.

[34] Yi-An Ma, Niladri Chatterji, Xiang Cheng, Nicolas Flammarion, Peter Bartlett, and Michael I Jordan. Is there an analog of nesterov acceleration for mcmc? *arXiv preprint arXiv:1902.00996*, 2019.

[35] Arnak S Dalalyan and Avetik Karagulyan. User-friendly guarantees for the langevin monte carlo with inaccurate gradient. *Stochastic Processes and their Applications*, 129(12):5278–5311, 2019.

A Extra discussions on ULD

A.1 Background

In this section, we introduce several such Markov chains as discretization of certain continuous stochastic processes and we roughly analyze discretization error of these methods with pointing out the bottleneck.

The simplest and most widely used process is the Langevin diffusion (LD) defined as following SDE:

$$d\boldsymbol{X}_t = -\nabla f(\boldsymbol{X}_t)dt + \sqrt{2}d\boldsymbol{B}_t\,, \tag{12}$$

where $\boldsymbol{B}_t$ is the standard Brownian motion. It is known that distribution of $\boldsymbol{X}_t$ converges to the exact target distribution exponentially [24]. The unadjusted Langevin algorithm (ULA) comes from applying Euler-Maruyama discretization [4] directly to LD. The update rule is:

$$\boldsymbol{x}_{k+1} = \boldsymbol{x}_k + \nabla f(\boldsymbol{x}_k)h + \sqrt{2}\boldsymbol{e}_k,\ \boldsymbol{e}_k = \int_0^t d\boldsymbol{B}_t \sim \mathcal{N}(\boldsymbol{0}, hI), \tag{13}$$

where $\boldsymbol{e}_k$ is standard Gaussian vector, and h is the step size. Compared with the ground-truth update $\boldsymbol{X}_h = \boldsymbol{x}_k - \int_0^h \nabla f(\boldsymbol{X}_t)dt + \sqrt{2}\int_0^t d\boldsymbol{B}_t$, where $\boldsymbol{X}_t$ is an LD starting from the $\boldsymbol{x}_k$, the discretization introduces an error $\sqrt{\mathbb{E}\|\boldsymbol{x}_{k+1} - \boldsymbol{X}_h\|_2^2} = O(h^{\frac{3}{2}})$ in each step. After accumulating this error in $\frac{T}{h}$ iterations, the final estimation error is $O(h^{\frac{1}{2}})$. Therefore, in order to sample from the distribution at accuracy ε, we need to select step size $h = O(\varepsilon^2)$, sampling time $T = O(\log(\varepsilon^{-1}))$ and the final iteration complexity is $T/h = \widetilde{O}(\varepsilon^{-2})$.

The analysis of ULA shows that the discretization error directly affects the sampling error, thus determines the sampling efficiency [15, 16]. More accurate approximation of the continuous diffusion process is desired.

The trajectory for LD is highly non-smooth, therefore is hard to approximate. In order to solve this problem, underdamped Langevin diffusion (ULD) [33] was proposed with using the following SDE:

$$d\boldsymbol{X}_t = \boldsymbol{V}_t dt,\ d\boldsymbol{V}_t = -\nabla f(\boldsymbol{X}_t)dt - \gamma \boldsymbol{V}_t dt + \sqrt{2\gamma}d\boldsymbol{B}_t. \tag{14}$$

We note that in previous works [5, 17, 34, 6], ULD shows up in multiple different forms which are essentially same up to a linear transformation. More detailed discussions can be found in Appendix A.3.

The ULD converges to extended distribution $p^*(\boldsymbol{x}, \boldsymbol{v}) \propto \exp(-f(\boldsymbol{x}) - \frac{1}{2}\|\boldsymbol{v}\|_2^2)$. The noise is injected into an additional momentum term $\boldsymbol{V}_t$ and then propagates to $\boldsymbol{X}_t$, therefore the trajectory of $\boldsymbol{X}_t$ is much smoother and easier to approximate.

Cheng et at. [5] introduced the LPM discretization scheme to leverage this smoothness. In order to illustrate the method, we first give the integral form of ULD as follows. The detailed derivation is shown in Appendix A.4.

$$\begin{aligned}
\boldsymbol{X}_t &= \boldsymbol{X}_0 + \psi_1(s)\boldsymbol{V}_0 - \int_0^t \psi_1(t-s)\nabla f(\boldsymbol{X}_s)ds + \boldsymbol{e}_{x,[0,t]}, e \\
\boldsymbol{V}_t &= \psi_0(t)\boldsymbol{V}_0 - \int_0^t \psi_0(t-s)\nabla f(\boldsymbol{X}_s)ds + \boldsymbol{e}_{v,[0,t]}.
\end{aligned} \tag{15}$$

$$\boldsymbol{e}_{x,[0,t]} = \sqrt{2\gamma}\int_0^t \psi_1(t-s)d\boldsymbol{B}_s,\ \ \boldsymbol{e}_{v,[0,t]} = \sqrt{2\gamma}\int_0^t \psi_0(t-s)d\boldsymbol{B}_s. \tag{16}$$

The auxiliary function $\psi_i(x)$ is defined as:

$$\psi_0(t) = e^{-\gamma t}, \psi_i(t) = \int_0^t \psi_{i-1}(u)du, \forall i \geq 1. \tag{17}$$

The basic idea of LPM is to estimate $\nabla f(\boldsymbol{X}_s)$ in (15) with gradient at initial point $\nabla f(\boldsymbol{X}_0)$. This gives following approximation at time point h.

$$\boldsymbol{X}_h^{(l)} = \boldsymbol{X}_0 + \psi_1(h)\boldsymbol{V}_0 - \psi_2(h)\nabla f(\boldsymbol{X}_0) + \boldsymbol{e}_{x,[0,h]},\quad \boldsymbol{V}_h^{(l)} = \psi_0(h)\boldsymbol{V}_0 - \psi_1(h)\nabla f(\boldsymbol{X}_0) + \boldsymbol{e}_{v,[0,h]}. \tag{18}$$

This gives $O(h^2)$ error in single step which is lower than ULA. After accumulation of T/h iterations, the discretization error is $O(h)$. With similar argument like ULA, the iteration complexity is $\widetilde{O}(\varepsilon^{-1})$.

Randomized midpoint method (RMM) [6], which enjoys best iteration complexity among all existing full gradient based sampling algorithms, tries to estimate the integration $\int_0^t \psi_i(t-s)\nabla f(\boldsymbol{X}_s)ds$ with a randomized midpoint $t\psi_i(t-at)\nabla f(\boldsymbol{X}_{at})$ where a is a uniform random variable in $[0,1]$. This is actually an unbiased estimation itself. However, $\nabla f(\boldsymbol{X}_{at})$ still cannot be calculated explicitly. Therefore, RMM uses LPM to calculate $\nabla f(\boldsymbol{X}_{at}^{(l)})$ as a proxy, which introduces bias into estimation. The final formula of RMM is shown as below:

$$\begin{aligned}\boldsymbol{X}_h^{(r)} &= \boldsymbol{X}_0 + \psi_1(h)\boldsymbol{V}_0 - h\psi_1(h-ah)\nabla f(\boldsymbol{X}_{ah}^{(l)}) + \boldsymbol{e}_{x,[0,h]},\\ \boldsymbol{V}_h^{(r)} &= \psi_0(h)\boldsymbol{V}_0 - h\psi_0(h-ah)\nabla f(\boldsymbol{X}_{ah}^{(l)}) + \boldsymbol{e}_{v,[0,h]},\\ \boldsymbol{X}_{ah}^{(l)} &= \boldsymbol{X}_0 + \psi_1(ah)\boldsymbol{V}_0 - \psi_2(ah)\nabla f(\boldsymbol{X}_0) + \boldsymbol{e}_{x,[0,ah]}.\end{aligned} \tag{19}$$

The bias and variance for single step can be controlled as $\sqrt{\mathbb{E}\|\mathbb{E}_a\boldsymbol{Z}_h^{(r)} - \boldsymbol{Z}_h\|_2^2} = O(h^4)$ and $\mathbb{E}\|\boldsymbol{Z}_h^{(r)} - \mathbb{E}_a\boldsymbol{Z}_h^{(r)}\|_2^2 = O(h^4)$ where $\boldsymbol{Z}$ is a vector combining both position $\boldsymbol{X}$ and momentum $\boldsymbol{V}$. After accumulation of T/h iterations, the total bias is $O(h^3)$, total variance is $O(h^3)$, and the error coming from variance is $O(h^{\frac{3}{2}})$. The accumulated bias for RMM is much smaller than LPM and the newly introduced variance is the bottleneck. Therefore, the final discretization error is $O(h^{\frac{3}{2}})$ and iteration complexity is $\widetilde{O}(\varepsilon^{-\frac{2}{3}})$.

A.2 Comparison with CV-ULD

Chatterji et al. [18] shows a gradient complexity for CV-ULD as $\widetilde{O}(N + d^{\frac{3}{2}}/(N^{\frac{3}{2}}\varepsilon^3))$, which is seemingly different from what is shown in Table 1. This is because (1) Chatterji et al. [18] defines mixing time as the number of steps to achieve $W_2(p_K, p^*) \le \varepsilon$ instead of $W_2(p_K, p^*) \le \varepsilon\sqrt{d/m}$, which is used throughout this paper. (2) Chatterji et al. [18] assumes gradient Lipschitz constant L (it actually uses letter M) and strongly convex constant m both scale linearly with the number of samples N.

In order to see that after adapting to the same setup, the $\widetilde{O}(N+\varepsilon^{-3})$ gradient complexity for CV-ULD is worse than $\widetilde{O}(N + N^{\frac{2}{3}}\varepsilon^{-\frac{2}{3}})$ gradient complexity for SVRG-ALUM and SAGA-ALUM, we just need to show that $\frac{7}{9}N + \frac{2}{9}\varepsilon^{-3} \ge N^{\frac{7}{9}}(\varepsilon^{-3})^{\frac{2}{9}} \ge N^{\frac{2}{3}}\varepsilon^{-\frac{2}{3}}$ and notice that the last inequality directly relaxes the order of N, therefore the inequality is asymptotically not tight.

A.3 Equivalent forms of ULD

The underdamped Langevin dynamics has many commonly used forms, and they only differ with a linear transformation. We next give two examples and corresponding linear transforms to connect them with simplified form in (14).

A.3.1 Form 1

$$\begin{gathered}d\overline{\boldsymbol{X}}_{\bar{t}} = \xi\overline{\boldsymbol{V}}_{\bar{t}}d\bar{t},\ d\overline{\boldsymbol{V}}_{\bar{t}} = -\boldsymbol{\nabla}\overline{f}(\overline{\boldsymbol{X}}_{\bar{t}})d\bar{t} - \gamma\xi\overline{\boldsymbol{V}}_{\bar{t}}d\bar{t} + \sqrt{2\gamma}d\overline{\boldsymbol{B}}_{\bar{t}}\\ t = \xi\bar{t}, \boldsymbol{X}_t = \sqrt{\xi}\overline{\boldsymbol{X}}_{\bar{t}}, \boldsymbol{V}_t = \sqrt{\xi}\overline{\boldsymbol{V}}_{\bar{t}}, \boldsymbol{B}_t = \sqrt{\xi}\overline{\boldsymbol{B}}_{\bar{t}}, f(\sqrt{\xi}\overline{\boldsymbol{X}}) = \overline{f}(\overline{\boldsymbol{X}})\end{gathered} \tag{20}$$

$\overline{\boldsymbol{B}}_{\bar{t}}$ is still standard Brownian motion in the sense that $\mathbb{E}\|\overline{\boldsymbol{B}}_{\bar{t}}\|_2^2 = \bar{t}^2$. The stationary distribution is

$$p^*(\overline{\boldsymbol{x}}, \overline{\boldsymbol{v}}) \propto \exp(-\overline{f}(\overline{\boldsymbol{x}}) - \frac{\xi}{2}\|\overline{\boldsymbol{v}}\|_2^2).$$

A.3.2 Form 2

$$\begin{gathered}d\boldsymbol{X}'_{t'} = \boldsymbol{V}'_{t'}dt',\ d\boldsymbol{V}'_{t'} = -u\boldsymbol{\nabla}f'(\boldsymbol{X}'_{t'})dt' - \gamma\boldsymbol{V}'_{t'}dt' + \sqrt{2\gamma u}d\boldsymbol{B}'_{t'}\\ t = t', \boldsymbol{X}_t = \frac{1}{\sqrt{u}}\boldsymbol{X}'_{t'}, \boldsymbol{V}_t = \frac{1}{\sqrt{u}}\boldsymbol{V}'_{t'}, \boldsymbol{B}_t = \boldsymbol{B}'_{t'}, f(\frac{1}{\sqrt{u}}\boldsymbol{X}') = f'(\boldsymbol{X}'),\end{gathered} \tag{21}$$

$\boldsymbol{B}'_{t'}$ is still standard Brownian motion in the sense that $\mathbb{E}\|\boldsymbol{B}'_{t'}\|_2^2 = {t'}^2$. The stationary distribution is

$$p^*(\boldsymbol{x}', \boldsymbol{v}') \propto \exp(-f'(\boldsymbol{x}') - \frac{1}{2u}\|\boldsymbol{v}'\|_2^2).$$

A.4 The integral form of ULD

$$\begin{aligned}
\boldsymbol{X}_t &= \boldsymbol{X}_0 + \int_0^t \boldsymbol{V}_s ds \\
&= \boldsymbol{X}_0 + \int_0^t \psi_0(s)\boldsymbol{V}_0 ds - \int_0^t \int_0^u \psi_0(u-s)\nabla f(\boldsymbol{X}_s) ds du + \sqrt{2\gamma}\int_0^t \int_0^u \psi_0(u-s) d\boldsymbol{B}_s du \\
&= \boldsymbol{X}_0 + \psi_1(s)\boldsymbol{V}_0 - \int_0^t \psi_1(t-s)\nabla f(\boldsymbol{X}_s) ds + \sqrt{2\gamma}\int_0^t \psi_1(t-s) d\boldsymbol{B}_s \\
\boldsymbol{V}_t &= e^{-\gamma t}\boldsymbol{V}_0 - \int_0^t e^{-\gamma(t-s)}\nabla f(\boldsymbol{X}_s) ds + \sqrt{2\gamma}\int_0^t e^{-\gamma(t-s)} d\boldsymbol{B}_s \\
&= \psi_0(t)\boldsymbol{V}_0 - \int_0^t \psi_0(t-s)\nabla f(\boldsymbol{X}_s) ds + \sqrt{2\gamma}\int_0^t \psi_0(t-s) d\boldsymbol{B}_s
\end{aligned} \tag{22}$$

A.5 Covariance of noise term in ALUM

For different k, $\boldsymbol{e}_{x,[0,h],k}$, $\boldsymbol{e}_{v,[0,h],k}$, $\boldsymbol{e}_{x,[0,a_k h],k}$ are independent with each other. For same k, the covaraince between these Gaussian random vector is as follows.

$$\begin{aligned}
\mathbb{E}\Big[\boldsymbol{e}_{x,[0,t]}\boldsymbol{e}_{x,[0,t]}^\top\Big] &= 2\gamma I\int_0^t \psi_1(s)^2 ds = \frac{2\gamma t - 3 + 4\exp(-\gamma t) - \exp(-2\gamma t)}{\gamma^2} I \\
\mathbb{E}\Big[\boldsymbol{e}_{x,[0,t]}\boldsymbol{e}_{v,[0,t]}^\top\Big] &= 2\gamma I\int_0^t \psi_1(s)\psi_0(s) ds = \frac{4\sinh^2\frac{\gamma t}{2}\exp(-\gamma t)}{\gamma} I \\
\mathbb{E}\Big[\boldsymbol{e}_{v,[0,t]}\boldsymbol{e}_{v,[0,t]}^\top\Big] &= 2\gamma I\int_0^t \psi_0(s)^2 ds = (1-\exp(-2\gamma t))I \\
\mathbb{E}\Big[\boldsymbol{e}_{x,[0,t]}\boldsymbol{e}_{x,[0,at]}^\top\Big] &= 2\gamma I\int_0^{at} \psi_1(t-s)\psi_1(at-s) ds = \frac{2a\gamma t - 2 - 4\exp(-\gamma t)\sinh^2\frac{a\gamma t}{2} + 2\exp(-a\gamma t)}{\gamma^2} I \\
\mathbb{E}\Big[\boldsymbol{e}_{v,[0,t]}\boldsymbol{e}_{x,[0,at]}^\top\Big] &= 2\gamma I\int_0^{at} \psi_0(t-s)\psi_1(at-s) ds = \frac{4\sinh^2\frac{a\gamma t}{2}\exp(-\gamma t)}{\gamma} I \\
\mathbb{E}\Big[\boldsymbol{e}_{x,[0,at]}\boldsymbol{e}_{x,[0,at]}^\top\Big] &= 2\gamma I\int_0^{at} \psi_1(at-s)^2 ds = \frac{2a\gamma t - 3 + 4\exp(-a\gamma t) - \exp(-2a\gamma t)}{\gamma^2} I
\end{aligned} \tag{23}$$

A.6 Full description of VR-ALUM

We give full description of VR-ALUM in Algorithm 2.

A.7 Initialization

In order to establish asymptotic convergence guarantee, we need to ensure that the initialization is not too far away from the target distribution. We introduce several popular initializations below that all can be summarized as $W_2(p_0, p^*) = O(1)\sqrt{d/m}$.

Start from optimal The global optimal could be chosen as initial point [6]. We could control the initial distance as $W_2(\delta_{\boldsymbol{x}^*}, p^*) \leq \sqrt{\frac{d}{m}}$.

[10] SAGA could be implemented in a cleverer way by caching the gradient, sum of gradient, and don't store $\boldsymbol{\phi}_k^i$.

Algorithm 2: Variance reduced ALUM Method

Input: Initial point $(\boldsymbol{x}_0^{(o)\widetilde{\nabla}}, \boldsymbol{v}_0^{(o)\widetilde{\nabla}})$, parameter γ, iteration number K batch size b, and step size $h > 0$.
for $k = 0$ **to** $K - 1$ **do**
  Randomly sample a_k uniformly from $[0, 1]$;
  Generate $\boldsymbol{e}_{x,[0,h],k}$, $\boldsymbol{e}_{v,[0,h],k}$, $\boldsymbol{e}_{x,[0,a_k h],k}$ according to Appendix A.5;
  $\boldsymbol{x}_k^{(e)\widetilde{\nabla}} = \boldsymbol{x}_k^{(o)\widetilde{\nabla}} + \psi_1(a_k h)\boldsymbol{v}_k^{(o)\widetilde{\nabla}} + \boldsymbol{e}_{x,[0,a_k h],k}$;
  Randomly sample without replacement a batch B_k of size b from $[N]$;
  if SVRG is used **then**
    if $k \mod \tau = 0$ **then**
      $\overline{\boldsymbol{x}} \leftarrow \boldsymbol{x}_k^{(e)\widetilde{\nabla}}$;
    end if
    $\widetilde{\nabla}_k = \frac{N}{b}\sum_{i\in B_k}(\nabla f_i(\boldsymbol{x}_k^{(e)\widetilde{\nabla}}) - \nabla f_i(\overline{\boldsymbol{x}})) + \sum_{i=1}^N \nabla f_i(\overline{\boldsymbol{x}})$;
  else if SAGA is used[10] **then**
    $\widetilde{\nabla}_k = \frac{N}{b}\sum_{i\in B_k}(\nabla f_i(\boldsymbol{x}_k^{(e)\widetilde{\nabla}}) - \nabla f_i(\boldsymbol{\phi}_k^i)) + \sum_{i=1}^N \nabla f_i(\boldsymbol{\phi}_k^i)$;
    for $i \in B_k$ **do**
      $\boldsymbol{\phi}_{k+1}^i = \boldsymbol{x}_k^{(e)\widetilde{\nabla}}$;
    end for
    for $i \notin B_k$ **do**
      $\boldsymbol{\phi}_{k+1}^i = \boldsymbol{\phi}_k^i$;
    end for
  end if
  $\boldsymbol{x}_{k+1}^{(o)\widetilde{\nabla}} = \boldsymbol{x}_k^{(o)\widetilde{\nabla}} + \psi_1(h)\boldsymbol{v}_k^{(o)\widetilde{\nabla}} - h\psi_1(h - a_k h)\widetilde{\nabla}_k + \boldsymbol{e}_{x,[0,h],k}$;
  $\boldsymbol{v}_{k+1}^{(o)\widetilde{\nabla}} = \psi_0(h)\boldsymbol{v}_k^{(o)\widetilde{\nabla}} - h\psi_0(h - a_k h)\widetilde{\nabla}_k + \boldsymbol{e}_{v,[0,h],k}$;
end for
Output: $\boldsymbol{x}_K^{(o)\widetilde{\nabla}}$.

Start from neighbor of optimal A starting point x_0 could be a fixed point that is not far away from global optimal [5] such that $\|\boldsymbol{x}_0 - \boldsymbol{x}^*\|_2 \le D$. We have $W_2(\delta_{\boldsymbol{x}_0}, p^*) \le \sqrt{\frac{d}{m}} + \gamma D$, therefore, if we can find a point $\boldsymbol{x}_0$ close enough to $\boldsymbol{x}^*$, such that $D = O(1)\sqrt{\frac{d}{m}}$, the assumption $W_2(\delta_{\boldsymbol{x}^*}, p^*) \le \sqrt{\frac{d}{m}}$ could be assured.

We emphasize that the assumption $W_2(p_0, p^*) = O(1)\sqrt{d/m}$ is only introduced to derive asymptotic results. Our non-asymptotic result in Theorems 1 to 4 doesn't use the assumption on the initialization at all. Therefore, our methods don't require a warm start, and non-asymptotic guarantees always hold regardless of what initialization we chose.

A.8 Derivation of iteration complexity for full gradient ALUM

For sampling problem, we choose step size $h = O(\min(\varepsilon^{\frac{2}{3}}, m))$ and run ALUM to estimate ULD at time $T = Kh = O(m^{-1}\log(1/(\varepsilon)))$ where K is the number of steps. According to theorem 1, we could achieve error in 2-Wasserstein distance as $O(\varepsilon\sqrt{\frac{d}{m}})$. Then we have the iteration complexity of full gradient ALUM as $K = \widetilde{O}(\kappa/\varepsilon^{\frac{2}{3}} + \kappa^2)$.

For ULD estimation problem, we just choose $h = O(\min(m^{\frac{2}{3}}\varepsilon^{\frac{2}{3}}d^{-\frac{1}{3}}, m))$, and run the algorithm for $K = T/h$ steps. According to theorem 2, we could achieve error in $\mathbb{L}_2$ distance as $O(\varepsilon)$.

A.9 Derivation of iteration complexity for variance-reduced ALUM

Sampling problem We choose step size $h = O(\varepsilon^{\frac{2}{3}}, m, m^{\frac{1}{3}}\varepsilon^{\frac{2}{3}}bN^{-\frac{2}{3}}, m^{\frac{1}{3}}bN^{-\frac{2}{3}})$. Select $T = O(m^{-1}\log(1/(\varepsilon)))$, then the iteration complexity is $K = T/h = \widetilde{O}(\max(\kappa\varepsilon^{-\frac{2}{3}}, \kappa^2, \kappa^{\frac{4}{3}}\varepsilon^{-\frac{2}{3}}N^{\frac{2}{3}}/b, \kappa^{\frac{4}{3}}N^{\frac{2}{3}}/b))$.

Both SAGA and SVRG requires initialization, which evaluates the full gradient at the beginning. In each iteration, SAGA evaluates b gradients, and SVRG uses $3b$ gradient in average. Therefore, the gradient complexity is

$$\begin{aligned} N + O(b)K =& \widetilde{O}(N + \max(b\kappa\varepsilon^{-\frac{2}{3}}, b\kappa^2, \kappa^{\frac{4}{3}}\varepsilon^{-\frac{2}{3}}N^{\frac{2}{3}}, \kappa^{\frac{4}{3}}N^{\frac{2}{3}})) \\ =& \widetilde{O}(N + \max(b\kappa\varepsilon^{-\frac{2}{3}}, b\kappa, b\kappa^2, \kappa^{\frac{4}{3}}\varepsilon^{-\frac{2}{3}}N^{\frac{2}{3}}, \kappa^{\frac{4}{3}}N^{\frac{2}{3}})) \\ =& \widetilde{O}(N + b\kappa\varepsilon^{-\frac{2}{3}} + b\kappa + b\kappa^2 + \kappa^{\frac{4}{3}}\varepsilon^{-\frac{2}{3}}N^{\frac{2}{3}} + \kappa^{\frac{4}{3}}N^{\frac{2}{3}}) \\ =& \widetilde{O}(N + (b\kappa + N^{\frac{2}{3}}\kappa^{\frac{4}{3}})(1 + \varepsilon^{-\frac{2}{3}}) + b\kappa^2). \end{aligned} \tag{24}$$

If we only consider the dependence of d, N, b and ε, we can see that gradient complexity is $\widetilde{O}(N + N^{\frac{2}{3}}\varepsilon^{-\frac{2}{3}})$ when $b \leq O(N^{\frac{2}{3}})$.

Estimating ULD We first derive the iteration complexity. Step size h has two ε independent upper bound in theorem 4, that is $h \leq \frac{m}{22}$ and $h^3 \leq \frac{1}{13824}b^3mN^{-2}$. We also require the right-hand side of inequality in theorem 4 to be smaller than ε. Therefore, we select $h = O(\min(m, bm^{\frac{1}{3}}N^{-\frac{2}{3}}, m^{\frac{2}{3}}d^{-\frac{1}{3}}\varepsilon^{\frac{2}{3}}, m^{\frac{2}{3}}d^{-\frac{1}{3}}\varepsilon^{\frac{2}{3}}bN^{-\frac{2}{3}}))$ and for a fixed T, we need iteration number as $K = T/h = O(\max(T\kappa, T\kappa^{\frac{1}{3}}N^{\frac{2}{3}}/b, T\kappa^{\frac{2}{3}}d^{\frac{1}{3}}\varepsilon^{-\frac{2}{3}}, \kappa^{\frac{2}{3}}d^{\frac{1}{3}}\varepsilon^{-\frac{2}{3}}N^{\frac{2}{3}}/b))$.

We next derive the gradient complexity.

$$\begin{aligned} N + O(b)K =& O(N + \max(T\kappa b, T\kappa^{\frac{1}{3}}N^{\frac{2}{3}}, T\kappa^{\frac{2}{3}}d^{\frac{1}{3}}\varepsilon^{-\frac{2}{3}}b, T\kappa^{\frac{2}{3}}d^{\frac{1}{3}}\varepsilon^{-\frac{2}{3}}N^{\frac{2}{3}})) \\ =& O(N + T\kappa b + T\kappa^{\frac{1}{3}}N^{\frac{2}{3}} + T\kappa^{\frac{2}{3}}d^{\frac{1}{3}}\varepsilon^{-\frac{2}{3}}b + T\kappa^{\frac{2}{3}}d^{\frac{1}{3}}\varepsilon^{-\frac{2}{3}}N^{\frac{2}{3}}) \\ =& O(N + T(\kappa b + \kappa^{\frac{1}{3}}N^{\frac{2}{3}}) + T\kappa^{\frac{2}{3}}d^{\frac{1}{3}}\varepsilon^{-\frac{2}{3}}(b + N^{\frac{2}{3}})). \end{aligned} \tag{25}$$

If we only consider the dependence of d, N, b and ε, we can see that gradient complexity is $O(N + N^{\frac{2}{3}}d^{\frac{1}{3}}\varepsilon^{-\frac{2}{3}})$ when $b \leq O(N^{\frac{2}{3}})$.

A.10 Conjecture on the tighter κ dependence for ALUM

The maximum upper bound of κ for ALUM is $O(\kappa^2)$. We first provide intuition on how that result is derived.

According to inequality (102), in each step, the approximation error A_k decreases with a multiplier $e^{-\frac{mh}{\gamma}}$. Meanwhile, we introduce $17h^4A_k^2$ amount of variance and h^3A_k amount of bias. In order to balance the decrease and increase in each step to ensure a decrease of error, we first treat error introduced by variance as bias (ignore the useful fact that variance accumulates slower than bias). Then we just need to balance the decrease with multiplier $e^{-\frac{mh}{\gamma}}$ and increases with noise $5h^2A_k$. This indicates $h = O(m)$. In the proof, we require $h \leq \frac{m}{22}$ to establish inequality (103). The maximum step size $h \leq \frac{m}{22}$ shows up in Theorem 1 and produce $O(\kappa^2)$ dependence for ALUM.

If (102) was replaced with some other analysis that doesn't accumulate variance as bias, then we only need to balance decrease and increase as h^3A_k, the upper bound of step size becomes $h = O(m^{1/2})$, and the final iteration complexity has $O(\kappa^{3/2})$ dependence.

We believe a different analysis could achieve the above condition. However, it complicates the proof a lot, and has no effect on our main result, which is optimal dependence on d,N,ε. Therefore, we leave the rigorous theoretical analysis for future work.

A.11 Piecewise noise terms

In this section, we show how to represent $\boldsymbol{e}_{x,[0,nt]}$, $\boldsymbol{e}_{v,[0,nt]}$, $\boldsymbol{e}_{x,[0,ant]}$ as a combination of $\boldsymbol{e}_{x,[it,(i+1)t]}$, $\boldsymbol{e}_{v,[it,(i+1)t]}$, $\boldsymbol{e}_{x,[\lfloor a\rfloor t,at]}$. This allows us to experimentally sample two ULD approximation with different step sizes, but the same realization of Brownian motion.

$$
\begin{aligned}
\boldsymbol{e}_{v,[0,nt]} =& \sqrt{2\gamma}\int_0^{nt} \psi_0(nt-s)d\boldsymbol{B}_s \\
=& \sqrt{2\gamma}\sum_{i=0}^{n-1}\int_{it}^{(i+1)t} \exp(-\gamma(nt-s))d\boldsymbol{B}_s \\
=& \sum_{i=0}^{n-1}\exp(-\gamma(n-i-1)t)\left(\sqrt{2\gamma}\int_{it}^{(i+1)t}\exp(-\gamma((i+1)t-s))d\boldsymbol{B}_s\right) \\
=& \sum_{i=0}^{n-1}\psi_0((n-i-1)t)\boldsymbol{e}_{v,[it,(i+1)t]}
\end{aligned}
\tag{26}
$$

$$
\begin{aligned}
\boldsymbol{e}_{x,[0,nt]} =& \sqrt{2\gamma}\int_0^{nt} \psi_1(nt-s)d\boldsymbol{B}_s \\
=& \sqrt{2\gamma}\sum_{i=0}^{n-1}\int_{it}^{(i+1)t} \psi_1(nt-s)d\boldsymbol{B}_s \\
=& \sqrt{2\gamma}\sum_{i=0}^{n-1}\int_{it}^{(i+1)t} \left(\psi_1((i+1)t-s)+\psi_1((n-i-1)t)\psi_0((i+1)t-s)\right)d\boldsymbol{B}_s \\
=& \sum_{i=0}^{n-1}\left(\boldsymbol{e}_{x,[it,(i+1)t]}+\psi_1((n-i-1)t)\boldsymbol{e}_{v,[it,(i+1)t]}\right)
\end{aligned}
\tag{27}
$$

We assume $0 \le a \le n$.

$$
\begin{aligned}
\boldsymbol{e}_{x,[0,at]} =& \sqrt{2\gamma}\int_0^{at} \psi_1(at-s)d\boldsymbol{B}_s \\
=& \sqrt{2\gamma}\sum_{i=0}^{\lceil a\rceil-1}\int_{it}^{\min(i+1,a)t} \psi_1(nt-s)d\boldsymbol{B}_s \\
=& \sqrt{2\gamma}\sum_{i=0}^{\lceil a\rceil-1}\begin{cases}\int_{it}^{at}\psi_1(at-s)d\boldsymbol{B}_s & i=\lceil a\rceil-1 \\ \int_{it}^{(i+1)t}\left(\psi_1((i+1)t-s)+\psi_1((a-i-1)t)\psi_0((i+1)t-s)\right)d\boldsymbol{B}_s & \text{otherwise}\end{cases} \\
=& \sum_{i=0}^{\lceil a\rceil-1}\begin{cases}\boldsymbol{e}_{x,[\lfloor a\rfloor t,at]} & i=\lceil a\rceil-1 \\ \boldsymbol{e}_{x,[it,(i+1)t]}+\psi_1((a-i-1)t)\boldsymbol{e}_{v,[it,(i+1)t]} & \text{otherwise}\end{cases} \\
=& \boldsymbol{e}_{x,[\lfloor a\rfloor t,at]}+\sum_{i=0}^{\lfloor a\rfloor-1}\left(\boldsymbol{e}_{x,[it,(i+1)t]}+\psi_1((a-i-1)t)\boldsymbol{e}_{v,[it,(i+1)t]}\right)
\end{aligned}
\tag{28}
$$

B Proof of convergence result and discretization error

We first unify the full gradient version and variance-reduced version in appendix B.1, then introduce some basic concepts in appendices B.2 to B.4, then we analyze the sampling error and approximation error in appendices B.5 and B.6.

B.1 Statement of general result

We first formulate a general version for theorem 1 and theorem 3, which uses the bounded MSE property defined in appendix B.3.

Theorem 7. *Suppose we use some unbiased gradient estimation method that satisfies bounded MSE property with parameter Θ. Suppose assumptions 1 to 3 holds. Given an initial distribution $p_0(\boldsymbol{x})$, we initialize an ALUM with random $\boldsymbol{x}_0^{(o)\tilde{\nabla}}$ based on probability p_0 and random $\boldsymbol{v}_0^{(o)\tilde{\nabla}}$ from standard*

Gaussian distribution. Assume $L = 1$ and let $\gamma = 2$, p_k be the distribution of $\boldsymbol{x}_k^{(o)^{\widetilde{\nabla}}}$ and p^* be the target distribution. Assume we use step size $h \leq \frac{m}{11\gamma}$ and $\frac{h^3\Theta}{m} \leq \frac{1}{2304}$. After running the ALUM for k iterations, for some $A_0 \leq \gamma W_2(p_0, p^*)$, we have the following upper bound of sampling error in 2-Wasserstein distance.

$$W_2(p_k, p^*) \leq (1 - \frac{mh}{2\gamma})^k A_0 + 46\sqrt{\frac{h^3}{m}}\sqrt{\Theta}A_0 + (12 + 57\sqrt{\Theta})\sqrt{\frac{h^3}{m}}\sqrt{d}. \tag{29}$$

The next theorem is general version result for theorem 2 and theorem 4.

Theorem 8. *With same assumptions and setup in theorem 7, we consider $\boldsymbol{X}_{kh}$ which comes from a continuous ULD starting from same position as $\boldsymbol{x}_0^{(o)^{\widetilde{\nabla}}}$ with probability 1. We have following upper bound of discretization error*

$$\|\boldsymbol{x}_k^{(o)} - \boldsymbol{X}_{kh}\|_{\mathbb{L}_2} \leq (19 + 46\sqrt{\Theta})\sqrt{\frac{h^3}{m}}A_0 + (31 + 57\sqrt{\Theta})\sqrt{\frac{h^3 d}{m}}. \tag{30}$$

In order to get all theorems in Section 5, we just need to use the fact that $\Theta = 0$ for full gradient ALUM, $\Theta \leq \frac{N^2}{b^3}$ for SVRG-ALUM and $\Theta \leq 2\frac{N^2}{b^3}$ for SAGA-ALUM.

B.2 Preliminary

We first introduce several notations.

$$\begin{aligned} \|\boldsymbol{v}\|_{\mathbb{L}_2} &= \sqrt{\mathbb{E}[\|\boldsymbol{v}\|_2^2]} \\ \|\boldsymbol{v}\|_{\mathbb{L}_2,B} &= \sqrt{\mathbb{E}_B[\|\boldsymbol{v}\|_2^2]} \\ \|\boldsymbol{v}\|_{\mathbb{L}_2,a} &= \sqrt{\mathbb{E}_a[\|\boldsymbol{v}\|_2^2]} \end{aligned} \tag{31}$$

$\mathbb{E}_B[\cdot]$ takes expectation with regard to random Brownian motion. $\mathbb{E}_a[\cdot]$ means average for random variable a which determines randomized midpoint in RMM or ALUM.

Next we introduce another assumption to simplify the analysis.

Assumption 4 (Optimal at Zero)**.** *Without loss of generality, we assume $\boldsymbol{x}^* = 0$ and $f(\boldsymbol{x}^*) = 0$ where $\boldsymbol{x}^*$ is the global minimum for the strongly convex potential energy function.*

Remark 3. *Assumption 4 doesn't mean that we have to calculate the global optimal of function $f(\boldsymbol{x})$ and shift the function. ULD is invariant under shifting the coordinate. More specifically, the stochastic process on a shifted potential function and shifted start point should be exactly the same as shifted process obtained based on original potential function and start point. The Wasserstein distance is also invariant under this shifting if we translate both target distribution and obtained distribution. Therefore, we can safely introduce Assumption 4 to simplify the analysis without really translate the potential.*

B.3 Bounded MSE property

Given $\boldsymbol{x}_k^{(e)}$ for $k \geq 0$ as a series of points provided sequentially for estimating the gradient. A gradient estimation method generates $\widetilde{\nabla}_k$ as random vectors for estimating $\nabla f(\boldsymbol{x}_k^{(e)})$. We let $\mathbb{E}_k[\cdot]$ means taking expectation for randomness only after k-th iteration in the gradient estimator. For example, if vanilla SGD, SVRG or SAGA is used, the randomness comes from the random batch and $\mathbb{E}_k[\widetilde{\nabla}_{k+1}]$ is same as $\mathbb{E}_{B_{k+1}}[\widetilde{\nabla}_{k+1}]$ that is expectation with respect to random batch in $(k+1)$-th iteration.

In this section, we propose bounded MSE property to control the mean-squared error (MSE) of variance reduction methods.

Definition 1 (Bounded MSE property)**.** *We say a gradient estimation method satisfies the bounded MSE property if (1) it is unbiased, which means $\mathbb{E}_k[\widetilde{\nabla}_{k+1}] = \nabla f(\boldsymbol{x}_{k+1}^{(e)}) = \sum_{i=1}^N \nabla f_i(\boldsymbol{x}_{k+1}^{(e)})$. (2) it*

has the following upper bound for some parameter Θ *and all* $k \geq 0$.

$$\begin{aligned} \mathbb{E}[\|\widetilde{\nabla}_{k+1} - \nabla f(\boldsymbol{x}_{k+1}^{(e)})\|_2^2] &\leq \Theta \max_{0\leq i\leq k} Q_i, \\ \|\widetilde{\nabla}_0 - \nabla f(\boldsymbol{x}_0^{(e)})\|_2^2 &= 0, \\ Q_k = N\sum_{i=1}^{N} \|\nabla f_i(\boldsymbol{x}_{k+1}^{(e)}) - \nabla f_i(\boldsymbol{x}_k^{(e)})\|_2^2. & \end{aligned} \tag{32}$$

Clearly, the full gradient estimator $\widetilde{\nabla}_k = \nabla f(\boldsymbol{x}_k^{(e)})$ satisfies bounded MSE property with $\Theta = 0$ because there is no gradient error. We next show both SVRG and SAGA satisfy bounded MSE property.

Lemma 1. *SVRG with epoch length* τ *satisfies bounded MSE property with* $\Theta = \frac{N-b}{N-1}\frac{(\tau-1)^2}{b} \leq \frac{\tau^2}{b}$.

Lemma 2. *SAGA satisfies bounded MSE property with* $\Theta = \frac{N(N-b)(2N-b)}{(N-1)b^3} \leq \frac{2N^2}{b^3}$.

We show the proof in appendix B.3.1 and appendix B.3.2 separately.

B.3.1 Proof of lemma 1 for SVRG

Recall the definition of SVRG as follows.

$$\widetilde{\nabla}_k^{\text{SVRG}} = \frac{N}{b}\sum_{i\in B_k}(\nabla f_i(\boldsymbol{x}_k^{(e)}) - \nabla f_i(\overline{\boldsymbol{x}})) + \sum_{i=1}^{N}\nabla f_i(\overline{\boldsymbol{x}}) \tag{33}$$

For $k = 0$, there is no gradient error because the full gradient is just calculated. For $k \geq 1$, we define $\boldsymbol{X}_i = \nabla f_i(\boldsymbol{x}_k^{(e)}) - \nabla f_i(\overline{\boldsymbol{x}})$, $\boldsymbol{Y}_i = N\boldsymbol{X}_i - \sum_{i=1}^{N}\boldsymbol{X}_i$. We then have

$$\sum_{i=1}^{N}\boldsymbol{Y}_i = 0 \tag{34}$$

$$\widetilde{\nabla}_k^{\text{SVRG}} - \sum_{i=1}^{N}\nabla f_i(\boldsymbol{x}_k^{(e)}) = \frac{1}{b}\sum_{i\in B_k}\boldsymbol{Y}_i \tag{35}$$

Lemma 3.

$$\mathbb{E}_{B_k}\left\|\frac{1}{b}\sum_{i\in B_k}\boldsymbol{Y}_i\right\|_2^2 = \frac{N-b}{N-1}\frac{1}{Nb}\sum_{i=1}^{N}\|\boldsymbol{Y}_i\|_2^2 \tag{36}$$

Due to the fact that batch B_k is sampling without replacement, controlling the norm is not that straightforward, therefore we show the proof separately in appendix B.3.3.

$$\sum_{i=1}^{N}\|\boldsymbol{Y}_i\|_2^2 = N^2\sum_{i=1}^{N}\|\boldsymbol{X}_i\|_2^2 - N\left\|\sum_{i=1}^{N}\boldsymbol{X}_i\right\|_2^2 \leq N^2\sum_{i=1}^{N}\|\boldsymbol{X}_i\|_2^2 \tag{37}$$

Therefore, we reach following inequality

$$\mathbb{E}_{B_k}\|\widetilde{\nabla}_k^{\text{SVRG}} - \nabla f_i(\boldsymbol{x}_k^{(e)})\|_2^2 \leq \frac{N-b}{N-1}\frac{N}{b}\sum_{i=1}^{N}\|\boldsymbol{X}_i\|_2^2 \tag{38}$$

We next give upper bound on $\sum_{i=1}^{N}\|\boldsymbol{X}_i\|_2^2$.

According to definition of SVRG, we know $\overline{\boldsymbol{x}} = \boldsymbol{x}_{k'}^{(e)}$ where k' is the last iteration that the algorithm update the full gradient. Therefore, we have $k - \tau + 1 \leq k' \leq k$.

$$\begin{aligned}
\sum_{i=1}^{N} \|\boldsymbol{X}_i\|_2^2 =& \sum_{i=1}^{N} \left\| \nabla f_i(\boldsymbol{x}_k^{(e)}) - \nabla f_i(\overline{\boldsymbol{x}}) \right\|_2^2 \\
=& \sum_{i=1}^{N} \left\| \nabla f_i(\boldsymbol{x}_k^{(e)}) - \nabla f_i(\boldsymbol{x}_{k'}^{(e)}) \right\|_2^2 \\
\leq& \sum_{i=1}^{N} (k - k') \sum_{t=k'}^{k-1} \left\| \nabla f_i(\boldsymbol{x}_{t+1}^{(e)}) - \nabla f_i(\boldsymbol{x}_t^{(e)}) \right\|_2^2 \\
=& (k - k') \sum_{t=k'}^{k-1} \sum_{i=1}^{N} \left\| \nabla f_i(\boldsymbol{x}_{t+1}^{(e)}) - \nabla f_i(\boldsymbol{x}_t^{(e)}) \right\|_2^2 \\
=& (k - k') \sum_{t=k'}^{k-1} \frac{1}{N} Q_t \\
\leq& \frac{(k - k')^2}{N} \max_{i<k} Q_i \\
\leq& \frac{(\tau - 1)^2}{N} \max_{i<k} Q_i
\end{aligned} \tag{39}$$

Finally, we have MSE upper bound as follows.

$$\mathbb{E}_{B_k} \|\widetilde{\nabla}_k^{\text{SVRG}} - \sum_{i=1}^{N} \nabla f_i(\boldsymbol{x}_k^{(e)})\|_2^2 \leq \frac{N - b}{N - 1} \frac{(\tau - 1)^2}{b} \max_{i<k} Q_i. \tag{40}$$

B.3.2 Proof of lemma 2 for SAGA

Recall the definition of SAGA as follows.

$$\widetilde{\nabla}_k^{\text{SAGA}} = \frac{N}{b} \sum_{i \in B_k} (\nabla f_i(\boldsymbol{x}_k^{(e)}) - \nabla f_i(\boldsymbol{\phi}_k^i)) + \sum_{i=1}^{N} \nabla f_i(\boldsymbol{\phi}_k^i) \tag{41}$$

Again, for $k = 0$, there is no gradient error, and for $k \geq 1$, we define $\boldsymbol{X}_i = \nabla f_i(\boldsymbol{x}_k^{(e)}) - \nabla f_i(\boldsymbol{\phi}_k^i)$. Similar to (38) in appendix B.3.1, we can reach the following result.

$$\mathbb{E}_{B_k} \|\widetilde{\nabla}_k^{\text{SAGA}} - \nabla f_i(\boldsymbol{x}_k^{(e)}))\|_2^2 \leq \frac{N - b}{N - 1} \frac{N}{b} \sum_{i=1}^{N} \|\boldsymbol{X}_i\|_2^2 \tag{42}$$

We next give upper bound on $\sum_{i=1}^{N} \|\boldsymbol{X}_i\|_2^2$.

We define $M_u = \sum_{i=1}^{N} \|\nabla f_i(\boldsymbol{x}_k^{(e)}) - \nabla f_i(\boldsymbol{\phi}_u^i)\|_2^2$ for $k \geq u \geq 0$. We can see that $\sum_{i=1}^{N} \|\boldsymbol{X}_i\|_2^2 = M_k$.

$$\begin{aligned}
M_0 =& \sum_{i=1}^{N} \|\nabla f_i(\boldsymbol{x}_k^{(e)}) - \nabla f_i(\boldsymbol{x}_0^{(e)})\|_2^2 \\
\leq& \sum_{i=1}^{N} k \sum_{t=0}^{k-1} \left\| \nabla f_i(\boldsymbol{x}_{t+1}^{(e)}) - \nabla f_i(\boldsymbol{x}_t^{(e)}) \right\|_2^2 \\
=& k \sum_{t=0}^{k-1} \sum_{i=1}^{N} \left\| \nabla f_i(\boldsymbol{x}_{t+1}^{(e)}) - \nabla f_i(\boldsymbol{x}_t^{(e)}) \right\|_2^2 \\
=& k \sum_{t=0}^{k-1} \frac{1}{N} Q_t \\
\leq& \frac{k^2}{N} \max_{i<k} Q_i
\end{aligned} \tag{43}$$

We next define indicator $\mathbb{I}_{i,u}=1$ if and only if $i\in B_u$ and $\mathbb{I}_{i,u}=0$ otherwise.

$$\begin{aligned}
\mathbb{E}_{B_{u-1}}[M_u] =&\mathbb{E}_{B_{u-1}}\sum_{i=1}^{N}\left(\mathbb{I}_{i,u-1}\|\nabla f_i(\boldsymbol{x}_k^{(e)})-\nabla f_i(\boldsymbol{x}_{u-1}^{(e)})\|_2^2+(1-\mathbb{I}_{i,u-1})\|\nabla f_i(\boldsymbol{x}_k^{(e)})-\nabla f_i(\boldsymbol{\phi}_{u-1}^{i})\|_2^2\right)\\
=&\frac{b}{N}\sum_{i=1}^{N}\|\nabla f_i(\boldsymbol{x}_k^{(e)})-\nabla f_i(\boldsymbol{x}_{u-1}^{(e)})\|_2^2+\frac{N-b}{N}M_{u-1}\\
\leq&\frac{b}{N}\sum_{i=1}^{N}(k-u+1)\sum_{t=u-1}^{k-1}\|\nabla f_i(\boldsymbol{x}_{t+1}^{(e)})-\nabla f_i(\boldsymbol{x}_t^{(e)})\|_2^2+\frac{N-b}{N}M_{u-1}\\
=&\frac{b}{N}(k-u+1)\sum_{t=u-1}^{k-1}\sum_{i=1}^{N}\|\nabla f_i(\boldsymbol{x}_{t+1}^{(e)})-\nabla f_i(\boldsymbol{x}_t^{(e)})\|_2^2+\frac{N-b}{N}M_{u-1}\\
=&\frac{b}{N}(k-u+1)\sum_{t=u-1}^{k-1}\frac{1}{N}Q_t+\frac{N-b}{N}M_{u-1}\\
\leq&\frac{b}{N^2}(k-u+1)^2\max_{i<k}Q_i+\frac{N-b}{N}M_{u-1}
\end{aligned}\tag{44}$$

Combining the above two inequalities, we have

$$\begin{aligned}
\mathbb{E}[M_u]\leq&\left((\frac{N-b}{N})^k\frac{k^2}{N}+\sum_{u=1}^{k}(\frac{N-b}{N})^{k-u}\frac{b(k-u+1)^2}{N^2}\right)\max_{i<k}Q_i\\
=&S(k)\max_{i<k}Q_i
\end{aligned}\tag{45}$$

The function $S(k)$ increases monotonically for k because $S(k+1)-S(k)=(\frac{N-b}{N})^k\frac{2k+1}{N}\geq 0$. We then have $S(k)\leq\lim_{k\to\infty}S(k)=\frac{2N-b}{b^2}$. Finally, we have MSE upper bound as follows.

$$\mathbb{E}\|\widetilde{\nabla}_k^{\text{SAGA}}-\nabla f_i(\boldsymbol{x}_k^{(e)}))\|_2^2\leq\frac{N(N-b)(2N-b)}{(N-1)b^3}\max_{i<k}Q_i.\tag{46}$$

B.3.3 Other

Proof of lemma 3. We define indicator $\mathbb{I}_i$ such that $\mathbb{I}_i=1$ if and only if $i\in B_k$ and $\mathbb{I}_0=0$ otherwise. Since B_k is a simple random sample of size b from a population of N elements, we have

$$\mathbb{E}_{B_k}[\mathbb{I}_i]=\frac{b}{N},\mathbb{E}_{B_k}[\mathbb{I}_i\mathbb{I}_j]=\frac{b}{N}\frac{b-1}{N-1},\forall i\neq j\tag{47}$$

$$\begin{aligned}
\mathbb{E}_{B_k}\left\|\sum_{i\in B_k}\boldsymbol{Y}_i\right\|_2^2=&\mathbb{E}_{B_k}\left(\sum_{i\in B_k}\|\boldsymbol{Y}_i\|_2^2+\sum_{i\neq j\in B_k}\langle\boldsymbol{Y}_i,\boldsymbol{Y}_j\rangle^2\right)\\
=&\mathbb{E}_{B_k}\left(\sum_{i=1}^{N}\mathbb{I}_i\|\boldsymbol{Y}_i\|_2^2+\sum_{i\neq j}\mathbb{I}_i\mathbb{I}_j\langle\boldsymbol{Y}_i,\boldsymbol{Y}_j\rangle^2\right)\\
=&\sum_{i=1}^{N}\frac{b}{N}\|\boldsymbol{Y}_i\|_2^2+\sum_{i\neq j}\frac{b}{N}\frac{b-1}{N-1}\langle\boldsymbol{Y}_i,\boldsymbol{Y}_j\rangle^2\\
=&\frac{N-b}{N-1}\frac{b}{N}\sum_{i=1}^{N}\|\boldsymbol{Y}_i\|_2^2+\frac{b}{N}\frac{b-1}{N-1}\left\langle\sum_{i=1}^{N}\boldsymbol{Y}_i,\sum_{j=1}^{N}\boldsymbol{Y}_j\right\rangle^2\\
=&\frac{N-b}{N-1}\frac{b}{N}\sum_{i=1}^{N}\|\boldsymbol{Y}_i\|_2^2
\end{aligned}\tag{48}$$

The last equality comes from the fact that $\sum_{i=1}^{N}\boldsymbol{Y}_i=0$. □

B.4 Continuous Contraction

We first define several vectors useful in the analysis by linear combination or direct sum of $\boldsymbol{X}$ and $\boldsymbol{V}$.

$$\boldsymbol{R}_t = \gamma \boldsymbol{X}_t + \boldsymbol{V}_t, \boldsymbol{S}_t = \boldsymbol{V}_t, \boldsymbol{Z}_t = \begin{bmatrix} \boldsymbol{R}_t \\ \boldsymbol{S}_t \end{bmatrix} \tag{49}$$

$$\boldsymbol{Z}_t = \begin{bmatrix} \boldsymbol{R}_t \\ \boldsymbol{S}_t \end{bmatrix} = \begin{bmatrix} \gamma & 1 \\ 0 & 1 \end{bmatrix} \begin{bmatrix} \boldsymbol{X}_t \\ \boldsymbol{V}_t \end{bmatrix} \tag{50}$$

$$\begin{bmatrix} \boldsymbol{X}_t \\ \boldsymbol{V}_t \end{bmatrix} = \frac{1}{\gamma} \begin{bmatrix} 1 & -1 \\ 0 & \gamma \end{bmatrix} \begin{bmatrix} \boldsymbol{R}_t \\ \boldsymbol{S}_t \end{bmatrix} \tag{51}$$

The following contraction result for continuous process is essentially the same as analysis in [17]. We rephrase them here in a form that is more coherent with the other part of this paper.

Lemma 4. *For any two ULD processes* $\begin{bmatrix} \boldsymbol{X}_t \\ \boldsymbol{Z}_t \end{bmatrix}$ *and* $\begin{bmatrix} \boldsymbol{X}'_t \\ \boldsymbol{Z}'_t \end{bmatrix}$ *with the same Brownian motion* $\boldsymbol{B}_t$*, we define* $\Delta \boldsymbol{X}_t = \boldsymbol{X}_t - \boldsymbol{X}'_t$ *and similarly for* $\Delta \boldsymbol{V}_t$*,* $\Delta \boldsymbol{R}_t$*,* $\Delta \boldsymbol{S}_t$ *and* $\Delta \boldsymbol{Z}_t$*. If* $\gamma \geq \sqrt{m+L}$*, then we have*

$$\|\Delta \boldsymbol{Z}_t\|_2 \leq e^{-\frac{m}{\gamma}t} \|\Delta \boldsymbol{Z}_0\|_2 \tag{52}$$

Proof of Lemma 4.

$$\begin{aligned} d\Delta \boldsymbol{Z}_t &= \begin{bmatrix} \gamma & 1 \\ 0 & 1 \end{bmatrix} \begin{bmatrix} d\Delta \boldsymbol{X}_t \\ d\Delta \boldsymbol{V}_t \end{bmatrix} \\ &= \begin{bmatrix} \gamma & 1 \\ 0 & 1 \end{bmatrix} \begin{bmatrix} \Delta \boldsymbol{V}_t \\ \nabla f(\boldsymbol{X}'_t) - \nabla f(\boldsymbol{X}_t) - \gamma \Delta \boldsymbol{V}_t \end{bmatrix} dt \\ \nabla f(\boldsymbol{X}'_t) - \nabla f(\boldsymbol{X}_t) &= -H_t \Delta \boldsymbol{X}_t \\ H_t &= \int_0^1 \boldsymbol{\nabla}^2 f(\boldsymbol{X}'_t + u\Delta \boldsymbol{X}_t) du \\ mI &\preccurlyeq H_t \preccurlyeq LI \end{aligned} \tag{53}$$

$$\begin{aligned} d\Delta \boldsymbol{Z}_t &= \begin{bmatrix} \gamma & 1 \\ 0 & 1 \end{bmatrix} \begin{bmatrix} 0 & 1 \\ -H_t & -\gamma \end{bmatrix} \begin{bmatrix} \Delta \boldsymbol{X}_t \\ \Delta \boldsymbol{V}_t \end{bmatrix} \\ &= \frac{1}{\gamma} \begin{bmatrix} \gamma & 1 \\ 0 & 1 \end{bmatrix} \begin{bmatrix} 0 & 1 \\ -H_t & -\gamma \end{bmatrix} \begin{bmatrix} 1 & -1 \\ 0 & \gamma \end{bmatrix} \begin{bmatrix} \Delta \boldsymbol{R}_t \\ \Delta \boldsymbol{S}_t \end{bmatrix} \\ &= \frac{1}{\gamma} \begin{bmatrix} -H_t & H_t \\ -H_t & H_t - \gamma^2 \end{bmatrix} \begin{bmatrix} \Delta \boldsymbol{R}_t \\ \Delta \boldsymbol{S}_t \end{bmatrix} \end{aligned} \tag{54}$$

$$\begin{aligned} d\|\Delta \boldsymbol{Z}_t\|_2^2 &= \frac{2}{\gamma} \begin{bmatrix} \Delta \boldsymbol{R}_t & \Delta \boldsymbol{S}_t \end{bmatrix} \begin{bmatrix} -H_t & 0 \\ 0 & H_t - \gamma^2 \end{bmatrix} \begin{bmatrix} \Delta \boldsymbol{R}_t \\ \Delta \boldsymbol{S}_t \end{bmatrix} \\ &\leq -\frac{2m}{\gamma} \|\Delta \boldsymbol{Z}_t\|_2^2 \end{aligned} \tag{55}$$

$$\|\Delta \boldsymbol{Z}_t\|_2^2 \leq e^{-\frac{2m}{\gamma}t} \|\Delta \boldsymbol{Z}_0\|_2^2 \tag{56}$$

□

B.5 Sampling error

We first define a ground truth path. The initial point $\boldsymbol{x}_0^*$,$\boldsymbol{v}_0^*$ is drawn from target distribution $p^*(\boldsymbol{x}^*, \boldsymbol{v}^*) \propto \exp(-f(\boldsymbol{x}^*) - \frac{\|\boldsymbol{v}^*\|_2^2}{2})$. Then we generate $\boldsymbol{x}_{k+1}^*$,$\boldsymbol{v}_{k+1}^*$ from $\boldsymbol{x}_k^*$,$\boldsymbol{v}_k^*$ by taking repeatedly applying a ULD process. More specifically, we let $\boldsymbol{x}_{k+1}^* = \boldsymbol{X}_h$,$\boldsymbol{v}_{k+1}^* = \boldsymbol{V}_h$ where $\boldsymbol{X}_t$,$\boldsymbol{V}_t$ is the ULD process starting from $\boldsymbol{x}_k^*$,$\boldsymbol{v}_k^*$. Clearly, the distribution of $\boldsymbol{x}_k^*$,$\boldsymbol{v}_k^*$ is still target distribution. Finally, we can define $\boldsymbol{z}_k^* = \begin{bmatrix} \gamma \boldsymbol{x}^* + \boldsymbol{v}^* \\ \boldsymbol{v}^* \end{bmatrix}$.

We then first define $A_k = \left\| \boldsymbol{z}_k^{(o)\widetilde{\nabla}} - \boldsymbol{z}_k^* \right\|_{\mathbb{L}_2}$ as the difference between the path $\boldsymbol{z}_k^{(o)\widetilde{\nabla}} = \begin{bmatrix} \gamma \boldsymbol{x}^{(o)\widetilde{\nabla}} + \boldsymbol{v}^{(o)\widetilde{\nabla}} \\ \boldsymbol{v}^{(o)\widetilde{\nabla}} \end{bmatrix}$ obtained by our algorithm and the ground truth path. Based on (50), we have $\|\Delta Z\|_{\mathbb{L}_2} \geq \frac{\gamma}{\sqrt{2}} \|\Delta X\|_{\mathbb{L}_2} \geq \|\Delta X\|_{\mathbb{L}_2}$. Therefore, A_k is an upper bound of $W_2(p_k, p^*)$.

At initialization, based on (51), we have $\left\| \begin{bmatrix} \Delta \boldsymbol{X} \\ \Delta \boldsymbol{V} \end{bmatrix} \right\|_{\mathbb{L}_2} \geq \frac{1}{\gamma} \|\Delta Z\|_{\mathbb{L}_2}$. Moreover, let distribution of $\boldsymbol{x}_0$ be $p_0(\boldsymbol{x})$, and distribution of $\boldsymbol{v}_0$ be a Gaussian distribution that is the same as $\boldsymbol{v}_0^*$. Let the coupling between $\begin{bmatrix} \boldsymbol{x}_0 \\ \boldsymbol{v}_0 \end{bmatrix}$ and $\begin{bmatrix} \boldsymbol{x}_0^* \\ \boldsymbol{v}_0^* \end{bmatrix}$ follows that $\boldsymbol{v}_0$ and $\boldsymbol{v}_0^*$ are exactly the same, and $\boldsymbol{x}_0$ and $\boldsymbol{x}_0^*$ are coupled according to the optimal transport between $p_0(\boldsymbol{x})$ and $p^*(\boldsymbol{x})$. In this way of initialization, we can get $\left\| \begin{bmatrix} \Delta \boldsymbol{x}_0 \\ \Delta \boldsymbol{v}_0 \end{bmatrix} \right\|_{\mathbb{L}_2} = W_2(p_0, p^*)$. Therefore, we have $A_0 \leq \gamma W_2(p_0, p^*)$.

The next ten pages of numerical analysis is a little bit long, so we provide an overview as follows.

B.5.1 Overview of proof

The main idea of controlling A_k is decomposing error and contraction as follows.

$$
\begin{aligned}
A_{k+1} =& \mathbb{E}\left[\left\| \boldsymbol{Z}_t^{(o)\widetilde{\nabla}} - \boldsymbol{Z}_t^* \right\|_2^2 \right] \\
\overset{①}{=}& \mathbb{E}\left[\left\| \boldsymbol{Z}_t^{(o)\widetilde{\nabla}} - \mathbb{E}_a \mathbb{E}_k \boldsymbol{Z}_t^{(o)\widetilde{\nabla}} \right\|_2^2 \right] \\
& + \mathbb{E}\left[\left\| \mathbb{E}_a \mathbb{E}_k \boldsymbol{Z}_t^{(o)\widetilde{\nabla}} - \boldsymbol{Z}_t^* \right\|_2^2 \right] \\
\overset{②}{\leq}& \mathbb{E}\left[\left\| \boldsymbol{Z}_t^{(o)\widetilde{\nabla}} - \mathbb{E}_a \boldsymbol{Z}_t^{(r)} \right\|_2^2 \right] \\
& + \mathbb{E}\left[\left\| \mathbb{E}_a \mathbb{E}_k \boldsymbol{Z}_t^{(o)\widetilde{\nabla}} - \boldsymbol{Z}_t^* \right\|_2^2 \right] \\
\overset{③}{=}& \mathbb{E}\left[\left\| \boldsymbol{Z}_t^{(o)\widetilde{\nabla}} - \mathbb{E}_a \boldsymbol{Z}_t^{(r)} \right\|_2^2 \right] \\
& + \mathbb{E}\left[\left\| \mathbb{E}_a \boldsymbol{Z}_t^{(o)} - \boldsymbol{Z}_t^* \right\|_2^2 \right] \\
\overset{④}{\leq}& 3\mathbb{E}\left[\left\| \boldsymbol{Z}_t^{(o)\widetilde{\nabla}} - \boldsymbol{Z}_t^{(o)} \right\|_2^2 \right] + 3\mathbb{E}\left[\left\| \boldsymbol{Z}_t^{(o)} - \boldsymbol{Z}_t^{(r)} \right\|_2^2 \right] \\
& + 3\mathbb{E}\left[\left\| \boldsymbol{Z}_t^{(r)} - \mathbb{E}_a \boldsymbol{Z}_t^{(r)} \right\|_2^2 \right] \\
& + \left(\left\| \mathbb{E}_a \boldsymbol{Z}_t^{(o)} - \mathbb{E}_a \boldsymbol{Z}_t^{(r)} \right\|_{\mathbb{L}_2} + \left\| \mathbb{E}_a \boldsymbol{Z}_t^{(r)} - \boldsymbol{Z}_t \right\|_{\mathbb{L}_2} + \| \boldsymbol{Z}_t - \boldsymbol{Z}_t^* \|_{\mathbb{L}_2} \right)^2
\end{aligned}
\tag{57}
$$

The vector $\boldsymbol{Z}^{(r)}$ is based on $\boldsymbol{X}^{(r)}$,$\boldsymbol{V}^{(r)}$ generated by RMM, which is defined in (19).

Inequality ① splits bias and variance and is based on the fact that $\mathbb{E}_a \mathbb{E}_k \boldsymbol{Z}_t^* = \boldsymbol{Z}_t^*$.

Inequality ② comes from the fact that $\mathbb{E}\left[\left\| \boldsymbol{Z}_t^{(o)\widetilde{\nabla}} - \mathbb{E}_a \boldsymbol{Z}_t^{(r)} \right\|_2^2 \right] = \mathbb{E}\left[\left\| \boldsymbol{Z}_t^{(o)\widetilde{\nabla}} - \mathbb{E}_a \mathbb{E}_k \boldsymbol{Z}_t^{(o)\widetilde{\nabla}} \right\|_2^2 \right] + \mathbb{E}\left[\left\| \mathbb{E}_a \mathbb{E}_k \boldsymbol{Z}_t^{(o)\widetilde{\nabla}} - \mathbb{E}_a \boldsymbol{Z}_t^{(r)} \right\|_2^2 \right]$.

Inequality ③ comes from the fact that variance reduction method we used are unbiased.

Inequality ④ is simply applying Young's inequality and triangle inequality.

The last term is $\|\boldsymbol{Z}_t - \boldsymbol{Z}_t^*\|_{\mathbb{L}_2} = e^{-\frac{m}{\gamma}t}\|\boldsymbol{Z}_0 - \boldsymbol{Z}_0^*\|_{\mathbb{L}_2} = e^{-\frac{m}{\gamma}t}A_k$. Therefore, we just need to control all other error term by term. We do that in Appendices B.5.3 to B.5.6.

During the analysis, we give upper bound of errors for A_k by using another value $Q_k = N\sum_{i=1}^N \mathbb{E}[\|\nabla f_i(\boldsymbol{x}_{k+1}^{(e)\widetilde{\nabla}}) - \nabla f_i(\boldsymbol{x}_k^{(e)\widetilde{\nabla}})\|_2^2]$. Q_k decides the magnitudes for gradient error. In Appendix B.5.8, we give the upper bound of Q_k by using A_k. Finally, we can give upper bound for both Q_k and A_k in Appendix B.5.9.

B.5.2 Some basic upper bounds for continuous process

Moments First, we derive the moments for equilibrium distribution.

Due to the fact that $\boldsymbol{V}_t^*$ follows standard Gaussian distribution,

$$\mathbb{E}\left[\|\boldsymbol{V}_t^*\|_2^2\right] = d. \tag{58}$$

Next we control the moment of $\nabla f(\boldsymbol{x})$.

$$\begin{aligned} Zd =& \int de^{-f(\boldsymbol{x})}d\boldsymbol{x} \\ =& \int \mathrm{div}(\boldsymbol{x})e^{-f(\boldsymbol{x})}d\boldsymbol{x} \\ =& \int \boldsymbol{x}\cdot\nabla f(\boldsymbol{x})e^{-f(\boldsymbol{x})}d\boldsymbol{x} \\ \geq& \frac{1}{L}\int \|\nabla f(\boldsymbol{x})\|_2^2 e^{-f(\boldsymbol{x})}d\boldsymbol{x} \end{aligned} \tag{59}$$

$$\mathbb{E}_{\boldsymbol{x}\sim p^*}\left[\|\nabla f(\boldsymbol{x})\|_2^2\right] = \frac{1}{Z}\int \|\nabla f(\boldsymbol{x})\|_2^2 e^{-f(\boldsymbol{x})}d\boldsymbol{x} \leq Ld \tag{60}$$

Then we control the moments for ULD process.

$$\begin{aligned} \|\boldsymbol{V}_t\|_{\mathbb{L}_2} \leq& \|\boldsymbol{V}_t^*\|_{\mathbb{L}_2} + \|\boldsymbol{V}_t - \boldsymbol{V}_t^*\|_{\mathbb{L}_2} \\ \leq& \sqrt{d} + \|\boldsymbol{Z}_t - \boldsymbol{Z}_t^*\|_{\mathbb{L}_2} \\ \leq& \sqrt{d} + \|\boldsymbol{Z}_0 - \boldsymbol{Z}_0^*\|_{\mathbb{L}_2} \\ =& \sqrt{d} + \left\|\boldsymbol{z}_k^{(o)\widetilde{\nabla}} - \boldsymbol{z}_k^*\right\|_{\mathbb{L}_2} \\ =& \sqrt{d} + A_k \end{aligned} \tag{61}$$

$$\begin{aligned} \|\nabla f(\boldsymbol{X}_t)\|_{\mathbb{L}_2} \leq& \|\nabla f(\boldsymbol{X}_t^*)\|_{\mathbb{L}_2} + \|\nabla f(\boldsymbol{X}_t) - \nabla f(\boldsymbol{X}_t^*)\|_{\mathbb{L}_2} \\ \leq& \sqrt{Ld} + L\|\boldsymbol{X}_t - \boldsymbol{X}_t^*\|_{\mathbb{L}_2} \\ \leq& \sqrt{Ld} + L\frac{\sqrt{2}}{\gamma}\|\boldsymbol{Z}_t - \boldsymbol{Z}_t^*\|_{\mathbb{L}_2} \\ \leq& \sqrt{Ld} + \frac{\sqrt{2}L}{\gamma}\|\boldsymbol{Z}_0 - \boldsymbol{Z}_0^*\|_{\mathbb{L}_2} \\ =& \sqrt{Ld} + \frac{\sqrt{2}L}{\gamma}\left\|\boldsymbol{z}_k^{(o)\widetilde{\nabla}} - \boldsymbol{z}_k^*\right\|_{\mathbb{L}_2} \\ =& \sqrt{Ld} + \frac{\sqrt{2}L}{\gamma}A_k \end{aligned} \tag{62}$$

Change Assume $t_2 \geq t_1 \geq 0$.

$$\begin{aligned}\|\boldsymbol{X}_{t_1} - \boldsymbol{X}_{t_2}\|_{\mathbb{L}_2} \leq & \left\| \int_{t_1}^{t_2} \boldsymbol{V}_s ds \right\|_{\mathbb{L}_2} \\ \leq & \int_{t_1}^{t_2} \|\boldsymbol{V}_s\|_{\mathbb{L}_2} ds \\ \leq & (t_2 - t_1) \max_{t_1 \leq u \leq t_2} \|\boldsymbol{V}_u\|_{\mathbb{L}_2}\end{aligned} \tag{63}$$

B.5.3 Error for LPM

$$\begin{aligned}\left\| \boldsymbol{V}_t^{(l)} - \boldsymbol{V}_t \right\|_{\mathbb{L}_2} = & \left\| \int_0^t \psi_0(t-s)(\nabla f(\boldsymbol{X}_s) - \nabla f(\boldsymbol{X}_0)) ds \right\|_{\mathbb{L}_2} \\ \leq & \int_0^t \|\nabla f(\boldsymbol{X}_s) - \nabla f(\boldsymbol{X}_0)\|_{\mathbb{L}_2} ds \\ \leq & L \int_0^t \|\boldsymbol{X}_s - \boldsymbol{X}_0\|_{\mathbb{L}_2} ds \\ \leq & L \int_0^t s \max_{0 \leq u \leq t} \|\boldsymbol{V}_u\|_{\mathbb{L}_2} ds \\ \leq & \frac{1}{2} L t^2 \max_{0 \leq u \leq t} \|\boldsymbol{V}_u\|_{\mathbb{L}_2}\end{aligned} \tag{64}$$

$$\begin{aligned}\left\| \boldsymbol{X}_t^{(l)} - \boldsymbol{X}_t \right\|_{\mathbb{L}_2} = & \left\| \int_0^t (\boldsymbol{V}_t^{(l)} - \boldsymbol{V}_t) ds \right\|_{\mathbb{L}_2} \\ \leq & \int_0^t \left\| \boldsymbol{V}_t^{(l)} - \boldsymbol{V}_t \right\|_{\mathbb{L}_2} ds \\ \leq & \frac{1}{2} L \int_0^t s^2 \max_{0 \leq u \leq s} \|\boldsymbol{V}_u\|_{\mathbb{L}_2} ds \\ \leq & \frac{1}{6} L t^3 \max_{0 \leq u \leq t} \|\boldsymbol{V}_u\|_{\mathbb{L}_2}\end{aligned} \tag{65}$$

B.5.4 Error for RMM

First term - Variance We aim to control the variance $\mathbb{E}\left[\left\| \boldsymbol{Z}_t^{(r)} - \mathbb{E}_a \boldsymbol{Z}_t^{(r)} \right\|_2^2 \right]$.

$$\begin{aligned}\mathbb{E}\left[\left\| \boldsymbol{Z}_t^{(r)} - \mathbb{E}_a \boldsymbol{Z}_t^{(r)} \right\|_2^2 \right] \leq & \mathbb{E}\left[\left\| \boldsymbol{Z}_t^{(r)} - \boldsymbol{Z}_t \right\|_2^2 \right] \\ = & \mathbb{E}\left[\left\| \begin{bmatrix} \boldsymbol{R}_t^{(r)} \\ \boldsymbol{S}_t^{(r)} \end{bmatrix} - \begin{bmatrix} \boldsymbol{R}_t \\ \boldsymbol{S}_t \end{bmatrix} \right\|_2^2 \right] \\ = & \mathbb{E}\left[\left\| \begin{bmatrix} \gamma & 1 \\ 0 & 1 \end{bmatrix} \begin{bmatrix} \boldsymbol{X}_t^{(r)} - \boldsymbol{X}_t \\ \boldsymbol{V}_t^{(r)} - \boldsymbol{V}_t \end{bmatrix} \right\|_2^2 \right] \\ \leq & 2\gamma^2 \mathbb{E}\left[\left\| \boldsymbol{X}_t^{(r)} - \boldsymbol{X}_t \right\|_2^2 \right] + 3\mathbb{E}\left[\left\| \boldsymbol{V}_t^{(r)} - \boldsymbol{V}_t \right\|_2^2 \right] \\ = & 2\gamma^2 \left\| \boldsymbol{X}_t^{(r)} - \boldsymbol{X}_t \right\|_{\mathbb{L}_2}^2 + 3 \left\| \boldsymbol{V}_t^{(r)} - \boldsymbol{V}_t \right\|_{\mathbb{L}_2}^2\end{aligned} \tag{66}$$

$$\begin{aligned}\left\|\boldsymbol{X}_t^{(r)}-\boldsymbol{X}_t\right\|_{\mathbb{L}_2} \leq & \left\|t\psi_1(t-at)\nabla f(\boldsymbol{X}_{at}^{(l)})-t\psi_1(t-at)\nabla f(\boldsymbol{X}_{at})\right\|_{\mathbb{L}_2} \\ & + \left\|t\psi_1(t-at)\nabla f(\boldsymbol{X}_{at})-\int_0^t \psi_1(t-at)\nabla f(\boldsymbol{X}_s)ds\right\|_{\mathbb{L}_2} \\ & + \left\|\int_0^t \psi_1(t-at)\nabla f(\boldsymbol{X}_s)ds-\int_0^t \psi_1(t-s)\nabla f(\boldsymbol{X}_s)ds\right\|_{\mathbb{L}_2}\end{aligned} \tag{67}$$

We denote above three terms as D_1,D_2 and D_3.

$$\begin{aligned}D_1 =& \left\|t\psi_1(t-at)\nabla f(\boldsymbol{X}_{at}^{(l)})-t\psi_1(t-at)\nabla f(\boldsymbol{X}_{at})\right\|_{\mathbb{L}_2} \\ \leq & \sqrt{\mathbb{E}_a\left[(t\psi_1(t-at)\|\nabla f(\boldsymbol{X}_{at}^{(l)})-\nabla f(\boldsymbol{X}_{at})\|_{\mathbb{L}_2,B})^2\right]} \\ \leq & \sqrt{\mathbb{E}_a\left[(t\psi_1(t-at)L\|\boldsymbol{X}_{at}^{(l)}-\boldsymbol{X}_{at}\|_{\mathbb{L}_2,B})^2\right]} \\ \leq & \sqrt{\mathbb{E}_a\left[\left(t\psi_1(t-at)L(\frac{1}{6}L(at)^3\max_{0\leq u\leq t}\|\boldsymbol{V}_u\|_{\mathbb{L}_2})\right)^2\right]} \\ \leq & \frac{\sqrt{7}}{252}L^2t^5\max_{0\leq u\leq t}\|\boldsymbol{V}_u\|_{\mathbb{L}_2}\end{aligned} \tag{68}$$

$$\begin{aligned}D_2 =& \left\|t\psi_1(t-at)\nabla f(\boldsymbol{X}_{at})-\int_0^t \psi_1(t-at)\nabla f(\boldsymbol{X}_s)ds\right\|_{\mathbb{L}_2} \\ =& \sqrt{\mathbb{E}_a\left[\psi_1(t-at)^2\mathbb{E}_B\left(\int_0^t(\nabla f(\boldsymbol{X}_{at})-\nabla f(\boldsymbol{X}_s))ds\right)^2\right]} \\ =& \sqrt{\mathbb{E}_a\left[\psi_1(t-at)^2\left\|\int_0^t(\nabla f(\boldsymbol{X}_{at})-\nabla f(\boldsymbol{X}_s))ds\right\|_{\mathbb{L}_2,B}^2\right]} \\ \leq & \sqrt{\mathbb{E}_a\left[\psi_1(t-at)^2\left(\int_0^t\|(\nabla f(\boldsymbol{X}_{at})-\nabla f(\boldsymbol{X}_s))\|_{\mathbb{L}_2,B}ds\right)^2\right]} \\ \leq & \sqrt{\mathbb{E}_a\left[\psi_1(t-at)^2L^2\left(\int_0^t\|(\boldsymbol{X}_{at}-\boldsymbol{X}_s)\|_{\mathbb{L}_2,B}ds\right)^2\right]} \\ \leq & \sqrt{\mathbb{E}_a\left[\psi_1(t-at)^2L^2\left(\int_0^t|at-s|\max_{0\leq u\leq t}\|\boldsymbol{V}_u\|_{\mathbb{L}_2}ds\right)^2\right]} \\ \leq & \frac{\sqrt{210}}{70}Lt^3\max_{0\leq u\leq t}\|\boldsymbol{V}_u\|_{\mathbb{L}_2}\end{aligned} \tag{69}$$

$$
\begin{aligned}
D_3 =& \left\| \int_0^t \psi_1(t-at)\nabla f(\boldsymbol{X}_s)ds - \int_0^t \psi_1(t-s)\nabla f(\boldsymbol{X}_s)ds \right\|_{\mathbb{L}_2} \\
=& \sqrt{\mathbb{E}_a \left\| \int_0^t (\psi_1(t-at)-\psi_1(t-s))\nabla f(\boldsymbol{X}_s)ds \right\|_{\mathbb{L}_2,B}^2} \\
\leq& \sqrt{\mathbb{E}_a (\int_0^t |\psi_1(t-at)-\psi_1(t-s)| \|\nabla f(\boldsymbol{X}_s)\|_{\mathbb{L}_2,B} ds)^2} \\
\leq& \sqrt{\mathbb{E}_a (\int_0^t |\psi_1(t-at)-\psi_1(t-s)| ds)^2} \max_{0\leq u\leq t} \|\nabla f(\boldsymbol{X}_u)\|_{\mathbb{L}_2} \\
\leq& \frac{\sqrt{105}}{30} t^2 \max_{0\leq u\leq t} \|\nabla f(\boldsymbol{X}_u)\|_{\mathbb{L}_2}
\end{aligned}
\tag{70}
$$

Therefore, we conclude the variance of $\boldsymbol{X}$ as following.

$$
\begin{aligned}
\left\| \boldsymbol{X}_t^{(r)} - \boldsymbol{X}_t \right\|_{\mathbb{L}_2} \leq& (\frac{\sqrt{210}}{70} L t^3 + \frac{\sqrt{7}}{252} L^2 t^5) \max_{0\leq u\leq t} \|\boldsymbol{V}_u\|_{\mathbb{L}_2} \\
&+ \frac{\sqrt{105}}{30} t^2 \max_{0\leq u\leq t} \|\nabla f(\boldsymbol{X}_u)\|_{\mathbb{L}_2}
\end{aligned}
\tag{71}
$$

$$
\begin{aligned}
\left\| \boldsymbol{V}_t^{(r)} - \boldsymbol{V}_t \right\|_{\mathbb{L}_2} \leq& \left\| t\psi_0(t-at)\nabla f(\boldsymbol{X}_{at}^{(l)}) - t\psi_0(t-at)\nabla f(\boldsymbol{X}_{at}) \right\|_{\mathbb{L}_2} \\
&+ \left\| t\psi_0(t-at)\nabla f(\boldsymbol{X}_{at}) - \int_0^t \psi_0(t-at)\nabla f(\boldsymbol{X}_s)ds \right\|_{\mathbb{L}_2} \\
&+ \left\| \int_0^t \psi_0(t-at)\nabla f(\boldsymbol{X}_s)ds - \int_0^t \psi_0(t-s)\nabla f(\boldsymbol{X}_s)ds \right\|_{\mathbb{L}_2}
\end{aligned}
\tag{72}
$$

We denote above three terms as E_1,E_2 and E_3.

$$
\begin{aligned}
E_1 =& \left\| t\psi_0(t-at)\nabla f(\boldsymbol{X}_{at}^{(l)}) - t\psi_0(t-at)\nabla f(\boldsymbol{X}_{at}) \right\|_{\mathbb{L}_2} \\
\leq& \sqrt{\mathbb{E}_a \left[(t\psi_0(t-at) \|\nabla f(\boldsymbol{X}_{at}^{(l)}) - \nabla f(\boldsymbol{X}_{at})\|_{\mathbb{L}_2,B})^2 \right]} \\
\leq& \sqrt{\mathbb{E}_a \left[(t\psi_0(t-at) L \|\boldsymbol{X}_{at}^{(l)} - \boldsymbol{X}_{at}\|_{\mathbb{L}_2,B})^2 \right]} \\
\leq& \sqrt{\mathbb{E}_a \left[\left(t\psi_0(t-at) L (\frac{1}{6} L (at)^3 \max_{0\leq u\leq t} \|\boldsymbol{V}_u\|_{\mathbb{L}_2}) \right)^2 \right]} \\
\leq& \frac{\sqrt{7}}{42} L^2 t^4 \max_{0\leq u\leq t} \|\boldsymbol{V}_u\|_{\mathbb{L}_2}
\end{aligned}
\tag{73}
$$

$$
\begin{aligned}
E_2 =& \left\| t\psi_0(t-at)\nabla f(\boldsymbol{X}_{at}) - \int_0^t \psi_0(t-at)\nabla f(\boldsymbol{X}_s)ds \right\|_{\mathbb{L}_2} \\
=& \sqrt{\mathbb{E}_a\left[\psi_0(t-at)^2 \mathbb{E}_B\left(\int_0^t (\nabla f(\boldsymbol{X}_{at}) - \nabla f(\boldsymbol{X}_s))ds\right)^2\right]} \\
=& \sqrt{\mathbb{E}_a\left[\psi_0(t-at)^2 \left\|\int_0^t (\nabla f(\boldsymbol{X}_{at}) - \nabla f(\boldsymbol{X}_s))ds\right\|_{\mathbb{L}_2,B}^2\right]} \\
\leq& \sqrt{\mathbb{E}_a\left[\psi_0(t-at)^2 \left(\int_0^t \|(\nabla f(\boldsymbol{X}_{at}) - \nabla f(\boldsymbol{X}_s))\|_{\mathbb{L}_2,B} ds\right)^2\right]} \\
\leq& \sqrt{\mathbb{E}_a\left[\psi_0(t-at)^2 L^2 \left(\int_0^t \|(\boldsymbol{X}_{at} - \boldsymbol{X}_s)\|_{\mathbb{L}_2,B} ds\right)^2\right]} \\
\leq& \sqrt{\mathbb{E}_a\left[\psi_0(t-at)^2 L^2 \left(\int_0^t |at-s| \max_{0\leq u\leq t}\|\boldsymbol{V}_u\|_{\mathbb{L}_2} ds\right)^2\right]} \\
\leq& \frac{\sqrt{105}}{30} L t^2 \max_{0\leq u\leq t}\|\boldsymbol{V}_u\|_{\mathbb{L}_2}
\end{aligned} \tag{74}
$$

$$
\begin{aligned}
E_3 =& \left\| \int_0^t \psi_0(t-at)\nabla f(\boldsymbol{X}_s)ds - \int_0^t \psi_0(t-s)\nabla f(\boldsymbol{X}_s)ds \right\|_{\mathbb{L}_2} \\
=& \sqrt{\mathbb{E}_a\left\|\int_0^t (\psi_0(t-at) - \psi_0(t-s))\nabla f(\boldsymbol{X}_s)ds\right\|_{\mathbb{L}_2,B}^2} \\
\leq& \sqrt{\mathbb{E}_a(\int_0^t |\psi_0(t-at) - \psi_0(t-s)| \|\nabla f(\boldsymbol{X}_s)\|_{\mathbb{L}_2,B} ds)^2} \\
\leq& \sqrt{\mathbb{E}_a(\int_0^t |\psi_0(t-at) - \psi_0(t-s)| ds)^2} \max_{0\leq u\leq t}\|\nabla f(\boldsymbol{X}_u)\|_{\mathbb{L}_2} \\
\leq& \frac{\sqrt{105}}{30}\gamma t^2 \max_{0\leq u\leq t}\|\nabla f(\boldsymbol{X}_u)\|_{\mathbb{L}_2}
\end{aligned} \tag{75}
$$

Therefore, we conclude the variance of $\boldsymbol{X}$ as following.

$$
\begin{aligned}
\left\|\boldsymbol{V}_t^{(r)} - \boldsymbol{V}_t\right\|_{\mathbb{L}_2} \leq& (\frac{\sqrt{105}}{30} L t^2 + \frac{\sqrt{7}}{42} L^2 t^4) \max_{0\leq u\leq t}\|\boldsymbol{V}_u\|_{\mathbb{L}_2} \\
&+ \frac{\sqrt{105}}{30}\gamma t^2 \max_{0\leq u\leq t}\|\nabla f(\boldsymbol{X}_u)\|_{\mathbb{L}_2}
\end{aligned} \tag{76}
$$

Finally, we can give the upper bound of variance as follows.

$$
\begin{aligned}
\mathbb{E}\left[\left\|\boldsymbol{Z}_t^{(r)} - \mathbb{E}_a\boldsymbol{Z}_t^{(r)}\right\|_2^2\right] \leq& \frac{7}{6}\gamma^2 t^4 \max_{0\leq u\leq t}\|\nabla f(\boldsymbol{X}_u)\|_{\mathbb{L}_2}^2 + \frac{7}{20} t^4 \max_{0\leq u\leq t}\|\boldsymbol{V}_u\|_{\mathbb{L}_2}^2 \\
&+ RL^2 t^6 \max_{0\leq u\leq t}\|\boldsymbol{V}_u\|_{\mathbb{L}_2}^2
\end{aligned} \tag{77}
$$

$$
R = \frac{\left(5\gamma^2 L^2 t^4 + 36\, L\sqrt{2}\gamma^2\sqrt{15}t^2 + 270 L^2 t^2 + 756\, L\sqrt{15} + 1944\,\gamma^2\right)}{22680}
$$

Second term - Bias We aim to control the bias $\left\|\mathbb{E}_a\boldsymbol{Z}_t^{(r)} - \boldsymbol{Z}_t\right\|_2$.

$$
\left\|\mathbb{E}_a\boldsymbol{Z}_t^{(r)} - \boldsymbol{Z}_t\right\|_{\mathbb{L}_2} \leq \gamma\left\|\mathbb{E}_a\boldsymbol{X}_t^{(r)} - \boldsymbol{X}_t\right\|_{\mathbb{L}_2} + 2\left\|\mathbb{E}_a\boldsymbol{V}_t^{(r)} - \boldsymbol{V}_t\right\|_{\mathbb{L}_2} \tag{78}
$$

$$
\begin{aligned}
\left\|\mathbb{E}_a \boldsymbol{X}_t^{(r)} - \boldsymbol{X}_t\right\|_{\mathbb{L}_2} =& \left\| \int_0^t \psi_1(t-s)\nabla f(\boldsymbol{X}_s^{(l)})ds - \int_0^t \psi_1(t-s)\nabla f(\boldsymbol{X}_s)ds \right\|_{\mathbb{L}_2} \\
=& \left\| \int_0^t \psi_1(t-s)(\nabla f(\boldsymbol{X}_s^{(l)}) - \nabla f(\boldsymbol{X}_s))ds \right\|_{\mathbb{L}_2} \\
\leq& \int_0^t \psi_1(t-s) \left\| \nabla f(\boldsymbol{X}_s^{(l)}) - \nabla f(\boldsymbol{X}_s) \right\|_{\mathbb{L}_2} ds \\
\leq& \int_0^t \psi_1(t-s) L \left\| \boldsymbol{X}_s^{(l)} - \boldsymbol{X}_s \right\|_{\mathbb{L}_2} ds \\
\leq& \int_0^t \psi_1(t-s) L (\frac{1}{6} L s^3 \max_{0\leq u\leq t} \|\boldsymbol{V}_u\|_{\mathbb{L}_2}) ds \\
\leq& \frac{1}{120} L^2 t^5 \max_{0\leq u\leq t} \|\boldsymbol{V}_u\|_{\mathbb{L}_2}
\end{aligned}
\tag{79}
$$

$$
\begin{aligned}
\left\|\mathbb{E}_a \boldsymbol{V}_t^{(r)} - \boldsymbol{V}_t\right\|_{\mathbb{L}_2} =& \left\| \int_0^t \psi_0(t-s)\nabla f(\boldsymbol{X}_s^{(l)})ds - \int_0^t \psi_0(t-s)\nabla f(\boldsymbol{X}_s)ds \right\|_{\mathbb{L}_2} \\
=& \left\| \int_0^t \psi_0(t-s)(\nabla f(\boldsymbol{X}_s^{(l)}) - \nabla f(\boldsymbol{X}_s))ds \right\|_{\mathbb{L}_2} \\
\leq& \int_0^t \psi_0(t-s) \left\| \nabla f(\boldsymbol{X}_s^{(l)}) - \nabla f(\boldsymbol{X}_s) \right\|_{\mathbb{L}_2} ds \\
\leq& \int_0^t \psi_0(t-s) L \left\| \boldsymbol{X}_s^{(l)} - \boldsymbol{X}_s \right\|_{\mathbb{L}_2} ds \\
\leq& \int_0^t \psi_0(t-s) L (\frac{1}{6} L s^3 \max_{0\leq u\leq t} \|\boldsymbol{V}_u\|_{\mathbb{L}_2}) ds \\
\leq& \frac{1}{24} L^2 t^4 \max_{0\leq u\leq t} \|\boldsymbol{V}_u\|_{\mathbb{L}_2}
\end{aligned}
\tag{80}
$$

$$
\left\|\mathbb{E}_a \boldsymbol{Z}_t^{(r)} - \boldsymbol{Z}_t\right\|_{\mathbb{L}_2} \leq \frac{1}{12} L^2 t^4 (1 + \frac{1}{10}\gamma L t) \max_{0\leq u\leq t} \|\boldsymbol{V}_u\|_{\mathbb{L}_2} \tag{81}
$$

B.5.5 Error for ALUM

Variance

$$
\begin{aligned}
&\mathbb{E}\left[\left\|\boldsymbol{Z}_t^{(o)}-\boldsymbol{Z}_t^{(r)}\right\|_2^2\right]\\
=&\mathbb{E}\left[\left\|\begin{bmatrix}\gamma & 1\\ 0 & 1\end{bmatrix}\begin{bmatrix}\boldsymbol{X}_t^{(o)}-\boldsymbol{X}_t^{(r)}\\ \boldsymbol{V}_t^{(o)}-\boldsymbol{V}_t^{(r)}\end{bmatrix}\right\|_2^2\right]\\
\leq&\mathbb{E}\left[\left\|\begin{bmatrix}\gamma & 1\\ 0 & 1\end{bmatrix}\begin{bmatrix}t\psi_1(t-at)(\nabla f(\boldsymbol{X}_{at}^{(e)\widetilde{\nabla}})-\nabla f(\boldsymbol{X}_{at}^{(l)}))\\ t\psi_0(t-at)(\nabla f(\boldsymbol{X}_{at}^{(e)\widetilde{\nabla}})-\nabla f(\boldsymbol{X}_{at}^{(l)}))\end{bmatrix}\right\|_2^2\right]\\
\leq&\mathbb{E}\left[t^2((\gamma\psi_1(t-at)+\psi_0(t-at))^2+\psi_0(t-at)^2)\left\|\nabla f(\boldsymbol{X}_{at}^{(e)\widetilde{\nabla}})-\nabla f(\boldsymbol{X}_{at}^{(l)})\right\|_2^2\right]\\
=&\mathbb{E}_a\left[t^2((\gamma\psi_1(t-at)+\psi_0(t-at))^2+\psi_0(t-at)^2)\left\|\nabla f(\boldsymbol{X}_{at}^{(e)\widetilde{\nabla}})-\nabla f(\boldsymbol{X}_{at}^{(l)})\right\|_{\mathbb{L}_2,B}^2\right]\\
\leq&\mathbb{E}_a\left[t^2((\gamma\psi_1(t-at)+\psi_0(t-at))^2+\psi_0(t-at)^2)L^2\left\|\boldsymbol{X}_{at}^{(e)\widetilde{\nabla}}-\boldsymbol{X}_{at}^{(l)}\right\|_{\mathbb{L}_2,B}^2\right]\\
=&\mathbb{E}_a\left[t^2((\gamma\psi_1(t-at)+\psi_0(t-at))^2+\psi_0(t-at)^2)L^2\|\psi_2(at)\nabla f(\boldsymbol{X}_0)\|_{\mathbb{L}_2,B}^2\right]\\
\leq&\mathbb{E}_a\left[t^2\psi_2(at)^2((\gamma\psi_1(t-at)+\psi_0(t-at))^2+\psi_0(t-at)^2)\right]L^2\max_{0\leq u\leq t}\|\nabla f(\boldsymbol{X}_t)\|_{\mathbb{L}_2}^2\\
\leq&\frac{1}{10}L^2t^6\max_{0\leq u\leq t}\|\nabla f(\boldsymbol{X}_t)\|_{\mathbb{L}_2}^2
\end{aligned}
\tag{82}
$$

$$
\begin{aligned}
&\mathbb{E}\left[\left\|\boldsymbol{X}_t^{(o)}-\boldsymbol{X}_t^{(r)}\right\|_2^2\right]\\
\leq&\mathbb{E}_a\left[t^2\psi_1(t-at)^2\psi_2(at)^2\right]L^2\max_{0\leq u\leq t}\|\nabla f(\boldsymbol{X}_t)\|_{\mathbb{L}_2}^2\\
\leq&\frac{1}{420}L^2t^8\max_{0\leq u\leq t}\|\nabla f(\boldsymbol{X}_t)\|_{\mathbb{L}_2}^2
\end{aligned}
\tag{83}
$$

$$
\begin{aligned}
&\mathbb{E}\left[\left\|\boldsymbol{V}_t^{(o)}-\boldsymbol{V}_t^{(r)}\right\|_2^2\right]\\
\leq&\mathbb{E}_a\left[t^2\psi_0(t-at)^2\psi_2(at)^2\right]L^2\max_{0\leq u\leq t}\|\nabla f(\boldsymbol{X}_t)\|_{\mathbb{L}_2}^2\\
\leq&\frac{1}{20}L^2t^6\max_{0\leq u\leq t}\|\nabla f(\boldsymbol{X}_t)\|_{\mathbb{L}_2}^2
\end{aligned}
\tag{84}
$$

Bias

$$
\begin{aligned}
&\left\|\mathbb{E}_a\boldsymbol{Z}_t^{(o)}-\mathbb{E}_a\boldsymbol{Z}_t^{(r)}\right\|_{\mathbb{L}_2}\\
=&\sqrt{\mathbb{E}\left\|\mathbb{E}_a\left[\boldsymbol{Z}_t^{(o)}-\boldsymbol{Z}_t^{(r)}\right]\right\|_2^2}\\
\leq&\sqrt{\mathbb{E}\left\|\boldsymbol{Z}_t^{(o)}-\boldsymbol{Z}_t^{(r)}\right\|_2^2}\\
\leq&\frac{1}{\sqrt{10}}Lt^3\max_{0\leq u\leq t}\|\nabla f(\boldsymbol{X}_t)\|_{\mathbb{L}_2}
\end{aligned}
\tag{85}
$$

B.5.6 Error introduced by gradient estimation

$$
\begin{aligned}
&\mathbb{E}\left[\left\|\boldsymbol{Z}_t^{(o)\widetilde{\nabla}}-\boldsymbol{Z}_t^{(o)}\right\|_2^2\right]\\
=&\mathbb{E}\left[\left\|\begin{bmatrix}\gamma & 1\\ 0 & 1\end{bmatrix}\begin{bmatrix}\boldsymbol{X}_t^{(o)\widetilde{\nabla}}-\boldsymbol{X}_t^{(o)}\\ \boldsymbol{V}_t^{(o)\widetilde{\nabla}}-\boldsymbol{V}_t^{(o)}\end{bmatrix}\right\|_2^2\right]\\
=&\mathbb{E}\left[\left\|\begin{bmatrix}\gamma & 1\\ 0 & 1\end{bmatrix}\begin{bmatrix}t\psi_1(t-at)(\widetilde{\nabla}_k-\nabla f(\boldsymbol{X}_{at}^{(e)\widetilde{\nabla}}))\\ t\psi_0(t-at)(\widetilde{\nabla}_k-\nabla f(\boldsymbol{X}_{at}^{(e)\widetilde{\nabla}}))\end{bmatrix}\right\|_2^2\right]\\
=&\mathbb{E}\left[t^2((\gamma\psi_1(t-at)+\psi_0(t-at))^2+\psi_0(t-at)^2)\left\|\widetilde{\nabla}_k-\mathbb{E}_k\widetilde{\nabla}_k\right\|_2^2\right]\\
\leq&\mathbb{E}\left[t^2((\gamma t+1)^2+1^2)\left\|\widetilde{\nabla}_k-\mathbb{E}_k\widetilde{\nabla}_k\right\|_2^2\right]\\
=&t^2((\gamma t+1)^2+1^2)\mathbb{E}\left[\left\|\widetilde{\nabla}_k-\mathbb{E}_k\widetilde{\nabla}_k\right\|_2^2\right]\\
\leq&t^2((\gamma t+1)^2+1)\Theta\max_{i<k}Q_i
\end{aligned}
\tag{86}
$$

The last inequality follows definition 1. We use $Q_k = N\sum_{i=1}^N \mathbb{E}[\|\nabla f_i(\boldsymbol{x}_{k+1}^{(e)\widetilde{\nabla}})-\nabla f_i(\boldsymbol{x}_k^{(e)\widetilde{\nabla}})\|_2^2]$. This has an extra expectation compared to Q_k in definition 1 because we need to consider the extra randomness coming from the Brownian motion instead of just random batch.

$$
\begin{aligned}
\mathbb{E}\left[\left\|\boldsymbol{X}_t^{(o)\widetilde{\nabla}}-\boldsymbol{X}_t^{(o)}\right\|_2^2\right]\leq&\mathbb{E}\left[\left\|t\psi_1(t-at)(\widetilde{\nabla}_k-\nabla f(\boldsymbol{X}_{at}^{(e)\widetilde{\nabla}}))\right\|_2^2\right]\\
\leq&t^4\Theta\max_{i<k}Q_i
\end{aligned}
\tag{87}
$$

$$
\begin{aligned}
\mathbb{E}\left[\left\|\boldsymbol{V}_t^{(o)\widetilde{\nabla}}-\boldsymbol{V}_t^{(o)}\right\|_2^2\right]\leq&\mathbb{E}\left[\left\|t\psi_0(t-at)(\widetilde{\nabla}_k-\nabla f(\boldsymbol{X}_{at}^{(e)\widetilde{\nabla}}))\right\|_2^2\right]\\
\leq&t^2\Theta\max_{i<k}Q_i
\end{aligned}
\tag{88}
$$

B.5.7 Summary of error in single step

By combining above error terms, we get follow error change in single step.

$$
\begin{aligned}
&\mathbb{E}\left[\langle\boldsymbol{Z}_t^{(o)\widetilde{\nabla}}-\mathbb{E}_a\mathbb{E}_k\boldsymbol{Z}_t^{(o)\widetilde{\nabla}},\mathbb{E}_a\mathbb{E}_k\boldsymbol{Z}_t^{(o)\widetilde{\nabla}}-\boldsymbol{Z}_t^{*}\rangle\right]\\
=&\mathbb{E}_B\left[\langle\mathbb{E}_a\mathbb{E}_k\boldsymbol{Z}_t^{(o)\widetilde{\nabla}}-\mathbb{E}_a\mathbb{E}_k\boldsymbol{Z}_t^{(o)\widetilde{\nabla}},\mathbb{E}_a\mathbb{E}_k\boldsymbol{Z}_t^{(o)\widetilde{\nabla}}-\boldsymbol{Z}_t^{*}\rangle\right]\\
=&0
\end{aligned}
\tag{89}
$$

$$
\begin{aligned}
\mathbb{E}\left[\left\|\boldsymbol{Z}_t^{(o)\widetilde{\nabla}}-\boldsymbol{Z}_t^*\right\|_2^2\right] =&\mathbb{E}\left[\left\|\boldsymbol{Z}_t^{(o)\widetilde{\nabla}}-\mathbb{E}_a\mathbb{E}_k\boldsymbol{Z}_t^{(o)\widetilde{\nabla}}\right\|_2^2\right]\\
&+\mathbb{E}\left[\left\|\mathbb{E}_a\mathbb{E}_k\boldsymbol{Z}_t^{(o)\widetilde{\nabla}}-\boldsymbol{Z}_t^*\right\|_2^2\right]\\
\leq&\mathbb{E}\left[\left\|\boldsymbol{Z}_t^{(o)\widetilde{\nabla}}-\mathbb{E}_a\boldsymbol{Z}_t^{(r)}\right\|_2^2\right]\\
&+\mathbb{E}\left[\left\|\mathbb{E}_a\boldsymbol{Z}_t^{(o)}-\boldsymbol{Z}_t^*\right\|_2^2\right]\\
\leq&3\mathbb{E}\left[\left\|\boldsymbol{Z}_t^{(o)\widetilde{\nabla}}-\boldsymbol{Z}_t^{(o)}\right\|_2^2\right]+3\mathbb{E}\left[\left\|\boldsymbol{Z}_t^{(o)}-\boldsymbol{Z}_t^{(r)}\right\|_2^2\right]\\
&+3\mathbb{E}\left[\left\|\boldsymbol{Z}_t^{(r)}-\mathbb{E}_a\boldsymbol{Z}_t^{(r)}\right\|_2^2\right]\\
&+\left(\left\|\mathbb{E}_a\boldsymbol{Z}_t^{(o)}-\mathbb{E}_a\boldsymbol{Z}_t^{(r)}\right\|_{\mathbb{L}_2}+\left\|\mathbb{E}_a\boldsymbol{Z}_t^{(r)}-\boldsymbol{Z}_t\right\|_{\mathbb{L}_2}+\|\boldsymbol{Z}_t-\boldsymbol{Z}_t^*\|_{\mathbb{L}_2}\right)^2\\
\leq&3t^2((\gamma t+1)^2+1)\Theta\max_{i<k}Q_i\\
&+\frac{7}{2}\gamma^2t^4\max_{0\leq u\leq t}\|\nabla f(\boldsymbol{X}_u)\|_{\mathbb{L}_2}^2+\frac{21}{20}t^4\max_{0\leq u\leq t}\|\boldsymbol{V}_u\|_{\mathbb{L}_2}^2\\
&+L^2t^6\left(\frac{3}{10}\max_{0\leq u\leq t}\|\nabla f(\boldsymbol{X}_t)\|_{\mathbb{L}_2}^2+3R\max_{0\leq u\leq t}\|\boldsymbol{V}_u\|_{\mathbb{L}_2}^2\right)\\
&+\left(\frac{1}{\sqrt{10}}Lt^3\max_{0\leq u\leq t}\|\nabla f(\boldsymbol{X}_t)\|_{\mathbb{L}_2}\right.\\
&+\frac{1}{12}L^2t^4(1+\frac{1}{10}\gamma Lt)\max_{0\leq u\leq t}\|\boldsymbol{V}_u\|_{\mathbb{L}_2}\\
&\left.+e^{-\frac{m}{\gamma}t}\|\boldsymbol{Z}_0-\boldsymbol{Z}_0^*\|_{\mathbb{L}_2}\right)^2
\end{aligned}
\tag{90}
$$

$$
R=\frac{\left(5\gamma^2L^2t^4+36\,L\sqrt{2}\gamma^2\sqrt{15}t^2+270L^2t^2+756\,L\sqrt{15}+1944\,\gamma^2\right)}{22680}
$$

B.5.8 Control Q_k with A_k

From here, we assume that a fixed step size h is used. In this section we introduce temporary notation a_k and $\boldsymbol{e}_{x,[0,a_kh],k}$, where k is inserted to specify the iteration.

We know that at each iteration, we calculate gradient estimation on point:

$$
\boldsymbol{x}_k^{(e)\widetilde{\nabla}}=\boldsymbol{x}_k^{(o)\widetilde{\nabla}}+\psi_1(a_kh)\boldsymbol{v}_k^{(o)\widetilde{\nabla}}+\boldsymbol{e}_{x,[0,a_kh],k}.
$$

Recall that value Q_k is introduced in Appendices B.3 and B.5.6 and is used for controlling gradient estimation error. We next give the upper bound of value Q_k.

$$
\begin{aligned}
Q_k=&N\sum_{i=1}^N\mathbb{E}[\|\nabla f_i(\boldsymbol{x}_{k+1}^{(e)\widetilde{\nabla}})-\nabla f_i(\boldsymbol{x}_k^{(e)\widetilde{\nabla}})\|_2^2]\\
\leq&N\sum_{i=1}^N(\frac{L}{N})^2\mathbb{E}[\|\boldsymbol{x}_{k+1}^{(e)\widetilde{\nabla}}-\boldsymbol{x}_k^{(e)\widetilde{\nabla}}\|_2^2]\\
=&L^2\|\boldsymbol{x}_{k+1}^{(e)\widetilde{\nabla}}-\boldsymbol{x}_k^{(e)\widetilde{\nabla}}\|_{\mathbb{L}_2}^2
\end{aligned}
\tag{91}
$$

$\boldsymbol{X}_h, \boldsymbol{V}_h$ starts from $\boldsymbol{x}_k^{(o)\widetilde{\nabla}}, \boldsymbol{v}_k^{(o)\widetilde{\nabla}}$.

$$
\begin{aligned}
&\|\boldsymbol{x}_{k+1}^{(e)\widetilde{\nabla}} - \boldsymbol{x}_k^{(e)\widetilde{\nabla}}\|_{\mathbb{L}_2} \\
=&\|(\boldsymbol{x}_{k+1}^{(o)\widetilde{\nabla}} - \boldsymbol{x}_k^{(o)\widetilde{\nabla}}) + \psi_1(a_{k+1}h)\boldsymbol{v}_{k+1}^{(o)\widetilde{\nabla}} - \psi_1(a_k h)\boldsymbol{v}_k^{(o)\widetilde{\nabla}} + \boldsymbol{e}_{x,[0,a_{k+1}h],k+1} - \boldsymbol{e}_{x,[0,a_k h],k}\|_{\mathbb{L}_2} \\
\leq&\|\boldsymbol{x}_{k+1}^{(o)\widetilde{\nabla}} - \boldsymbol{x}_k^{(o)\widetilde{\nabla}}\|_{\mathbb{L}_2} + \|\psi_1(a_{k+1}h)\boldsymbol{v}_{k+1}^{(o)\widetilde{\nabla}}\|_{\mathbb{L}_2} + \|\psi_1(a_k h)\boldsymbol{v}_k^{(o)\widetilde{\nabla}}\|_{\mathbb{L}_2} \\
&+ \|\boldsymbol{e}_{x,[0,a_{k+1}h],k+1}\|_{\mathbb{L}_2} + \|\boldsymbol{e}_{x,[0,a_k h],k}\|_{\mathbb{L}_2}
\end{aligned} \tag{92}
$$

$$
\begin{aligned}
&\|\boldsymbol{x}_{k+1}^{(o)\widetilde{\nabla}} - \boldsymbol{x}_k^{(o)\widetilde{\nabla}}\|_{\mathbb{L}_2} \\
=&\|\boldsymbol{X}_h^{(o)\widetilde{\nabla}} - \boldsymbol{X}_0\|_{\mathbb{L}_2} \\
\leq&\|\boldsymbol{X}_h^{(o)\widetilde{\nabla}} - \boldsymbol{X}_h^{(o)}\|_{\mathbb{L}_2} + \|\boldsymbol{X}_h^{(o)} - \boldsymbol{X}_h^{(r)}\|_{\mathbb{L}_2} + \|\boldsymbol{X}_h^{(r)} - \boldsymbol{X}_h\|_{\mathbb{L}_2} + \|\boldsymbol{X}_h - \boldsymbol{X}_0\|_{\mathbb{L}_2} \\
\leq&h^2\sqrt{\Theta}\max_{i<k}\sqrt{Q_i} + h\max_{0\leq u\leq h}\|\boldsymbol{V}_u\|_{\mathbb{L}_2} \\
&+ (\frac{\sqrt{210}}{70}Lh^3 + \frac{\sqrt{7}}{252}L^2h^5)\max_{0\leq u\leq t}\|\boldsymbol{V}_u\|_{\mathbb{L}_2} \\
&+ (\frac{\sqrt{105}}{30}h^2 + \frac{1}{\sqrt{420}}Lh^4)\max_{0\leq u\leq t}\|\nabla f(\boldsymbol{X}_u)\|_{\mathbb{L}_2}
\end{aligned} \tag{93}
$$

$$
\|\psi_1(a_{k+1}h)\boldsymbol{v}_{k+1}^{(o)\widetilde{\nabla}}\|_{\mathbb{L}_2} \leq h\|\boldsymbol{v}_{k+1}^{(o)\widetilde{\nabla}}\|_{\mathbb{L}_2} = h\|\boldsymbol{V}_h^{(o)\widetilde{\nabla}}\|_{\mathbb{L}_2} \tag{94}
$$

$$
\begin{aligned}
&\|\boldsymbol{V}_h^{(o)\widetilde{\nabla}}\|_{\mathbb{L}_2} \\
\leq&\|\boldsymbol{V}_h^{(o)\widetilde{\nabla}} - \boldsymbol{V}_h^{(o)}\|_{\mathbb{L}_2} + \|\boldsymbol{V}_h^{(o)} - \boldsymbol{V}_h^{(r)}\|_{\mathbb{L}_2} + \|\boldsymbol{V}_h^{(r)} - \boldsymbol{V}_h\|_{\mathbb{L}_2} + \|\boldsymbol{V}_h\|_{\mathbb{L}_2} \\
\leq&h\sqrt{\Theta}\max_{i<k}\sqrt{Q_i} + \max_{0\leq u\leq h}\|\boldsymbol{V}_u\|_{\mathbb{L}_2} \\
&+ (\frac{\sqrt{105}}{30}Lh^2 + \frac{\sqrt{7}}{42}L^2h^4)\max_{0\leq u\leq t}\|\boldsymbol{V}_u\|_{\mathbb{L}_2} \\
&+ (\frac{\sqrt{105}}{30}\gamma h^2 + \frac{1}{\sqrt{20}}Lh^3)\max_{0\leq u\leq t}\|\nabla f(\boldsymbol{X}_u)\|_{\mathbb{L}_2}
\end{aligned} \tag{95}
$$

$$
\|\psi_1(a_k h)\boldsymbol{v}_k^{(o)\widetilde{\nabla}}\|_{\mathbb{L}_2} \leq h\|\boldsymbol{v}_k^{(o)\widetilde{\nabla}}\|_{\mathbb{L}_2} = h\|\boldsymbol{V}_0\|_{\mathbb{L}_2} \leq h\max_{0\leq u\leq t}\|\boldsymbol{V}_u\|_{\mathbb{L}_2} \tag{96}
$$

$$
\begin{aligned}
&\|\boldsymbol{e}_{x,[0,a_{k+1}h],k+1}\|_{\mathbb{L}_2} = \|\boldsymbol{e}_{x,[0,a_k h],k}\|_{\mathbb{L}_2} \\
=&\sqrt{\mathbb{E}\left[\|\boldsymbol{e}_{x,[0,a_k h],k}\|_2^2\right]} \\
=&\sqrt{\mathbb{E}_a\left[(2\gamma d\int_0^{a_k h}\psi_1(u)^2du)^2\right]} \\
\leq&\frac{1}{\sqrt{6}}\sqrt{\gamma d h^3}
\end{aligned} \tag{97}
$$

$$
\begin{aligned}
\sqrt{Q_k} \leq&2Lh^2\sqrt{\Theta}\max_{i<k}\sqrt{Q_i} + 3Lh\max_{0\leq u\leq t}\|\boldsymbol{V}_u\|_{\mathbb{L}_2} + \frac{2}{\sqrt{6}}\sqrt{\gamma d h^3} \\
&+ ((\frac{\sqrt{210}}{70} + \frac{\sqrt{105}}{30})L^2h^3 + (\frac{\sqrt{7}}{252} + \frac{\sqrt{7}}{40})L^3h^5)\max_{0\leq u\leq t}\|\boldsymbol{V}_u\|_{\mathbb{L}_2} \\
&+ (\frac{\sqrt{105}}{30}(1+\gamma h)Lh^2 + (\frac{1}{\sqrt{420}} + \frac{1}{\sqrt{20}})L^2h^4)\max_{0\leq u\leq t}\|\nabla f(\boldsymbol{X}_u)\|_{\mathbb{L}_2}
\end{aligned} \tag{98}
$$

B.5.9 Upper bound of Q_k and A_k

Starting from this section, we assume $L = 1$ and $\gamma = 2$. We further assume $h < \frac{1}{10}$ to simplify upper bounds in previous sections.

$$\sqrt{Q_k} \leq 2h^2\sqrt{\Theta}\max_{i<k}\sqrt{Q_i} + 4hA_k + 4h\sqrt{d} \tag{99}$$

In order to give a tractable upper bound of A_{k+1}, we further apply Young's inequalities to $\|\boldsymbol{V}_t\|_{\mathbb{L}_2}^2$ and $\|\nabla f(\boldsymbol{X}_u)\|_{\mathbb{L}_2}^2$.

$$\|\boldsymbol{V}_t\|_{\mathbb{L}_2}^2 \leq 2d + 2A_k^2 \tag{100}$$

$$\|\nabla f(\boldsymbol{X}_u)\|_{\mathbb{L}_2}^2 \leq 2Ld + 4\frac{L^2}{\gamma^2}A_k^2 \tag{101}$$

$$\begin{aligned}
A_{k+1}^2 =& \mathbb{E}\left[\left\|\boldsymbol{Z}_t^{(o)\widetilde{\nabla}} - \boldsymbol{Z}_t^*\right\|_2^2\right] \\
\leq& 8h^2\Theta\max_{i<k}Q_i + 17h^4A_k^2 + 31h^4d \\
&+ \left(h^3A_k + h^3\sqrt{d} + e^{-\frac{m}{\gamma}t}A_k\right)^2 \\
\leq& 8h^2\Theta\max_{i<k}Q_i + 31h^4d \\
&+ \left(\sqrt{17}h^2A_k + h^3A_k + h^3\sqrt{d} + e^{-\frac{m}{\gamma}h}A_k\right)^2 \\
\leq& 8h^2\Theta\max_{i<k}Q_i + 31h^4d \\
&+ \left(5h^2A_k + h^3\sqrt{d} + e^{-\frac{m}{\gamma}h}A_k\right)^2
\end{aligned} \tag{102}$$

We further assume $h \leq \frac{1}{11}\frac{m}{\gamma}$, which implies $h \leq \frac{\frac{m}{\gamma}}{(\frac{m}{\gamma})^2+10}$ and $h \leq \frac{1}{22} \leq \frac{1}{10}$.

$$e^{-\frac{mh}{\gamma}} + 5h^2 = 1 - \frac{mh}{2\gamma} + h(-\frac{m}{2\gamma} + (\frac{m^2}{2\gamma^2} + 5)h) \leq 1 - \frac{mh}{2\gamma} \tag{103}$$

By [35, Lemma 7], if $x_{k+1}^2 \leq ((1-\alpha)x_k + B)^2 + A$, then

$$x_k \leq (1-\alpha)^k x_0 + \frac{B}{\alpha} + \frac{A}{B + \sqrt{\alpha(2-\alpha)A}} \leq (1-\alpha)^k x_0 + \frac{B}{\alpha} + \frac{\sqrt{A}}{\sqrt{\alpha}} \tag{104}$$

Therefore, we have

$$\begin{aligned}
A_k =& (1 - \frac{mh}{2\gamma})^k A_0 + \frac{2\gamma\sqrt{h^4d}}{m} + \sqrt{\frac{16h\gamma}{m}\Theta\max_{i<k}Q_i + \frac{62\gamma h^4 d}{m}} \\
\leq& (1 - \frac{mh}{2\gamma})^k A_0 + 4\sqrt{\frac{h\gamma}{m}}\sqrt{\Theta}\max_{i<k}\sqrt{Q_i} + (\frac{4\sqrt{h}}{\sqrt{m}} + \sqrt{62\gamma})\sqrt{\frac{h^3 d}{m}} \\
\leq& (1 - \frac{mh}{2\gamma})^k A_0 + 4\sqrt{\frac{h\gamma}{m}}\sqrt{\Theta}\max_{i<k}\sqrt{Q_i} + 12\sqrt{\frac{h^3 d}{m}}
\end{aligned} \tag{105}$$

We can then control $\max_{i<k}\sqrt{Q_i}$ as follows.

$$\begin{aligned}
\sqrt{Q_k} \leq& 24\sqrt{\frac{h^3}{m}}\sqrt{\Theta}\max_{i<k}\sqrt{Q_i} + 5h\sqrt{d} + 4h(1 - \frac{mh}{2\gamma})^k A_0 \\
\leq& 24\sqrt{\frac{h^3}{m}}\sqrt{\Theta}\max_{i<k}\sqrt{Q_i} + 5h\sqrt{d} + 4hA_0
\end{aligned} \tag{106}$$

Assume $\frac{h^3\Theta}{m} \leq \frac{1}{2304}$.

$$\sqrt{Q_k} \leq \frac{1}{2}\max_{i<k}\sqrt{Q_i} + 5h\sqrt{d} + 4hA_0. \tag{107}$$

$$\max_{i<k} \sqrt{Q_i} \leq 10h\sqrt{d} + 8hA_0 \tag{108}$$

Finally we can give upper bound of A_k.

$$\begin{aligned} A_k \leq & (1 - \frac{mh}{2\gamma})^k A_0 + 46\sqrt{\frac{h^3}{m}}\sqrt{\Theta}A_0 + (12 + 57\sqrt{\Theta})\sqrt{\frac{h^3}{m}}\sqrt{d} \\ \leq & 2A_0 + 2\sqrt{d} \end{aligned} \tag{109}$$

B.6 Discretization error

Consider a ULD process $\boldsymbol{Z}_t$ starting from the same initial point as the algorithm. Let $\boldsymbol{z}_k = \boldsymbol{Z}_{kh}$ and $B_k = \left\| \boldsymbol{z}_k^{(e)^{\widetilde{\nabla}}} - \boldsymbol{z}_k \right\|_{\mathbb{L}_2}$. Based on (50), we have $B_k \geq \|\boldsymbol{x}_k^{(o)^{\widetilde{\nabla}}} - \boldsymbol{X}_{kh}\|_{\mathbb{L}_2}$.

We can control the error B_k similarly to what we have done for A_k. Actually we don't need to analyze the error from scratch again. The following result can be obtained directly by modifying (102). This is because the error in variance and bias terms is the same, and the only difference is that we are controlling difference between $\boldsymbol{z}_k^{(e)^{\widetilde{\nabla}}}$ and $\boldsymbol{z}_k$ instead of between $\boldsymbol{z}_k^{(e)^{\widetilde{\nabla}}}$ and $\boldsymbol{z}_k^*$.

$$\begin{aligned} B_{k+1}^2 \leq & 8h^2\Theta \max_{i<k} Q_i + 17h^4 A_k^2 + 31h^4 d \\ & + \left(h^3 A_k + h^3\sqrt{d} + e^{-\frac{m}{\gamma}h} B_k \right)^2. \end{aligned} \tag{110}$$

We use simplified upper bounds for A_k and Q_k in eqs. (108) and (109):

$$\begin{aligned} A_k \leq & 2A_0 + 2\sqrt{d} \\ \max_{i<k} \sqrt{Q_i} \leq & 10h\sqrt{d} + 8hA_0. \end{aligned} \tag{111}$$

With $B_0 = 0$ and inequality [35, Lemma 7] or (104), we can derive the following result

$$B_k \leq (19 + 46\sqrt{\Theta})\sqrt{\frac{h^3}{m}}A_0 + (31 + 57\sqrt{\Theta})\sqrt{\frac{h^3 d}{m}}. \tag{112}$$

C Proof of information-based complexity lower bound

We first introduce some notations in appendix C.1. We prove theorems 5 and 6 for $d = 1$ case in appendices C.2 and C.3. Then we generalize these results to high dimension in appendix C.4. Finally, we prove corollary 2 in appendix C.5.

C.1 Preliminary

We let $[N]$ means $\{i \in \mathbb{N} | 1 \leq i \leq N\}$. For set Θ, $|\Theta|$ means the cardinality or number of elements if Θ is finite.

C.2 Flat error when $n < N$

We first show the intuition behind Theorem 5 as follows. Then we give rigorous analysis.

In our definition of problem class $\mathcal{U}$, the mean of the distribution is restricted to a small ball. However, the minimum of each component of the potential is not restricted. Therefore, we can construct a family of adversarial models, such that each component potential function has a minimum being very far away from the origin, in the meantime, the sum potential has a minimum close to the origin. In this case, every component could affect the mean of the final distribution arbitrarily, and the lack of information for even just one component makes the prediction very uninformative.

C.2.1 Proof of theorem 5 for 1-d Case

We consider the class of randomized algorithms $\mathcal{A}_n$ with step number $n < N$. We first assume N to be positive odd integer in the following proof. At the end of this subsection, we extend the method to even integer N.

A $N-1$-steps algorithm could ignore the last $N-1-n$ oracle evaluation and be essentially the same as a n-steps algorithms. Therefore, $e_{\mathcal{A}_{N-1},\mathcal{U}} \leq e_{\mathcal{A}_n,\mathcal{U}}$ and we can only consider $n = N-1$ without loss of generality.

Parameterized model We consider a class of parameterized model as a subset of $\mathcal{U}$ to give a lower bound of $e_{\mathcal{A},\mathcal{U}}$.

Let parameter be $\theta \in \Theta = \{(a_0, \dots, a_N) \in \{-1,1\}^{N+1} | \sum_0^N a_i = 0\}$. We define potentials $f_i(x) = \frac{u}{2N}x^2 - \sqrt{u}a_i x$, such that $\sum_i^N f_i(x) = \frac{u}{2}x^2 - \sqrt{u}(\sum_1^N a_i)x$ and global minimum is $x^* = \frac{1}{\sqrt{u}}\sum_1^N a_i = -\frac{1}{\sqrt{u}}a_0 \in \{-\frac{1}{\sqrt{u}}, \frac{1}{\sqrt{u}}\}$. We assume $m \leq u \leq L$, and it is easy to see that $U = (f_1, \dots, f_N)$ is inside $\mathcal{U}$.

We extend the notation to use $\boldsymbol{X}_T(\omega, \theta)$ and $A(\omega, \widetilde{\omega}, \theta)$ to mean $\boldsymbol{X}_T(\omega, U)$ and $A(\omega, \widetilde{\omega}, U)$ where U is above model with parameter θ.

$$
\begin{aligned}
e^2_{\mathcal{A}_n,\mathcal{U}} &= \inf_{A\in\mathcal{A}_n} \sup_{U\in\mathcal{U}} \mathbb{E}_{\omega\in\mathbb{P}}\mathbb{E}_{\widetilde{\omega}\in\widetilde{\mathbb{P}}}[\boldsymbol{X}_T(\omega, U) - A(\omega, \widetilde{\omega}, U)]^2 \\
&\geq \inf_{A\in\mathcal{A}_n} \sup_{\theta\in\Theta} \mathbb{E}_{\omega\in\mathbb{P}}\mathbb{E}_{\widetilde{\omega}\in\widetilde{\mathbb{P}}}[\boldsymbol{X}_T(\omega, \theta) - A(\omega, \widetilde{\omega}, \theta)]^2 \\
&\geq \inf_{A\in\mathcal{A}_n} \frac{1}{|\Theta|}\sum_{\theta\in\Theta} \mathbb{E}_{\omega\in\mathbb{P}}\mathbb{E}_{\widetilde{\omega}\in\widetilde{\mathbb{P}}}[\boldsymbol{X}_T(\omega, \theta) - A(\omega, \widetilde{\omega}, \theta)]^2 \\
&\geq \inf_{A\in\mathcal{A}_n} \mathbb{E}_{\omega\in\mathbb{P}}\mathbb{E}_{\widetilde{\omega}\in\widetilde{\mathbb{P}}} \frac{1}{|\Theta|}\sum_{\theta\in\Theta} [\boldsymbol{X}_T(\omega, \theta) - A(\omega, \widetilde{\omega}, \theta)]^2
\end{aligned}
\tag{113}
$$

We next give a lower bound on the quantity $\frac{1}{|\Theta|}\sum_{\theta\in\Theta}[\boldsymbol{X}_T(\omega, \theta) - A(\omega, \widetilde{\omega}, \theta)]^2$ under a fixed ω and $\widetilde{\omega}$. The basic idea is that due to lack of information, multiple θ could generate same $A(\omega, \widetilde{\omega}, \theta)$, therefore the error could be lower-bounded by differences between $\boldsymbol{X}_T(\omega, \theta)$ with equivalence θ.

Mask We use a mask on parameters to represent how much information could be accessed by the algorithm.

The algorithm takes $N-1$ steps to calculate $A(\omega, \widetilde{\omega}, \theta)$. During this process, $N-1$ oracle are evaluated. Therefore, there is at most $N-1$ gradient oracle evaluation $\Upsilon_U(i, x)$. Those indexes i that appear at least once in these gradient evaluations are collected into a mask.

Let $\mathcal{J} = \{m \subseteq [N]\} = 2^{[N]}$, we define a mapping $\beta : \theta \in \Theta \mapsto \beta(\theta) \in \mathcal{J}$ to represent the mask. More specifically, $\beta(\theta)$ contains index i if and only if, at a certain step during calculating $A(\omega, \widetilde{\omega}, \theta)$, the algorithm evaluates the gradient oracle $\Upsilon_U(i, x)$ with some x.

Expanded mask We have $|\beta(\theta)| \leq N-1$, since there is at most $N-1$ gradient evaluation. We next expand this mask into $\beta'(\theta)$ to make sure $|\beta'(\theta)| = N-1$. This is done by simply adding the largest element in $[N]$ that is still not inside $\beta(\theta)$ until the size reaches $N-1$. More specifically, we can always find k, such that $|\beta(\theta) \cup \{i \in \mathbb{N}^+ | k \leq i \leq N\}| = N-1$ and we let $\beta'(\theta) = \beta(\theta) \cup \{i \in \mathbb{N}^+ | k \leq i \leq N\}$.

Complementary mask We define $\widetilde{\beta}'(\theta) = \{i \in \mathbb{N} | i \leq N\} \setminus \beta'(\theta)$ as complementary mask to represent how much information is not relevant to the algorithm output. It is easy to see that $|\widetilde{\beta}'(\theta)| = 2$ and $0 \in \widetilde{\beta}'(\theta)$.

Equivalent parameters For each $i \in \widetilde{\beta}'(\theta)$, the gradient of $f_i(x)$ is not used in the algorithm, and therefore changing the function f_i or parameter a_i will not affect algorithm output $A(\omega, \widetilde{\omega}, \theta)$.

Therefore, we say two parameters to be equivalent if they have the same mask, and they are the same under this mask. More specifically, two parameters $\theta = (a_0, \ldots, a_N)$ and $\theta' = (a'_0, \ldots, a'_N)$ are equivalent if and only if $\beta'(\theta) = \beta'(\theta')$ and for any $i \in \beta'(\theta)$, $a_i = a'_i$. For any two equivalent parameters θ and θ', the algorithm gives the same output $A(\omega, \widetilde{\omega}, \theta) = A(\omega, \widetilde{\omega}, \theta')$.

Equivalent class We divide the parameter space Θ into a family of disjoint equivalent class Θ_i, such that $\Theta = \cup_i \Theta_i$.

Lemma 5. *For any equivalent class, the size is either* 1 *or* 2*. Moreover, the number of equivalent classes with* 2 *elements is at least* $\frac{|\Theta|}{4}$.

Proof of lemma 5. We first show that the size of each equivalent class is either 1 or 2. For each parameter $\theta = (a_0, \ldots, a_N)$, we have $|\widetilde{\beta}'(\theta)| = 2$ and $0 \in \widetilde{\beta}'(\theta)$. We denote the other element in $\widetilde{\beta}'(\theta)$ to be u such that $\widetilde{\beta}'(\theta) = \{0, u\}$. Then we have $\sum_{i \in \beta(\theta)} a_i = -\sum_{i \in \beta'(\theta)} a_i = -a_0 - a_u \in \{-2, 0, 2\}$. If $\sum_{i \in \beta(\theta)} a_i = -2$, then it is mandatory that $a_0 = -1$ and $a_u = -1$, therefore, there is no other parameter to be equivalent to θ and the size of equivalent class is 1. The situation is similar if $\sum_{i \in \beta(\theta)} a_i = 2$. When $\sum_{i \in \beta(\theta)} a_i = 0$, there are two possible value for a_0, a_u. $a_0 = 1, a_u = -1$ and $a_0 = -1, a_u = 1$ are both valid, so the size of the equivalent class is 2.

Before we control the number of equivalent classes, we extend the notation to represent the "path" of the mask and construct a bijection between parameters Θ and the path. Recall that $\beta'(\theta)$ can be constructed sequentially. We can start from an empty mask $\beta'_0(\theta)$ and $i = 0$. At each step of the algorithm, if gradient oracle is evaluated, we denote the index parameter for gradient oracle as t_{i+1}, we add it into the mask as $\beta'_{i+1}(\theta) = \beta'_i(\theta) \cup \{t_{i+1}\}$ and set $i \leftarrow i + 1$. At the end of the algorithm, we still have $i \leq N + 1$. We then repeatedly select largest index from $\{c \in \mathbb{N} | c \leq N, c \notin \beta'_i(\theta)\}$ as t_{i+1}, then append it to mask to form $\beta'_{i+1}(\theta)$ and increase i by 1. The above process is repeated until $i = N + 1$. It is easy to see that $|\beta'_i(\theta)| = i$ and $\beta'(\theta) = \beta'_{N-1}(\theta)$.

We define the mapping $p : \theta \in \Theta \mapsto (a_{t_1}, \ldots, a_{t_{N+1}}) \in \Theta$. This mapping is injective, as two different θ will give a_{t_i} at certain step in the construction. In the meantime, p is also a self-map. Therefore, p is a bijection, and every path $(a_{t_1}, \ldots, a_{t_{N+1}}) \in \Theta$ can be realized by exactly one $\theta \in \Theta$.

We next show that the number of equivalent classes with 2 elements is at least $\frac{|\Theta|}{4}$. First, we have $|\Theta| = \binom{N+1}{\frac{N+1}{2}}$. This is because choosing a θ is equivalent to selecting $\frac{N+1}{2}$ indexes from all $N + 1$ indexes to set 1 and set -1 for all other indexes. Next, we consider all θ that has distinct equivalent parameter. $\exists! \theta' \in \Theta, \theta \neq \theta', \beta'(\theta) = \beta'(\theta') \iff \sum_{i \in \beta'(\theta)} a_i = 0 \iff \sum_{i=1}^{N-1} a_{t_i} = 0$. Selecting a θ that has distinct equivalent parameter is equivalent to selecting half indexes for previous $N - 1$ elements in $(a_{t_1}, \ldots, a_{t_{N+1}})$ to be -1, one of a_N and a_{N+1} to be -1, and all others to be 1, and finally mapped back to θ with p^{-1}. Therefore, the number of θ that has distinct equivalent parameter is $2\binom{N-1}{\frac{N-1}{2}}$. Finally, the number of equivalent classes with 2 elements is $\binom{N-1}{\frac{N-1}{2}} = \frac{1}{4}(1 + \frac{1}{N})|\Theta| \geq \frac{1}{4}|\Theta|$. □

We only consider equivalent classes with 2 elements to derive a lower bound as follows.

$$
\begin{aligned}
&\frac{1}{|\Theta|}\sum_{\theta\in\Theta}[\boldsymbol{X}_T(\omega,\theta)-A(\omega,\widetilde{\omega},\theta)]^2\\
\geq&\frac{1}{|\Theta|}\sum_{\substack{\Theta_i\\|\Theta_i|=2}}\sum_{\theta\in\Theta_i}[\boldsymbol{X}_T(\omega,\theta)-A(\omega,\widetilde{\omega},\theta)]^2\\
\geq&\frac{1}{|\Theta|}\sum_{\substack{\Theta_i\\|\Theta_i|=2}}([\boldsymbol{X}_T(\omega,\theta)-A(\omega,\widetilde{\omega},\theta)]^2+[\boldsymbol{X}_T(\omega,\theta')-A(\omega,\widetilde{\omega},\theta)]^2)\big|_{\theta,\theta_i\in\Theta_i,\theta\neq\theta_i}\\
\geq&\frac{1}{|\Theta|}\sum_{\substack{\Theta_i\\|\Theta_i|=2}}\frac{1}{2}[\boldsymbol{X}_T(\omega,\theta)-\boldsymbol{X}_T(\omega,\theta')]^2\big|_{\theta,\theta_i\in\Theta_i,\theta\neq\theta_i}\\
\overset{①}{\geq}&\frac{1}{|\Theta|}\sum_{\substack{\Theta_i\\|\Theta_i|=2}}\frac{1}{2}C(T)^2\frac{1}{u}\\
\geq&\frac{1}{|\Theta|}\frac{1}{4}|\Theta|\frac{1}{2}C(T)^2\frac{1}{u}\\
=&\frac{1}{8}C(T)^2\frac{1}{u}
\end{aligned}
\tag{114}
$$

Inequality ① comes from lemma 6. We can just set $u=m$ for largest error.

If N is even integer, we just need to modify our construction of parameterized model. We define $\theta\in\Theta=\{(a_0,\dots,a_N)\in\{-1,1\}^{N+1}|\sum_0^N a_i=1\}$, and $f_i(x)=\frac{u}{2N}x^2-\sqrt{u}(a_i-1/N)x$ such that the global minimum still falls in $\{-\frac{1}{\sqrt{u}},\frac{1}{\sqrt{u}}\}$. Similarly, we can still define masks, equivalent parameters, equivalent class, and we can still have the number of equivalent classes with exactly two elements being larger than $\frac{1}{4}$ times total number of parameters. Finally, we can still give a lower bound in the same form.

C.2.2 Explicit ULD solution for 1-d quadratic potential

We consider ULD process on potential function $f(x)=\frac{u}{2}x^2$ starting from x_0,v_0.

$$
d\begin{bmatrix}x_t\\v_t\end{bmatrix}=\begin{bmatrix}0&1\\-u&-\gamma\end{bmatrix}\begin{bmatrix}x_t\\v_t\end{bmatrix}dt+\begin{bmatrix}0\\\sqrt{2\gamma}\end{bmatrix}dB_t \tag{115}
$$

We define $H=\begin{bmatrix}0&1\\-u&-\gamma\end{bmatrix}$. It is easy to verify that the following solution solves the SDE.

$$
\begin{bmatrix}x_t\\v_t\end{bmatrix}=e^{Ht}\begin{bmatrix}x_0\\v_0\end{bmatrix}+\int_0^t e^{H(t-s)}\begin{bmatrix}0\\\sqrt{2\gamma}\end{bmatrix}dB_t \tag{116}
$$

We can also derive e^{Ht} explicitly.

$$
e^{Ht}=\frac{1}{\lambda_+-\lambda_-}\left(e^{\lambda_- t}\begin{bmatrix}\lambda_+&1\\-u&-\lambda_-\end{bmatrix}-(e^{\lambda_+ t}\begin{bmatrix}\lambda_-&1\\-u&-\lambda_+\end{bmatrix}\right) \tag{117}
$$

$$
\lambda_\pm=\frac{\gamma\pm\sqrt{\gamma^2-4u}}{2} \tag{118}
$$

C.2.3 Difference between two ULD processes with same Brownian motion but different quadratic potential

Lemma 6. *Given two quadratic potential $f(x)=\frac{u}{2}x^2-\sqrt{u}x$ and $f'(x)=\frac{u}{2}x^2+\sqrt{u}x$, consider two ULD process $X_T(\omega,f)$ and $X_T(\omega,f')$ starting from same initialization $X_0=0,V_0=0$. Then, we have*

$$
0\leq X_T(\omega,f)-X_T(\omega,f')\leq C(T)\frac{1}{\sqrt{u}},
$$

where $C(T)$ only depends on T, γ, u.

Proof. First consider a quadratic potential $\widetilde{f}(x) = \frac{u}{2}x^2$. Then we have $X_T(\omega, f) = \frac{1}{\sqrt{u}} + \widetilde{X}_T(\omega, \widetilde{f})$ where $\widetilde{X}_T(\omega, \widetilde{f})$ is ULD process starting from $X_0 = -\frac{1}{\sqrt{u}}$. Similarly, $X_T(\omega, f') = -\frac{1}{\sqrt{u}} + \widetilde{X}'_T(\omega, \widetilde{f})$ where $\widetilde{X}'_T(\omega, \widetilde{f})$ is ULD process starting from $X_0 = \frac{1}{\sqrt{u}}$.

$\widetilde{X}_T(\omega, \widetilde{f})$ and $\widetilde{X}'_T(\omega, \widetilde{f})$ and be calculated explicitly by result in appendix C.2.2. Therefore, we have the following result.

$$0 \le X_T(\omega, f) - X_T(\omega, f') \le (1 - \frac{e^{-\lambda_- T}\lambda_+ - e^{\lambda_+ T}\lambda_-}{\lambda_+ - \lambda_-})\frac{2}{\sqrt{u}} \tag{119}$$

□

C.3 Error by perturbation

With similar tools in previous section, we can derive a lower bound by applying perturbation on a quadratic potential function.

C.3.1 Proof of theorem 6 for 1-d Case

Parameterized model For positive values $m < u < L$,C_x and ε, we define $x_i = \frac{NC_x}{2n}(i - \frac{n}{N})$ for $0 \le i \le \frac{2n}{N}$, $I_i = [x_i, x_{i+1})$ for $0 \le i < \frac{2n}{N}$, and $f_0(x) = \frac{u}{2N}x^2$.

Let parameter be $\theta \in \Theta = \{0, 1\}^{2n}$, we define $f_i(x)$ by it's gradient and global optimal. We require that $\nabla f_i(x) = \nabla f_0(x) + \sum_{j=0}^{\frac{2n}{N}-1} \theta_{jN+i}\, g(x - x_j)$ and $0 = \operatorname{argmin}_x f_i(x)$ for $1 \le i \le N$.

The function g represents a local perturbation.

$$g(x) := \begin{cases} \frac{4n\xi}{N^2 C_x}x^2 & x \in [0, \frac{NC_x}{8n}] \\ \frac{4n\xi}{N^2 C_x}[-(x - \frac{NC_x}{4n})^2 + 2(\frac{NC_x}{8n})^2] & x \in [\frac{NC_x}{8n}, \frac{3NC_x}{8n}] \\ \frac{4n\xi}{N^2 C_x}(x - \frac{NC_x}{2n})^2 & x \in [\frac{3NC_x}{8n}, \frac{NC_x}{2n}] \\ 0 & x \notin [0, \frac{NC_x}{2n}] \end{cases} \tag{120}$$

It can be easily verify that $\|g'\|_\infty = \frac{\xi}{N}$, $\|g\|_\infty = \frac{C_x\xi}{8n}$ and when $u - m \le \xi \le L - u$, we have $U = (f_1, \ldots, f_N) \in \mathcal{U}$ for every parameter θ.

Similar to the flat error case, we extend the notation to use $\boldsymbol{X}_T(\omega, \theta)$ and $A(\omega, \widetilde{\omega}, \theta)$ to mean $\boldsymbol{X}_T(\omega, U)$ and $A(\omega, \widetilde{\omega}, U)$ where U is above model with parameter θ.

$$e^2_{\mathcal{A}_n, \mathcal{U}} \ge \inf_{A \in \mathcal{A}_n} \mathbb{E}_{\omega \in \mathbb{P}} \mathbb{E}_{\widetilde{\omega} \in \widetilde{\mathbb{P}}} \frac{1}{|\Theta|} \sum_{\theta \in \Theta} [\boldsymbol{X}_T(\omega, \theta) - A(\omega, \widetilde{\omega}, \theta)]^2 \tag{121}$$

Mask The algorithm takes n steps to calculate $A(\omega, \widetilde{\omega}, \theta)$. During this process, n oracle are evaluated. Therefore, there is at most n gradient oracle evaluation $\Upsilon_U(i, x)$. For each gradient oracle evaluation, if $x \in [-\frac{C_x}{2}, \frac{C_x}{2})$, then there exists exactly one j such that $x \in I_j$. In this case, we add $jN + i$ into the mask.

Let $\mathcal{J} = \{m \subseteq [2n]\} = 2^{[2n]}$, we define a mapping $\beta : \theta \in \Theta \mapsto \beta(\theta) \in \mathcal{J}$ to represent the mask. More specifically, $\beta(\theta)$ contains index $jN + i$ if and only if, at a certain step during calculating $A(\omega, \widetilde{\omega}, \theta)$, the algorithm evaluates the gradient oracle $\Upsilon_U(i, x)$ with $x \in I_j$.

Expanded mask We have $|\beta(\theta)| \le n$, since there is at most n gradient evaluation. We expand this mask into $\beta'(\theta)$ to make sure $|\beta'(\theta)| = n$ by repeatedly adding the largest element in $[2n]$ that is still not inside $\beta(\theta)$ until the size reaches n. More specifically, we can always find k, such that $|\beta(\theta) \cup \{i \in \mathbb{N}^+ | k \le i \le 2n\}| = n$ and we let $\beta'(\theta) = \beta(\theta) \cup \{i \in \mathbb{N}^+ | k \le i \le 2n\}$.

Complementary mask We define $\widetilde{\beta}'(\theta) = \{i \in \mathbb{N}^+ | i \le 2n\} \setminus \beta'(\theta)$ as complementary mask to represent how much information is not relevant to the algorithm output. It is easy to see that $|\widetilde{\beta}'(\theta)| = n$.

Equivalent parameters We say two parameters to be equivalent if they have the same mask, and they are the same under this mask. More specifically, two parameters θ and θ' are equivalent if and only if $\beta'(\theta) = \beta'(\theta')$ and for any $i \in \beta'(\theta)$, $\theta_i = \theta'_i$. For any two equivalent parameters θ and θ', the algorithm gives the same output $A(\omega, \widetilde{\omega}, \theta) = A(\omega, \widetilde{\omega}, \theta')$.

Equivalent class We divide the parameter space Θ into a family of disjoint equivalent class Θ_i, such that $\Theta = \cup_i \Theta_i$.

For each parameter θ, by altering different digits at $\widetilde{\beta}'(\theta)$, we can construct 2^n different equivalent parameter, therefore, the size of any equivalent class is always 2^n. Then the number of equivalent classes is just $2^{2n}/2^n = 2^n$.

We next construct a pairing between parameters in each equivalent class Θ_i with a self-map S on Θ_i. For any $\theta, \theta' \in \Theta_i$, we construct an order between them $\theta \succ \theta' \iff \forall i \in \widetilde{\beta}'(\theta), \theta_i \geq \theta'_i$. Based on this order, all 2^n elements in Θ_i forms a Boolean lattice. The rank of θ in this lattice is just $\rho(\theta) = |\{i \in \widetilde{\beta}'(\theta) | \theta_i = 1\}|$. We select a symmetric chain decomposition $\mathcal{C}$ for this Boolean lattice. For any parameter $\theta \in \Theta_i$, there exist only one symmetric chain $C \in \mathcal{C}$ that contains θ. We pick the element θ' in chain C with rank $\rho(\theta') = n - \rho(\theta)$. This always possible because the chain is rank-symmetric and saturated. We then define the map $S : \theta \mapsto \theta'$. This mapping is bijective and $S(S(\theta)) = \theta$.

$$
\begin{aligned}
&\frac{1}{|\Theta|}\sum_{\theta\in\Theta}[\boldsymbol{X}_T(\omega,\theta) - A(\omega,\widetilde{\omega},\theta)]^2 \\
=&\frac{1}{|\Theta|}\sum_{\Theta_i}\sum_{k=0}^{n}\sum_{\substack{\theta\in\Theta_i\\ \rho(\theta)=k}}[\boldsymbol{X}_T(\omega,\theta) - A(\omega,\widetilde{\omega},\theta)]^2 \\
=&\frac{1}{|\Theta|}\sum_{\Theta_i}\sum_{k=0}^{n}\sum_{\substack{\theta\in\Theta_i\\ \rho(\theta)=k}}\frac{1}{2}([\boldsymbol{X}_T(\omega,\theta) - A(\omega,\widetilde{\omega},\theta)]^2 + [\boldsymbol{X}_T(\omega,S(\theta)) - A(\omega,\widetilde{\omega},\theta)]^2) \\
\geq&\frac{1}{|\Theta|}\sum_{\Theta_i}\sum_{k=0}^{n}\sum_{\substack{\theta\in\Theta_i\\ \rho(\theta)=k}}\frac{1}{4}[\boldsymbol{X}_T(\omega,\theta) - \boldsymbol{X}_T(\omega,S(\theta))]^2 \\
\overset{①}{\geq}&\frac{1}{|\Theta|}\sum_{\Theta_i}\sum_{k=0}^{n}\sum_{\substack{\theta\in\Theta_i\\ \rho(\theta)=k}}\frac{1}{4}[C\frac{N\xi}{n^2}(n-k-k)]^2\mathbb{I}_{\mathcal{E}}(\omega) \\
=&\frac{1}{2^{2n}}2^n\sum_{k}^{n}\binom{n}{k}\frac{1}{4}[C\frac{N\xi}{n^2}(n-k-k)]^2\mathbb{I}_{\mathcal{E}}(\omega) \\
=&\frac{1}{4}C^2\xi^2\frac{N^2}{n^4}\mathbb{I}_{\mathcal{E}}(\omega)
\end{aligned}
\tag{122}
$$

Inequality ① comes from lemma 7.

$$
\begin{aligned}
e^2_{\mathcal{A}_n,\mathcal{U}} \geq& \inf_{A\in\mathcal{A}_n}\mathbb{E}_{\omega\in\mathbb{P}}\mathbb{E}_{\widetilde{\omega}\in\widetilde{\mathbb{P}}}\frac{1}{|\Theta|}\sum_{\theta\in\Theta}[\boldsymbol{X}_T(\omega,\theta) - A(\omega,\widetilde{\omega},\theta)]^2 \\
\geq& \inf_{A\in\mathcal{A}_n}\mathbb{E}_{\omega\in\mathbb{P}}\mathbb{E}_{\widetilde{\omega}\in\widetilde{\mathbb{P}}}\frac{1}{4}C^2\xi^2\frac{N^2}{n^3}\mathbb{I}_{\mathcal{E}}(\omega) \\
=&\frac{1}{4}C^2\xi^2\mathbb{P}(\mathcal{E})\frac{N^2}{n^3}
\end{aligned}
\tag{123}
$$

Then we can optimize all free parameter including ξ,C_x and C_v introduced in appendix C.3.2 to derive final result.

$$
e^2_{\mathcal{A}_n,\mathcal{U}} \geq C_2\frac{N^2}{n^3} \tag{124}
$$

According to the discussion in appendix C.3.2, $\varepsilon = \frac{NC_x\xi}{8n} \leq \frac{C_x\xi}{8}$ and we can always select parameters, so that ε is small enough and C_v is large enough such that $\mathbb{P}(\mathcal{E}) > 0$. Therefore, we have $C_2 > 0$.

C.3.2 Perturbation error

For positive values $\varepsilon > 0$,$C_v > 0$ we define

$$\mathcal{U}_{u,\varepsilon} = \{(f_1, \ldots, f_N) \in \mathcal{U} | \| \sum_{i}^{N} \nabla f_i(x) - ux\|_\infty \leq \varepsilon\} \tag{125}$$

$$\begin{aligned}\mathcal{E} = \{\omega \in \mathbb{M} | \forall U \in \mathcal{U}_{u,\varepsilon},\ &\sup_{0\leq t\leq T} \boldsymbol{X}_t(\omega, U) \geq C_x, \\ &\inf_{0\leq t\leq T} \boldsymbol{X}_t(\omega, U) \leq -C_x,\ \sup_{0\leq t\leq T} \boldsymbol{V}_t(\omega, U) \leq C_v\}\end{aligned} \tag{126}$$

[10, Lemma 2.3, Lemma 3.2] When ε is small enough and C_v is large enough, the event $\mathcal{E}$ happens with a positive probability. More specifically, there exists $\overline{\varepsilon} > 0$ that only depends on L, u, C_x, C_v and $\overline{C_v}$ that only depends on L, u, C_x , such that when $\varepsilon \leq \overline{\varepsilon}$ and $C_v \geq \overline{C_v}$, we have $\mathbb{P}(\mathcal{E}) > 0$.

[10, Proposition 3.1] Given $U^{(1)}, U^{(2)} \in \mathcal{U}_{u,\varepsilon}$, $\mathcal{I} \subseteq [-\frac{C_x}{2}, \frac{C_x}{2}]$ as finite union of closed bounded interval, such that

$$g(x) = \sum_{i=1}^{N} \nabla f_i^{(1)}(x) - \sum_{i=1}^{N} \nabla f_i^{(2)}(x) \geq c\varepsilon \mathbb{I}_{\mathcal{I}}(x), \forall x \in \mathbb{R}$$

where $\mathbb{I}$ is the indicator function. Then for every $\omega \in \mathcal{E}$ we have

$$\boldsymbol{X}_T(\omega, U^{(2)}) - \boldsymbol{X}_T(\omega, U^{(1)}) \geq \overline{C} c\varepsilon \mu(\mathcal{I})$$

where $\overline{C}$ is always positive and only depends on L, u, C_x, C_v.

Remark 4. *The statement in the above proposition is not exactly the same as the original statement in [10]. Some modification is made to adapt to this paper's setup. We address these differences as follows.*

Value u_R: The original statement in [10] assumes $\nabla^2 U(x) \leq u_R \leq L$. Here we just assume $u_R = L$ for simplicity.

Sign: The original statement in [10, Proposition 3.1] only gives lower bounds for absolute value $|\boldsymbol{X}_T(U^{(1)}, \omega) - \boldsymbol{X}_T(U^{(2)}, \omega)|$. However, [10, Lemma 3.7] already shows that $\boldsymbol{X}_T(U^{(1)}, \omega) - \boldsymbol{X}_T(U^{(2)}, \omega) \leq 0$.

Scale of $g(x)$: The original statement in [10, Proposition 3.1] assumes $c = \frac{1}{2}$, however, this is not necessary. In the proof of [10, Proposition 3.1], $g(x)$ is used linearly, therefore the proposition should be valid for all c. We always have $c \leq 2$ because $U^{(1)}, U^{(2)} \in \mathcal{U}_{u,\varepsilon}$.

Scale of ULD process: The SDE for ULD in [10] has different scale than this paper, this can be resolved by a linear transformation as discussed in Appendix A.3 or simply assuming $\gamma = 2$ and $L = 1$.

Lemma 7. *Let $\varepsilon = \frac{NC_x\xi}{8n}$. If $\omega \in \mathcal{E}$, then for any two parameter θ, θ' in an equivalent class Θ_i, if $\theta \prec \theta'$, we have*

$$\boldsymbol{X}_T(\omega, \theta) - \boldsymbol{X}_T(\omega, \theta') \geq C\frac{N\xi}{n^2}(\rho(\theta') - \rho(\theta))$$

where C is always positive and only depends on L, u, C_x, C_v.

Proof of lemma 7. For any θ, we have $U \in \mathcal{U}_{u,\varepsilon}$.

Recall that Θ_i forms a finite Boolean lattice with order $\succ$. Therefore, we can always find a saturated chain $\theta^{(\rho(\theta))} \prec \theta^{(\rho(\theta))+1} \prec \cdots \prec \theta^{(\rho(\theta'))}$, so that $\theta = \theta^{(\rho(\theta))}$ and $\theta' = \theta^{(\rho(\theta'))}$.

For any two adjacent element in this chain $\theta^{(u)}, \theta^{(u+1)} \in 2^{[2n]}$, we know that $\theta^{(u+1)}$ is only greater than $\theta^{(u)}$ at one index $jN + i$. Therefore, the corresponding functions $f^{(u)} = \sum_{i=1}^{N} f_i^{(u)}(x)$ and

$f^{(u+1)} = \sum_{i=1}^{N} f_i^{(u+1)}(x)$ only differ at $f_i(x)$ within interval I_j. More specifically, $\nabla f^{(u+1)}(x) - \nabla f^{(u)}(x) = g(x - x_j) \geq \frac{1}{2N}\varepsilon \mathbb{I}_{\mathcal{I}}$ where $\mathcal{I} = [x_j + \frac{NC_x}{8n}, x_j + \frac{3NC_x}{8n}]$. [10, Proposition 3.1] can be applied to give

$$\boldsymbol{X}_T(\omega, U^{(u)}) - \boldsymbol{X}_T(\omega, U^{(u+1)}) \geq \overline{C}\frac{NC_x^2\xi}{64n^2}$$

Telescoping the above inequality for all u, we have

$$\boldsymbol{X}_T(\omega, U^{(\rho(\theta))}) - \boldsymbol{X}_T(\omega, U^{(\rho(\theta'))}) \geq \overline{C}\frac{NC_x^2\xi}{64n^2}(\rho(\theta') - \rho(\theta))$$

□

C.4 High dimension case

In this section we extend the proof in previous sections to high dimensional space.

We have already established a parameterized model for controlling both flat error and perturbation error in 1 -dimensional space. We now define a parameterized model for high dimensional space. The parameter space is just the Cartesian product of parameters for a single dimension $\Theta = \times_{i=1}^{d}\Theta^{(i)}$. Given a parameter $(\theta^{(1)}, \ldots, \theta^{(d)}) \in \Theta$, we construct a potential function as follows. For each $1 \leq i \leq d$, let $\widetilde{f^{(i)}}$ be the 1-d potential corresponding to $\theta^{(i)}$. Then we define $f(\boldsymbol{X}) = \sum_{i=1}^{d} f^{(i)}(\boldsymbol{X}) = \sum_{i=1}^{d} \widetilde{f^{(i)}}(\boldsymbol{X}^{(i)})$. Clearly, the different dimension components of ULD decouple with each other, so $\boldsymbol{X}_T^{(i)}$ is just a ULD on the 1-dimensional potential $\widetilde{f^{(i)}}$ and is only affected by $\theta^{(i)}$.

$$\begin{aligned}
e_{\mathcal{A},\mathcal{U}}^2 &= \inf_{A\in\mathcal{A}}\sup_{U\in\mathcal{U}}\mathbb{E}_{\omega\in\mathbb{P}}\mathbb{E}_{\widetilde{\omega}\in\widetilde{\mathbb{P}}}\|\boldsymbol{X}_T(\omega, U) - A(\omega, \widetilde{\omega}, U)\|_2^2 \\
&= \inf_{A\in\mathcal{A}}\sup_{U\in\mathcal{U}}\mathbb{E}_{\omega\in\mathbb{P}}\mathbb{E}_{\widetilde{\omega}\in\widetilde{\mathbb{P}}}\sum_{i=1}^{d}[\boldsymbol{X}_T^{(i)}(\omega, U) - A^{(i)}(\omega, \widetilde{\omega}, U)]^2 \\
&\geq \inf_{A\in\mathcal{A}}\frac{1}{\prod_{i=1}^{d}|\Theta^{(i)}|}\sum_{\substack{\theta^{(i)}\in\Theta^{(i)} \\ i=1,\ldots,d}}\mathbb{E}_{\omega\in\mathbb{P}}\mathbb{E}_{\widetilde{\omega}\in\widetilde{\mathbb{P}}}\sum_{i=1}^{d}[\boldsymbol{X}_T^{(i)}(\omega, \theta) - A^{(i)}(\omega, \widetilde{\omega}, \theta)]^2 \\
&\geq \inf_{A\in\mathcal{A}}\sum_{i=1}^{d}\frac{1}{\prod_{j\neq i}|\Theta^{(j)}|}\sum_{\substack{\theta^{(j)}\in\Theta^{(j)} \\ j\neq i}}\mathbb{E}_{\omega\in\mathbb{P}}\mathbb{E}_{\widetilde{\omega}\in\widetilde{\mathbb{P}}} \\
&\qquad\qquad \frac{1}{|\Theta^{(i)}|}\sum_{\theta^{(i)}\in\Theta^{(i)}}[\boldsymbol{X}_T^{(i)}(\omega, \theta) - A^{(i)}(\omega, \widetilde{\omega}, \theta)]^2
\end{aligned} \tag{127}$$

By fixing dimension index i, all other parameters $\theta^{(j)} \in \Theta^{(j)}$ with $j \neq i$, random events $\omega, \widetilde{\omega}$, we reduce the problem into constructing lower bounds for $\frac{1}{|\Theta^{(i)}|}\sum_{\theta^{(i)}\in\Theta^{(i)}}[\boldsymbol{X}_T^{(i)}(\omega, \theta) - A^{(i)}(\omega, \widetilde{\omega}, \theta)]^2$. This is exactly the same as the case for 1-d problem, and we can again define the mask, expanded mask, complementary mask, equivalent parameters under this setting and generate the same lower bounds. Therefore, the lower bound for error of d dimensional space is just d times the result from 1 dimensional case.

C.5 Proof of corollary 2

When $\varepsilon^2 < dC_1$, according to theorem 5, we know that $n \geq N$.

Let $n' = \lceil \frac{n}{N} \rceil N$, we have $n \leq n' \leq n + N - 1$. According to theorem 6, we have $e_{\mathcal{A}_{n'},\mathcal{U}}^2 \geq dC_2\frac{N^2}{n'^3}$. According to monotonicity, we have $e_{\mathcal{A}_n,\mathcal{U}} \geq e_{\mathcal{A}_{n'},\mathcal{U}}$. We also have $\varepsilon \geq e_{\mathcal{A}_n,\mathcal{U}}$. Combining the above inequities gives us $n \geq C_2^{\frac{1}{3}}d^{\frac{1}{3}}N^{\frac{2}{3}}\varepsilon^{-\frac{2}{3}} - N + 1$.

We then combine above two lower bounds to finish the proof.

$$\begin{aligned} n \geq & \frac{2}{3}N + \frac{1}{3}(C_2^{\frac{1}{3}} d^{\frac{1}{3}} N^{\frac{2}{3}} \varepsilon^{-\frac{2}{3}} - N + 1) \\ \geq & \frac{1}{3}(N + C_2^{\frac{1}{3}} d^{\frac{1}{3}} N^{\frac{2}{3}} \varepsilon^{-\frac{2}{3}} + 1) \end{aligned} \tag{128}$$

D Extra discussion on experiments

D.1 Estimating the discretization error

We wish to calculate discretization error $\sqrt{\|\boldsymbol{x}_K - \boldsymbol{X}_{Kh}\|_2^2 + \|\boldsymbol{v}_K - \boldsymbol{V}_{Kh}\|_2^2}$ for comparing different algorithms, where $\boldsymbol{x}_k$,$\boldsymbol{v}_k$ are generated by the algorithm, and $\boldsymbol{X}_t$,$\boldsymbol{V}_t$ are the true solution.

For an arbitrary non-linear model, the true solution of ULD process might not be available in closed form. Therefore, instead of calculating the error between an algorithm and the true solution, we calculate the error between an algorithm and another algorithm which is guaranteed to have much smaller discretization error. This typically can be achieved with a full gradient RMM with small enough step size.

Naturally, a following question is how to make sure these two algorithms are approximating the same ULD process. In another word, we need to make sure that the noise terms in these two algorithms are derived from the same realization of Brownian motion. We introduce a novel technique by accumulating the noise terms in the algorithms with smaller step size to generate the noise term for algorithms with larger step size. If the two algorithms uses step size h' and nh' respectively with positive integer n, we show that the noise terms $\boldsymbol{e}_{x,[0,nh']}$, $\boldsymbol{e}_{v,[0,nh']}$, $\boldsymbol{e}_{x,[0,anh']}$ can be represented as a combination of $\boldsymbol{e}_{x,[ih',(i+1)h']}$, $\boldsymbol{e}_{v,[ih',(i+1)h']}$, $\boldsymbol{e}_{x,[\lfloor an \rfloor h',anh']}$. The detailed derivation can be found in appendix A.11.

Finally, we calculate an average of errors along the path instead of at last iterate to reduce variance. We call this as trajectory error.

The final method to estimate the discretization error is shown in Algorithm 3. Typically, we select algorithm B as RMM with full gradient and segments number $n = 10$ to approximate discretization error for an algorithm A.

A following question is: how accurate this estimation is to the real trajectory error $\frac{1}{K}\sum_{i=1}^{K}\sqrt{\|\boldsymbol{x}_k - \boldsymbol{X}_{kh}\|_2^2 + \|\boldsymbol{v}_k - \boldsymbol{V}_{kh}\|_2^2}$? We know that when n increases, $h' = \frac{h}{n}$ decreases, so the reference path converge to the real solution. Therefore, by selecting a large enough n, we can approximate the trajectory error to arbitrary accuracy. We apply Algorithm 3 to estimate the trajectory error of RMM with fixed step size under different segments number n. Figure 4 shows that selecting $n = 10$ could generate an accurate enough estimate.

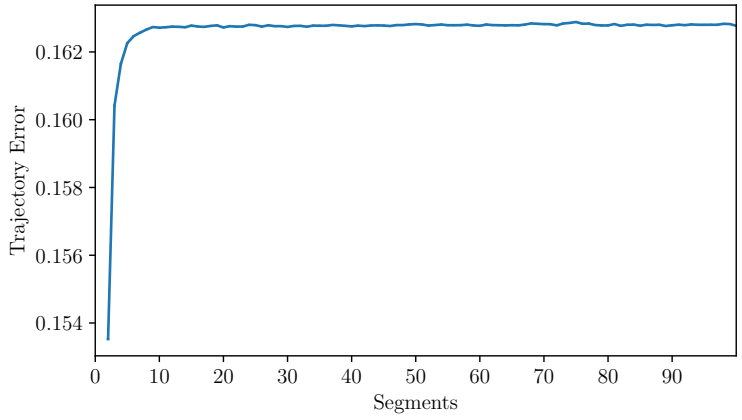

Figure 4: Estimated trajectory error of RMM with different segments number.

Algorithm 3: Method to estimating trajectory error.

Input: Initial point $(\boldsymbol{x}_0, \boldsymbol{v}_0)$, parameter γ, iteration number K and step size $h > 0$.
Input: Two algorithms $A, B \in \{\text{LPM}, \text{RMM}, \text{ALUM}, \text{VR-ALUM}, \dots\}$, number of segments n.
Initialize $\boldsymbol{x}'_0 = \boldsymbol{x}_0$,$\boldsymbol{x}'_0 = \boldsymbol{x}_0$.
for $k = 0$ **to** $K - 1$ **do**
  $h' = \frac{h}{n}$;
  // Generate noise terms
  for $i = 0$ **to** $n - 1$ **do**
    Randomly sample a_i uniformly from $[0, 1]$;
    Generate $\boldsymbol{e}_{x,[ih',(i+1)h']}$, $\boldsymbol{e}_{v,[ih',(i+1)h']}$, $\boldsymbol{e}_{x,[ih',(i+a_i)h']}$ according to appendix A.5;
  end for
  // Generate reference path
  Initialize $\boldsymbol{x}''_0 = \boldsymbol{x}'_k$,$\boldsymbol{x}''_0 = \boldsymbol{x}'_k$.
  for $i = 0$ **to** $n - 1$ **do**
    Generate $\boldsymbol{x}''_{i+1}$ and $\boldsymbol{v}''_{i+1}$ by algorithm B with input $\boldsymbol{x}''_i$ and $\boldsymbol{v}''_i$ and noise terms $\boldsymbol{e}_{x,[ih',(i+1)h']}$, $\boldsymbol{e}_{v,[ih',(i+1)h']}$, $\boldsymbol{e}_{x,[ih',(i+a_i)h']}$;
  end for
  $\boldsymbol{x}'_{k+1} = \boldsymbol{x}''_n$,$\boldsymbol{v}'_{k+1} = \boldsymbol{v}''_n$.
  // Accumulate noise terms
  Randomly sample $j \in \{0, \dots, n-1\}$ with uniform distribution and let $a' = j + a_j$, $a = \frac{a'}{n}$;
  $\boldsymbol{e}_{x,[0,h]} = \sum_{i=0}^{n-1} \left(\boldsymbol{e}_{x,[ih',(i+1)h']} + \psi_1((n-i-1)h')\boldsymbol{e}_{v,[ih',(i+1)h']}\right)$;
  $\boldsymbol{e}_{v,[0,h]} = \sum_{i=0}^{n-1} \psi_0((n-i-1)h')\boldsymbol{e}_{v,[ih',(i+1)h']}$;
  $\boldsymbol{e}_{x,[0,ah]} = \boldsymbol{e}_{x,[\lfloor a' \rfloor h', a'h']} + \sum_{i=0}^{\lfloor a' \rfloor - 1} \left(\boldsymbol{e}_{x,[ih',(i+1)h']} + \psi_1((a'-i-1)h')\boldsymbol{e}_{v,[ih',(i+1)h']}\right)$;
  // Generate original path with large step size
  Generate $\boldsymbol{x}_{k+1}$ and $\boldsymbol{v}_{k+1}$ by algorithm A with input $\boldsymbol{x}_k$ and $\boldsymbol{v}_k$ and noise terms $\boldsymbol{e}_{v,[0,h]}$, $\boldsymbol{e}_{v,[0,h]}$, $\boldsymbol{e}_{x,[0,ah]}$;
end for
Output: $\frac{1}{K}\sum_{i=1}^{K} \sqrt{\|\boldsymbol{x}_k - \boldsymbol{x}'_k\|_2^2 + \|\boldsymbol{v}_k - \boldsymbol{v}'_k\|_2^2}$.

There also exists theoretical guarantee on the accuracy of this trajectory error estimation. Since we use RMM for algorithm B, we have discretization error for this reference path as $O(h'^{\frac{3}{2}}) = O(h^{\frac{3}{2}} n^{-\frac{3}{2}})$. Therefore, by selecting $n = 10$, we know the discretization error for this reference path is at least $10^{\frac{3}{2}} \approx 30$ times smaller than RMM with original step size. The accuracy can then be derived as $\|\boldsymbol{z}_k - \boldsymbol{Z}_{kh}\|_{\mathbb{L}_2} - \|\boldsymbol{z}'_k - \boldsymbol{Z}_{kh}\|_{\mathbb{L}_2} \le \|\boldsymbol{z}_k - \boldsymbol{z}'_k\|_{\mathbb{L}_2} \le \|\boldsymbol{z}_k - \boldsymbol{Z}_{kh}\|_{\mathbb{L}_2} + \|\boldsymbol{z}'_k - \boldsymbol{Z}_{kh}\|_{\mathbb{L}_2}$. [11]

D.2 Detailed setup

Datasets For Gaussian model:

$$f_i(\boldsymbol{x}) = \frac{1}{2N}(\boldsymbol{d}_i - \boldsymbol{x})^\top \Sigma^{-1}(\boldsymbol{d}_i - \boldsymbol{x}), \tag{129}$$

we let $d = 5$ and $N = 100$. The vectors $\boldsymbol{d}_i$ are generated from $\mathcal{N}(\mathbf{2}, 2I)$, where $\mathbf{2}$ is a vector with 2 in all its elements. Σ is generated by QR decomposition of a random Gaussian matrix and then re normalized to have smallest and largest eigenvalue of $m = 1$,$L = 10$.

For logistic regression:

$$f_i(\boldsymbol{x}) = \frac{m}{2N}\|\boldsymbol{x}\|_2^2 + \sum_{i=1}^{N} \log(1 + \exp(-y_i \boldsymbol{a}_i^\top \boldsymbol{x})), \tag{130}$$

we summarize four datasets used in Table 4. We split the dataset by half randomly for training and testing model. We set parameter m according to $L = \frac{1}{4}\sigma_{\max}(A^\top A) + m$ such that the final condition number κ is 10^4 for australian, 10^5 for phishing dataset, 10^3 for german dataset, and 10 for mushromms dataset.

[11] Actually, this analysis is not tight. As we can see in fig. 4, $n = 2$ could achieve about $1/10$ relative accuracy, but the theory predicts about $2^{\frac{3}{2}} \approx 1/3$. Most error of RMM comes from the variance instead of bias, which affects the estimate error differently. We leave the tight analysis of trajectory error estimation for future works.

Table 4: The summary of different datasets used in our experiments.

Dataset	australian	german	phishing	mushrooms
N	690	1000	11055	8124
d	14	24	68	112

Hyperparameters If there is no further explanation, we use $b = 20$ for Gaussian model and $b = 40$ for Logistic regression models.

We use $\tau \approx N/b$ for SVRG. More specifically, we update the full gradient after every N evaluations of the single component gradient $\nabla f_i(x)$. This means that the epoch length of different epochs can vary up to 1. This setup doesn't affect our theoretical result, as the bounded MSE property in Appendix B.3 always holds for SVRG with $\Theta = \frac{N^2}{b^3}$.

Tasks

1. Discussing the relationship between error and gradient evaluation number: We first transform the potential to satisfy $L = 1$, as discussed in Remark 1. Then we choose certain step size h, run different algorithms to estimate ULD till time T. Time T is $T = 10$ for Gaussian model and $T = 100$ for logistic regression. For any chosen step size h, we can record how many gradient oracles $\nabla f_i(x)$ was evaluated for x-axis and record the trajectory error as y-axis.
2. Discussing the relationship between error and step size: We use same T and other settings as above. The only difference is that we report step size in x-axis.
3. Discussing the relationship between error and batch size: We select a group of batch sizes b. For each b, we use the same settings as Item 1 to generate the plot.
4. Sampling: The detailed setup for sampling is shown in Appendix D.6.

D.3 Results on other datasets

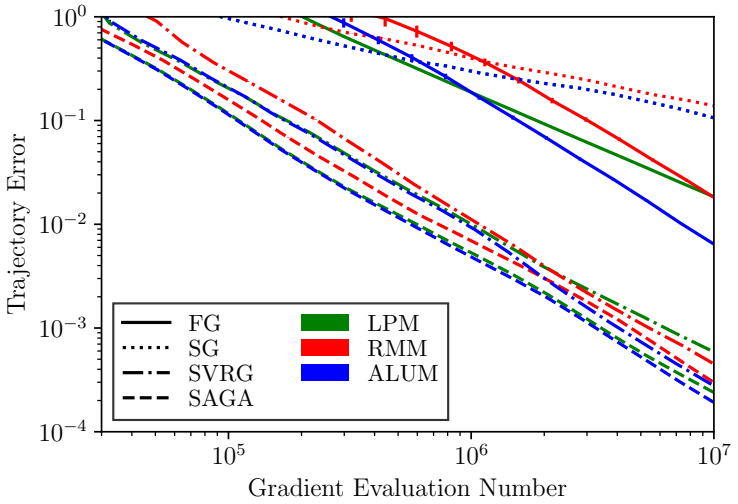

Figure 5: Logistic regression on phishing dataset.

We show discretization error on phishing, german, and mushrooms datasets in Figures 5 to 7.

We can see that SAGA-ALUM constantly outperforms all other algorithms.

Although in Figure 5, the difference between SAGA-ALUM and SAGA-LPM seems small when we only consider less than 10^7 gradient evaluations, we know that gradient complexity of LPM has worse dependence on accuracy ε, therefore the difference will grow larger when we increase the budget of gradient evaluations.

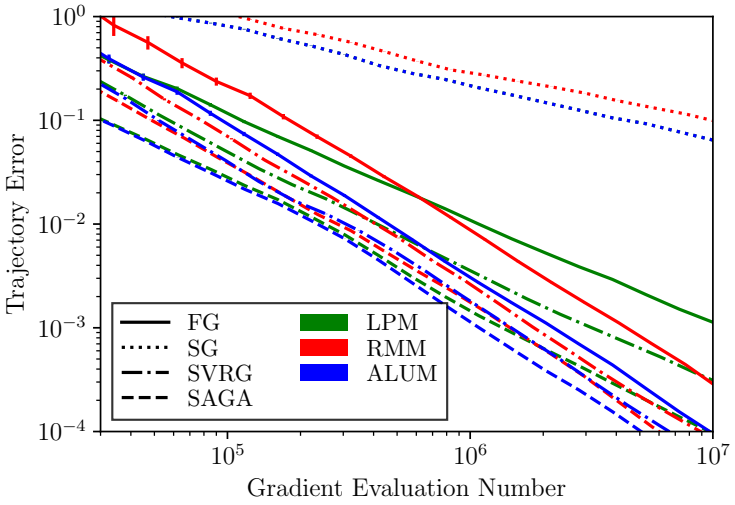

Figure 6: Logistic regression on german dataset.

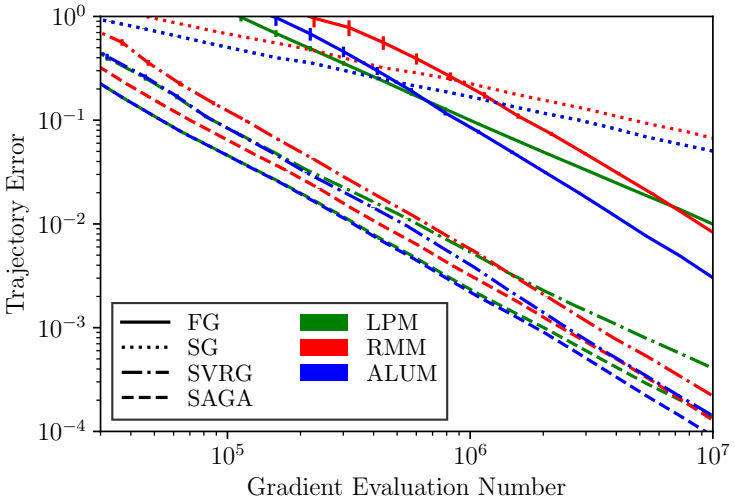

Figure 7: Logistic regression on mushrooms dataset.

D.4 Dependency on step size

In contrast to Figure 1, we adopt a different point of view in this section by considering the relationship between accuracy and step size.

Figure 8 verifies our theoretical result that discretization error is $O(h^{\frac{3}{2}})$ for ALUM.

We can also see that SAGA-ALUM has higher discretization error than SVRG-ALUM when using same step size. However, practically, SAGA uses less gradient evaluations per iteration, therefore achieves better gradient efficiency.

We also notice that given the same step size, the SAGA-RMM and SVRG-RMM have smaller error than SAGA-ALUM and SVRG-ALUM respectively. However, ALUM uses only one gradient evaluation per iteration in contrast to RMM which takes two, therefore ALUM based algorithms achieves better gradient efficiency.

Finally, we note that our theory analysis is only valid for small enough step size. For example, Theorem 4 requires $h^3 \leq \frac{1}{2304c} b^3 m N^{-2}$ and $h \leq \frac{m}{22}$. For a given step size h, our theory might not be applicable if N is too large or b is too small. This happens on phishing and mushrooms datasets where sample size N is much larger than australian and german datasets, but we use the same batch

size. Figures 8c and 8e shows that trajectory error's dependence of step size h is roughly $O(h^{1/2})$ when step size is relatively large, and then becomes $O(h^{3/2})$ when step size keeps decreasing.

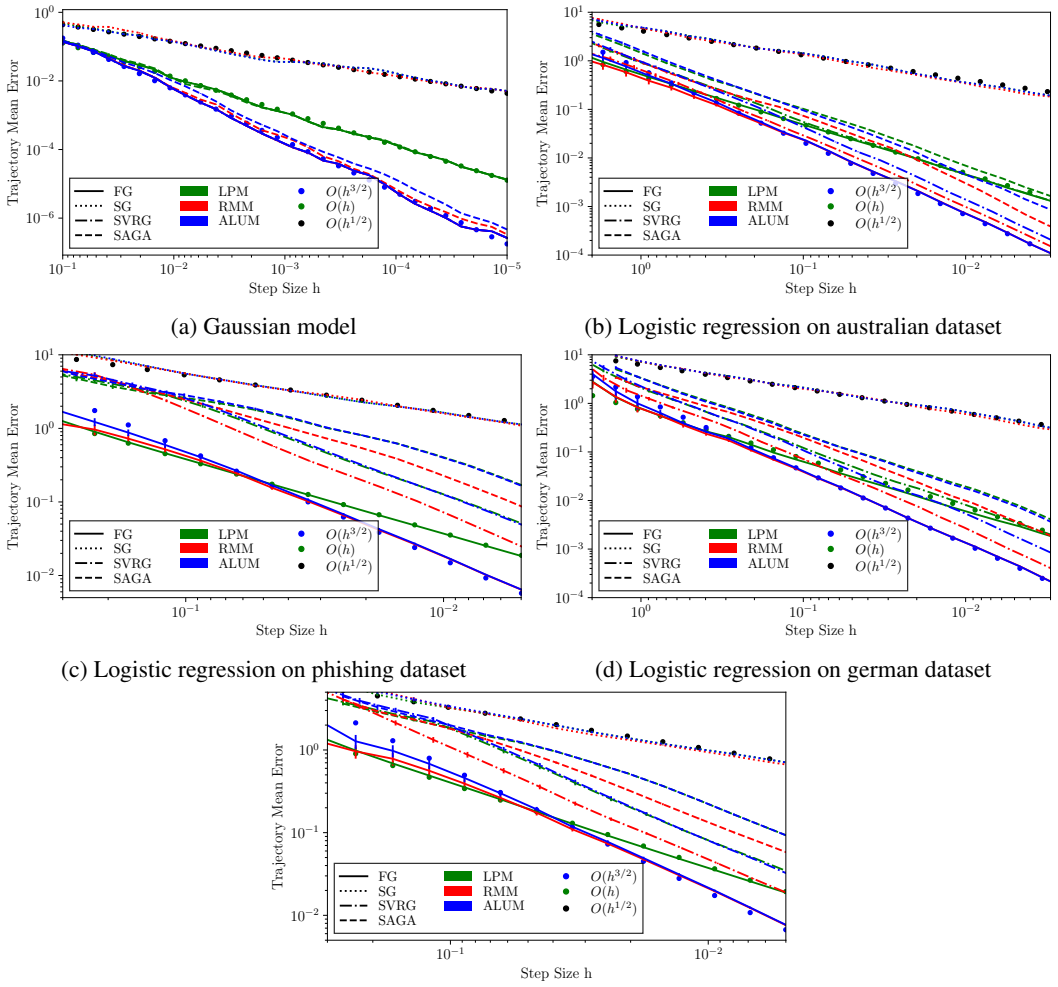

(a) Gaussian model

(b) Logistic regression on australian dataset

(c) Logistic regression on phishing dataset

(d) Logistic regression on german dataset

(e) Logistic regression on mushrooms dataset

Figure 8: Discretization error on australian dataset for different algorithms under different step size.[12]

D.5 Dependency on batch size

Here, we give an intuition why our method is not sensitive to batch size when batch size is relatively small, and why the efficiency deteriorate for very large batch size.

We can roughly split the discretization error between the vector generated by the VR-ALUMs $\boldsymbol{z}_k^{(o)\widetilde{\nabla}}$ and true solution $\boldsymbol{Z}_{kh}$ as two part: (1) Difference between $\boldsymbol{z}_k^{(o)\widetilde{\nabla}}$ and $\boldsymbol{z}_k^{(o)}$ generated by the full gradient ALUM. We denote $E_1 = \|\boldsymbol{z}_k^{(o)\widetilde{\nabla}} - \boldsymbol{z}_k^{(o)}\|_{\mathbb{L}_2}^2$. (2) Difference between $\boldsymbol{z}_k^{(o)}$ and $\boldsymbol{Z}_{kh}$ as two part. We denote $E_2 = \|\boldsymbol{z}_k^{(o)} - \boldsymbol{Z}_{kh}\|_{\mathbb{L}_2}^2$.

According to analysis in Appendix B, we have $E_1 = O(h^3 \frac{N^2}{b^3})$ and $E_2 = O(h^3)$.

Next, we show that E_1 is irrelevant to b if we fix the total number of gradient evaluation n. Since every iteration need $O(b)$ gradient evaluation, we can have at most $K = O(\frac{n}{b})$ iterations. Then the

[12] On phishing dataset and mushrooms datasets, SAGA-LPM, SVRG-LPM highly overlap with SAGA-ALUM and SVRG-ALUM respectively.

step size is $h = \frac{T}{K} = O(\frac{Tb}{n})$. Therefore, we can see $E_1 = \frac{T^3N^2}{n^3}$ so this part of error doesn't change with respect to batch size.

On the other hand, $E_2 = h^3 = O(\frac{T^3b^3}{n^3})$, therefore E_2 will increase as batch size increases.

When $b = O(N^{\frac{2}{3}})$, E_1 is larger than or at same order as E_2, and the change in E_2 doesn't affect the overall performance too much. Therefore, our methods are not sensitive to batch size when batch size is relatively small. When b is very large, E_2 is dominant, and E_2 increases as batch size increases. Therefore, the overall efficiency deteriorates significantly for extremely large batch size.

Finally, we show Figure 9 which is larger and contains more information than Figure 3.

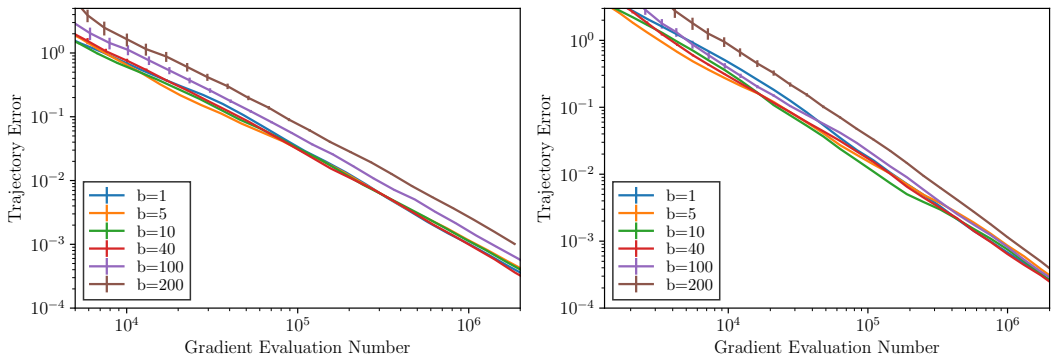

(a) SVRG-ALUM (b) SAGA-ALUM

Figure 9: Discretization error for SVRG-ALUM and SAGA-ALUM with different batch sizes on australian dataset.

D.6 ALUM for Sampling

In previous subsections, we discussed the accuracy of ALUM for approximating a ULD process and show that ALUM achieves smaller discretization error on estimating a ULD process than LPM and RMM with same number of gradient evaluation. When time T is very large, the continuous ULD process converge to the target distribution. Therefore, any output of ALUM can be used as a sample approximately drawn from the target distribution.

In this section, we apply ALUM to sample from the posterior of a Bayesian logistic regression model. We use prior distribution as $p(\boldsymbol{x}) \sim \mathcal{N}(0, mI)$, likelihood as $p(y_i|\boldsymbol{a}_i, \boldsymbol{x}) = \frac{1}{1+\exp(-y_i\boldsymbol{a}_i^\top \boldsymbol{x})}$ for $y_i \in \{1, -1\}$ and y_i,$\boldsymbol{a}_i$ comes from training set. The posterior is just $p^*(\boldsymbol{x}) \propto \exp(\sum_{i=1}^N f_i(\boldsymbol{x}))$ where the potentials f_i are defined as in Appendix D.2.

Within any gradient evaluation budgets, ALUM and VR-ALUMs can generate a sample $\boldsymbol{x}$ from a distribution that is similar to target distribution $p^*(\boldsymbol{x})$. We evaluate these sampling algorithms with the following tasks:

1. Estimating the mean potential: we sample $M = 100$ number of independent $\boldsymbol{x}_m$ by ALUM or VR-ALUMs, and report the mean potential $\frac{1}{M}\sum_{m=1}^M f(\boldsymbol{x}_m) = \frac{1}{M}\sum_{m=1}^M \sum_{i=1}^N f_i(\boldsymbol{x}_m)$.
2. Estimating the mean accuracy on test set: we sample $M = 100$ number of independent $\boldsymbol{x}_m$ by ALUM or VR-ALUMs, and report the mean accuracy $\frac{1}{M}\sum_{m=1}^M \frac{1}{N'}\sum_{i=1}^{N'} \mathbb{I}(y_i\boldsymbol{a}_i^\top \boldsymbol{x}_m > 0)$ where N' is the size of test set, y_i, $\boldsymbol{a}_i$ comes from test set and $\mathbb{I}$ is the indicator function.
3. Estimating the posterior predictive distribution: we sample $M = 100$ number of independent $\boldsymbol{x}_m$ by ALUM or VR-ALUMs, and report the estimated posterior predictive distribution $\frac{1}{N'}\sum_{i=1}^{N'} \frac{1}{M}\sum_{m=1}^M \frac{1}{1+\exp(-y_i\boldsymbol{a}_i^\top \boldsymbol{x}_m)}$ where N' is the size of test set and y_i, $\boldsymbol{a}_i$ comes from test set. This should approximate the true posterior predictive distribution $\frac{1}{N'}\sum_{i=1}^{N'} p(y_i|D_{\text{train}}) = \frac{1}{N'}\sum_{i=1}^{N'} \int p(y_i|\boldsymbol{a}_i, \boldsymbol{x})p^*(\boldsymbol{x})d\boldsymbol{x}$.

Although our theory in Theorems 1 and 3 control the sampling error in 2-Wasserstein distance, we don't conduct experiments to measure sampling error directly due to high computational cost.[13]

In order to apply ALUM for sampling, we first transform the potential to satisfy $L = 1$ as discussed in Remark 1, then we use hyperparameters $b = 1$ and $h = \frac{1}{40}$.

The results for the above tasks are shown in Figures 10 to 13, where the x-axis represent the number of gradient evaluations needed to generate a single sample. We can see that SAGA-ALUM and SVRG-ALUM converge much faster than full gradient version, since only a small batch is used for each iteration. SVRG-ALUM has multiple "plateau" in the plot, which represent the periodic update of full gradient.

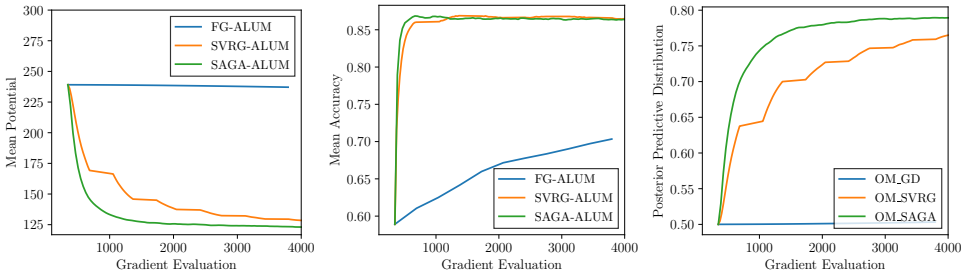

Figure 10: Sampling from posterior of Bayesian logistic regression model on australian dataset.

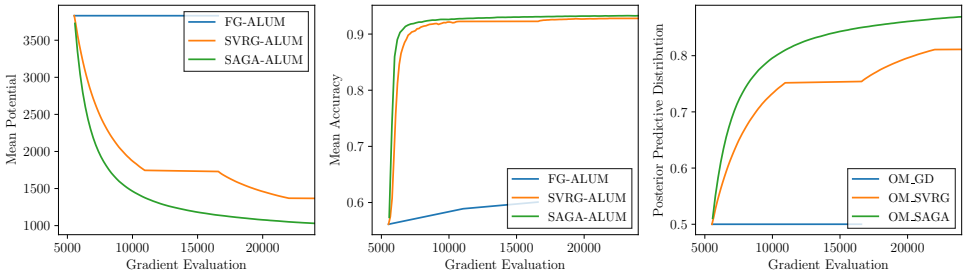

Figure 11: Sampling from posterior of Bayesian logistic regression model on phishing dataset.

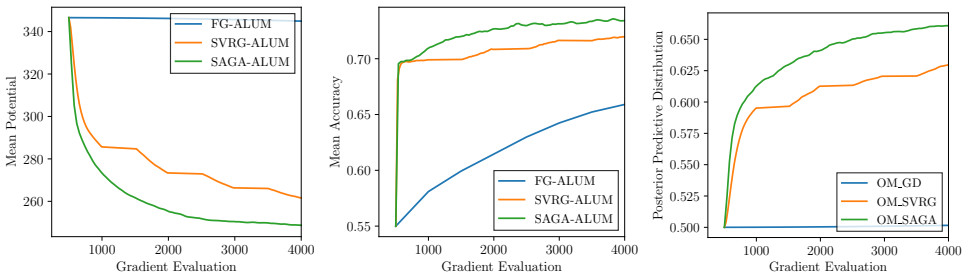

Figure 12: Sampling from posterior of Bayesian logistic regression model on german dataset.

[13]The 2-Wasserstein distance between these two continuous distributions cannot be calculated directly, therefore we must draw many samples from these distributions and calculate 2-Wasserstein distance between two discrete distribution as an approximation. The final stationary distribution of ALUM and VR-ALUMs could have very small sampling error (e.g. about 10^{-2}). In order to experimentally measure this error, we must be able to approximate the 2-Wasserstein distance between two continuous distributions up to an accuracy which is at least one order of magnitude smaller than sampling error. Due to the curse of dimension, we need an exponentially large number of samples to do that. The cost of generating these samples and the cost of calculating the distance afterwards are unaffordable in high dimensional space.

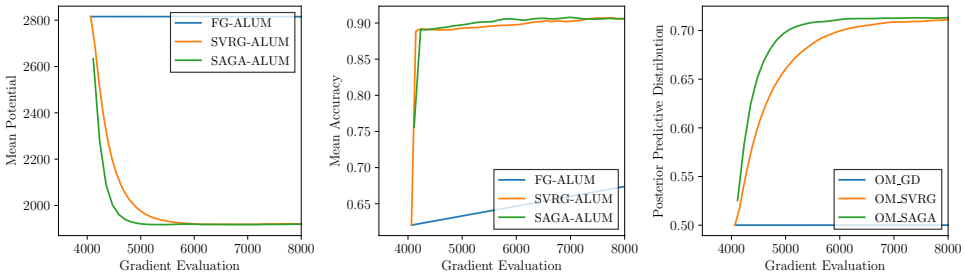

Figure 13: Sampling from posterior of Bayesian logistic regression model on mushrooms dataset.

We call the sampling error of ALUM and VR-ALUMs after running infinite steps with a fixed step size as flat sampling error. All results in this subsection illustrate how quickly the ALUM and VR-ALUMs converge with a fixed step size, but don't directly measure the flat sampling error. According to Section 5, we know both the discretization error and the flat sampling error have upper bound of $O(h^{3/2})$. We show in Appendix D.4 that this upper bound is tight for discretization error. However, it is still not clear whether the upper bound is tight for the flat sampling error.